



Fermi National Accelerator Laboratory

FERMILAB-Conf-84/101-T
October, 1984
Revised March, 1985

Eleven lectures on the Physics of the Quark-Gluon Plasma*

LARRY MCLERRAN
Fermi National Accelerator Laboratory
P. O. Box 500, Batavia, IL 60510

*(Lectures presented at a Workshop on the Physics of the Quark-Gluon Plasma, held at Hua-Zhong Normal University, Wuhan, People's Republic of China, September, 1983)



Operated by Universities Research Association Inc. under contract with the United States Department of Energy

Acknowledgements: I wish to thank my friend and colleague Liu Lian-sou for arranging this stimulating meeting in Wuhan, at Hua-Zhong Normal University. The conversations with colleagues and students who attended this meeting have been very useful to my research in this field, and provided a stimulus to write up these lectures. I especially thank my friend and colleague Gao Chong-shou who patiently read these lectures and offered advice and criticism which I hope I have successfully incorporated into the lectures. I also especially thank Ni Guang-jiong for interesting conversations on real time response theory, and Lee Jur-rong for discussions concerning photon and di-lepton emission.

Abstract: These lectures are intended to be an introduction to the physics of the quark-gluon plasma, and were presented at a workshop on The Physics of the Quark-Gluon Plasma held at Hua-Zhong Normal University in Wuhan, People's Republic of China in September, 1983. The lectures cover perturbation theory of the plasma at high temperature as well as the non-perturbative methods and results of lattice gauge theory computations. Physical models of the confinement-deconfinement phase transition and the modes of chiral symmetry breaking are presented. The possibility that a quark-gluon plasma might be produced in ultra-relativistic nuclear collisions is analyzed.

Lecture 0 : An Introduction to the Physics of the Quark-Gluon Plasma and How It Might Be Produced in Hadronic Collisions

The simplest systems studied in physics are those consisting of one, two, or infinite numbers of particles. The symmetries and dynamics of particle interactions may simply manifest themselves in systems such as an isolated electron, a hydrogen atom or an Ising spin system. The dynamics of the motion of an isolated electron probes the Lorentz and translation invariance of the vacuum, and is manifest in conservation laws which describe the electron's motion. The non-existence of isolated quarks in the vacuum is the most compelling evidence for the confining nature of the theory which describes strong interactions, Quantum Chromodynamics (QCD). In two particle systems such as the hydrogen atom, the dynamics of particle interactions are isolated and may be simply studied. In multi-particle systems such as are described by Ising models and their ilk, the symmetries of particle interactions may arise in the phase structure of the systems as symmetries are broken or realized. In the Ising model, the magnetization-demagnetization phase transition reflects a realization of a spontaneous breaking, i. e. realization of the rotational invariance of spin-spin interactions. For infinite particle systems the dynamics simplifies since it may be studied by powerful statistical mechanical methods. The dynamics of few particle systems containing three or more particles but not infinite numbers of particles, are intrinsically complicated and extracting the fundamental particle symmetries and dynamics is difficult.

Much progress in understanding strong interaction physics has arisen from studying systems which are approximately composed of two particles. For example, in a high energy electron-positron collision, a high energy quark-antiquark pair is formed. The quark-antiquark pair form a pair of very high energy jets as they travel in opposite directions to detectors. As this happens, further high energy jets might be formed when the quark-antiquark

pair emits gluons or quark-antiquark pairs with high transverse momentum relative to the jet axis. If the energy is however high enough, it is a good approximation to ignore the subsequent emission of these jets, and secondary jet emissions may be computed in a convergent expansion in the number of jets. The complications of the hadronic final state, when the quarks and gluons are converted into hadrons, is miraculously irrelevant for the computation of certain physical observables which characterize the jets.

The simplicity of jet formation in electron-positron annihilation arises from the asymptotic freedom of strong interactions. At high energies, or short distances, the strong interactions become weak. Since strong interactions change particle number, the creation of particles is suppressed at high energies and short distances. This fact allows for a systematic expansion in powers of the strong interaction coupling constant when computing the properties of jets. Such an expansion is essentially an expansion in the number of jets. Of course, as the quark-antiquark pair initially produced in the collision separate to larger distances, the strong interactions become strong and multi-particle degrees of freedom become important. A remarkable feature of QCD is that in this hadronization process, where quarks and gluons are converted into ordinary colorless hadronic particles, certain physical observables which characterize the jets are unmodified.

The fact that strong interactions (when the interactions are truly strong) are intimately tied to multiparticle dynamics seems to be an inevitable consequence of the particle number non-conserving nature of the strong interactions. Even the ground state vacuum of quantum chromodynamics is a state consisting of an infinite number virtual quarks, antiquarks and gluons. Statistical mechanics techniques seem ideally suited for analyzing such systems.

These considerations demonstrate the dual nature of QCD studies. One goal of such studies is to verify that QCD in fact

describes strong interaction processes. For this purpose, studies of few particle systems should be adequate. Another goal is to study the dynamics of QCD when interactions are truly strong. These studies may lead to fundamental understanding of the nature of confinement, that is, the non-existence of isolated colored particles in nature, and the nature of chiral symmetry breaking, that is why the proton is so massive compared to the pion, or put another way, how the quarks which initially are to a good approximation massless in the dynamical equations which describe QCD acquire effective masses through interactions.

Since the study of strong interaction dynamics demands the study of multiparticle systems, we should ask what are the simplest multiparticle systems to study. The vacuum or ground state of QCD is perhaps the simplest such system, but suffers from having no adjustable parameter which might allow for simplification of the properties of the vacuum for certain ranges of such an adjustable parameter. It is also difficult to imagine carrying out non-trivial experiments on the vacuum in order to probe the dynamics of QCD.

The simplest set of systems characterized by a minimal set of adjustable parameters are finite temperature and baryon number density hadronic systems. Two parameters characterize these systems, the temperature T and the baryon number density, ρ_B . Baryon number density is the number of baryons minus antibaryons per unit volume. Baryon number is conserved by the strong interactions. In the limit that $T \rightarrow 0$ and $\rho_B \rightarrow 0$, these systems reduce to the vacuum. Another remarkable fact is that the method of computation of the spectrum and propagation of single particle excitations of these systems is in close parallel with the method of computations for the vacuum.

To have a reasonable range of parameters to probe the structure of QCD it is necessary to have very high energy density hadronic systems. High energy density hadronic matter might be composed of bound states of quarks and gluons in ordinary hadrons, or might be an unconfined plasma of quarks and gluons. Such high energy density hadronic matter occurs in a variety of physically interesting situations. Cold, baryon rich hadronic matter of almost infinite extent occurs in the cores of neutron stars, and baryon number densities of maybe 10-20 times that of ordinary nuclear matter. Since the natural time scale for interactions in strongly interacting systems is the time it takes light to travel a Fermi, 10^{-23} sec., and since neutron stars have macroscopic lifetimes, the cores of neutron stars almost certainly contain matter which is in local thermal equilibrium and may be well described using equilibrium thermodynamics.

Another example of a high energy density system is provided by the big bang. In the big bang energy densities may have existed up to those where at least quantum gravity becomes important, $\rho \sim 10^{70-80}$ times that of nuclear matter. When the energy density was that of ordinary nuclear matter, the universe was expanding with a characteristic time scale of $t \sim 10^{-6}$ sec. Since this is orders of magnitude larger than the natural time scale for strong interactions, the universe was probably in local thermal equilibrium.

Another place where hot, baryon rich matter might be produced is in ultra-relativistic heavy ion collisions. The result of such a collision is shown in Fig. 1. Here the two Lorentz contracted nuclei have passed through one another leaving hot hadronic matter in their wake. In the region of the Lorentz contracted nuclei, hot, baryon rich matter presumably exists. The conjecture that the two nuclei pass through one another at very high energies will be explained later in this lecture. This situation is much different than that at very low energies where the nuclei are almost impenetrable, and is a consequence of the Lorentz time dilation of hadronic interactions of ultra-relativistic particles. Reasonable estimates of the energy densities achieved in these collisions are 10-400 times that of ordinary nuclear matter. The time scales for expansion of such matter are perhaps only a few times to 10 times the natural time scale for hadronic interactions, and although the system may be

to a fair approximation in local thermal equilibrium, non-equilibrium processes will also be important for the dynamics.

The description of hadronic matter by QCD is adequate for energy densities less than those for which heavy W and Z bosons form an important component of the matter. Electromagnetic effects must be included and are more important than strong interactions for describing dynamics at energy densities less than those of nuclear matter. Strong interactions are not so important at these low densities since hadrons are well separated and strong interactions are short range. At extremely high energy densities, $\rho = 10^{60-80}$ times that of nuclear matter, particles with the degrees of freedom associated with grand unification, and eventually even quantum gravity, may play a dominant role. At any energy density at which new degrees of freedom play an important role, a variety of phase changes may take place. Such energy densities are shown in Table I. We shall be interested in matter in the range of energy densities $10^{10} \text{ GeV/Fm}^3 > \rho > 1 \text{ Gev/Fm}^3$, where QCD adequately and simply describes matter. (At these densities, electromagnetic particles contribute to the dynamics, but play a trivial role since their interactions are unimportant)

There are several values of the energy density for which the dynamics of hadronic matter is quite different. At energy densities which are very large or very small compared to some natural scale, we might expect the dynamics of the matter to simplify. At energy densities close to some natural scale we might expect that the dynamics would be complicated, but perhaps more interesting than in the asymptotic regimes. At energy densities close to a natural scale, a variety of phase transitions might occur which involve dramatic changes in the properties of hadronic matter, and their existence might reflect symmetries of the QCD interactions.

The natural density scale for QCD is the energy density at which hadrons begin to overlap. At this energy density scale, the quark and gluon degrees of freedom become important for the description of the matter. This energy density scale should be

of the order of the energy density of matter inside a proton, which is $\rho = 1 \text{ Gev}/(\frac{4}{3}\pi R^3) \sim 500 \text{ Mev/Fm}^3$, where we have used R as the r.m.s. charge radius of the proton, $R = .3 \text{ Fm}$. This is reasonably close to the estimate of $\rho = \Lambda_{\text{MS}}^4 \sim 200 \text{ Mev/Fm}^3$, with $\Lambda_{\text{MS}} \sim 200 \text{ Mev}$ as the dimensional scale parameter typica of QCD. This energy density is also not large compared to the energy density of nuclear matter, $\rho = 150 \text{ Mev/Fm}^3$, which to the accuracy of these order of magnitude estimates is the same as that of the natural scale for hadronic matter. There are of course large uncertainties in this crude order of magnitude estimate. Reasonable variations of the value of the parameter R in the estimate of the energy density inside a proton give an order of magnitude uncertainty in the value of this scale. Uncertainties in current lattice Monte-Carlo estimates of the energy densities for which there may be phase transitions in QCD are perhaps a factor of 20 (1-6).

At energy densities which are very large compared to this natural scale, hadronic matter is a plasma of quarks and gluons unconfined into hadrons. At such very high energy densities, the average separation between the constituents of the quark-gluon plasma may become $d \ll 1 \text{ Fm}$. The strength of the QCD interactions between these closely packed quarks and gluons is weak due to asymptotic freedom, since QCD interactions become weak at short distances. Of course, there may be some long range interactions which are not shielded in the plasma and for such long range interactions the strength is not small. Such long range interactions do not however significantly affect the bulk properties of the plasma, but might significantly alter long distance correlations between particles in the plasma. Since the interactions which affect the average bulk properties of the plasma are weak, they provide small corrections to the kinetic energies of the quarks and gluons when bulk quantities such as the energy density and the pressure are computed. Hadronic matter therefore becomes an ideal gas at very high energy densities.

At extremely low energy densities, hadronic matter is

composed of widely separated hadrons. Since the range of strong interactions is finite, these widely separated hadrons will, on the average, interact weakly. Hadronic matter becomes an ideal hadron gas at these low energy densities.

The properties of hadronic matter simplify at very high and very low energy densities, when hadronic matter becomes an ideal gas. The degrees of freedom of these ideal gases are of course quite different. For a zero baryon number density system, the low temperature system is a pion gas with three degrees of freedom. At very high temperatures there are colored spin 1/2 quarks and antiquarks with three colors corresponding to 12 degrees of freedom plus eight colored helicity 1 gluons corresponding to 16 degrees of freedom. For intermediate energy densities, hadronic matter is interpolating between these degrees of freedom.

At intermediate interpolating energy densities phase transitions may occur. As the quarks and gluons become liberated from hadrons, a confinement-deconfinement phase transition might arise. Also a chiral symmetry restoration phase transition might take place. The existence of phase transitions is often associated with a spontaneous realization or breakdown of a symmetry. Chiral symmetry is a symmetry of the QCD interactions for massless up and down quark masses. Since these quarks have small but finite masses, such a symmetry is only approximate. If the chiral phase transition is first order, the introduction of small up and down quark masses should not remove the phase transition since the system changes discontinuously across a first order transition, and a small continuous change should only slightly modify the magnitude of this discontinuity.

The confinement-deconfinement phase transition may be shown to arise as a consequence of a symmetry for QCD as it describes gluons, and ignoring quarks. Confinement arises as a consequence of symmetry realization, and deconfinement as a consequence of symmetry breaking. For QCD this phase transition is first order, and in so far as the effects of quarks are small,

this phase transition might remain when quarks are properly accounted for.

To probe the gluon plasma (in the absence of dynamical quarks), heavy test quarks may be inserted into the plasma. The free energy of these test quarks may be found by computing the expectation values of spatially local operators $L(\vec{r})$. It is possible to show that the free energy of an isolated test quark at the position \vec{r} is

$$\langle L(\vec{r}) \rangle = e^{-\beta F(\vec{r})} = \begin{cases} 0 & \text{Confinement} \\ \text{Finite} & \text{Deconfinement} \end{cases} \quad (1)$$

The operator L is an order parameter since its expectation value is zero in the confined phase, where the free energy of an isolated test quark is infinite. In the deconfined phase, the free energy is finite.

The operator L may be shown to be analogous to the spin variable of a Z_3 spin system. In this analogy, the temperature of the Z_3 spin system is

$$T_{\text{Eff}} = g^2 \quad (2)$$

where g is the QCD coupling strength. The effective temperature depends on the physical temperature since g^2 depends upon T . Recall that at high temperatures, the coupling strength decreases due to asymptotic freedom. Eq. 2 predicts that as the physical temperature increases, the effective temperature decreases and vice-versa.

The operator L is analogous to spin variable. For a theory with N^2-1 gluons ($N = 3$ for QCD) the QCD equations of motion are invariant under a global transformation which flips L :

$$L(\vec{r}) \rightarrow e^{\frac{2\pi i j}{N}} L(\vec{r}) \quad (3)$$

where j is an integer. This Z_3 spin flip symmetry, which we shall call the center symmetry, guarantees that $\langle L \rangle = 0$ if the symmetry is realized.

At very high effective temperatures of the Z_3 spin system, the spin system should be disordered, $\langle L \rangle = 0$, and the system confines. As the effective temperature decreases, there may be a critical temperature for which the spin system orders, $\langle L \rangle \neq 0$, and the system deconfines. It can be shown that if the effective spin system exhibits a first order phase transition, then this will also be true for the QCD finite temperature theory. For Z_3 spin systems, corresponding to QCD, the phase transition is predicted to be first order. Since effective temperature and physical temperature are inversely correlated, low physical temperatures correspond to symmetry restoration and confinement, while high physical temperatures correspond to symmetry breaking and deconfinement.

This picture of the confinement-deconfinement phase transition for a gluon plasma may be studied using lattice Monte-Carlo methods.⁽¹⁻⁸⁾ The latticization starts by discretizing space-time in a finite four volume, and physical quantities are extracted in the zero lattice spacing infinite three volume limit. The fourth length of the four volume may be shown to be $\beta = 1/T$. Using a discretization of coordinates is a familiar technique for solving partial differential equations and is of great use for numerically solving QCD. The phase structure at finite temperature arises in the zero lattice spacing, infinite three volume limit as the length of the fourth dimension of the box, $1/\beta$, is varied. This length might be varied by changing the coupling since temperature and coupling are related through asymptotic freedom.

Once QCD is discretized and placed on a four dimensional lattice, it may be studied by lattice Monte-Carlo simulation techniques. These techniques are entirely analogous to the techniques applied to study spin systems such as the Ising model. Various gluon field configurations which give contributions to the partition function may be selectively sampled by an algorithm which finds those contributions which dominate the sum over configurations. The error in this selective sampling is approximately the inverse square root of

the independently sampled gluon field configurations.

Hypothetical results of a Monte-Carlo simulation of $\langle L \rangle$ are shown in Fig. 2. For $N = 3$, corresponding to QCD, there is a sharp break at the critical temperature corresponding to a first order phase transition, and actual Monte-Carlo computations yield curves for $\langle L \rangle$ similar to that shown.⁽¹⁻⁶⁾ The specific heat and energy density as a function of temperature have also been computed.⁽⁴⁻⁸⁾ At high temperatures, these quantities approach ideal gas values. The energy density jumps rapidly at T_c' , and a first order phase transition is strongly indicated. The latent heat of this phase transition appears to be $1-2$ GeV/Fm³, with uncertainties of undetermined magnitude arising from the small size of lattices used in the computations, but which might be as large as an order of magnitude.⁽⁵⁻⁶⁾ The critical temperature is determined to be $T_c = 200$ Mev with uncertainty of perhaps a factor of 2.

When dynamical quarks are included in finite temperature QCD computations, the confinement-deconfinement transition might disappear.⁽⁹⁻¹¹⁾ To understand how this might happen, consider the free energy of an isolated test quark. In a system with dynamical quarks, this free energy is always finite since the test quark may always form finite energy bound states with the dynamical quarks. The operator L is no longer an order parameter, since it always has a finite expectation value. In the analogy with a spin system, the dynamical quarks are analogous to an external magnetic field since their presence guarantees that the magnetization $\langle L \rangle$ is always finite. Since the effects of dynamical quarks disappear as the quark mass becomes infinite, the external magnetic field goes to zero in this limit.

In spin systems such as the Ising model, the presence of an external magnetic of arbitrarily small strength can destroy the magnetization phase transition. The case for QCD is somewhat more complicated since in the absence of dynamical quarks, the confinement-deconfinement phase transition is first order, where for the Ising model the phase transition in the absence of an

external magnetic field is second order. A first order phase transition involves a discontinuous change in the properties of a system, and a small perturbation may only continuously deform this change. Only if the effects of quarks become sufficiently large may the phase transition be removed. We therefore conclude that if the quark masses are sufficiently small and if there are a sufficiently large number of quark flavors, then the phase transition might be removed.

These arguments are complicated by the possibility of a chiral symmetry restoration phase transition. Chiral symmetry is a symmetry of the QCD equations of motion when the up and down quark masses are taken to zero. (This symmetry might be enlarged by taking the strange quark mass as zero, which is a fair approximation.) The chiral symmetry appropriate to this limit is only approximate in nature since the up and down quark masses are small but finite. If chiral symmetry was exact, either all baryons would be massless, or for every massive baryon there would be a partner which would be degenerate in mass. The meson masses would be unconstrained. The spectrum of states realized in nature has large mass baryons which do not occur in parity doublets, and the pion has a small mass. This situation corresponds to chiral symmetry breaking. When a symmetry such as chiral symmetry is broken, Goldstone's theorem guarantees that there must be a massless scalar particle, here corresponding to the pion. The finite pion mass is presumably a consequence of the finite quark masses in the QCD equations of motion.

A simple model for chiral symmetry breaking is the σ model where a spin zero, even parity and even charge conjugation σ meson condenses in the vacuum and induces chiral symmetry breaking. In QCD, this σ meson is presumably a bound quark-antiquark pair. As quarks and gluons begin to become deconfined from hadrons, the σ mesons become ionized. Since fermions do not condense by themselves, and since there are no longer any σ mesons to condense, chiral symmetry breaking may end. Since chiral symmetry breaking generates dynamical masses

for baryons such as quarks, and since the strength of the effective magnetic field which might destroy the confinement-deconfinement phase transition increases with decreasing quark mass, the confinement-deconfinement phase transition and the chiral phase transition are intimately related. The chiral phase transition for three flavors of massless quarks may be studied using effective chiral interactions, and is almost certainly first order.(12-13) As the up, down, and strange quarks acquire small but finite masses, this first order phase transition should not disappear. Since the strange quark mass is perhaps not so small, this argument is somewhat soft, but even for two massless flavors, which should be a very good approximation, there are arguments that the chiral phase transition is first order.(14)

A possible phase diagram for the chiral and confinement phase transitions is shown in Fig. 3. The upper and bottom horizontal axis are the temperature while the vertical axis is $e^{-1/m}$. This latter variable approaches 1 for infinite mass quarks, and approaches 0 for zero mass quarks. The upper T axis therefore corresponds to a theory in the absence of dynamical quarks. Along this axis there is a first order phase transition. As the mass decreases from infinity, a line of first order phase transitions may evolve in the $T, e^{-1/m}$ plane. This line might terminate in a first order phase transition as shown in Fig. 3a or it might evolve all the way to zero T as in Fig. 3b. Along the bottom T axis, the quark mass is zero. There should be a chiral phase transition along this axis which may be first or higher order. If the phase transition is first order as is assumed in Fig. 3, then the chiral transition evolves into the $T, e^{-1/m}$ plane. This line might either terminate somewhere in this plane, as is assumed in Fig. 3a, or it might join on to the upper axis. The most elegant possibility is that the line emanating from the deconfinement transition joins the chiral transition. In this sense, the confinement-deconfinement phase transition and the chiral phase transition would be identified. There are of course many more

phase diagrams than are illustrated in Fig. 3, and the actual diagram realized in nature is not yet known. It is also important to recognize that although quark masses may be varied in a theory, in nature masses are fixed, and the issue of whether or not there are true phase transitions in QCD is whether or not for some fixed values of masses, the first order phase lines are crossed while varying the temperature T . Numerical Monte-Carlo simulations of lattice gauge theories are still in a very primitive state, and knowledge of the phase diagram for QCD is very scant. Early attempts to include fermions concluded that there was a first order confinement-deconfinement phase transition which could be identified with a chiral transition.⁽⁵⁾ These so called quenched approximations were then improved to include fermions in an expansion in inverse powers of the fermion masses. Such hopping parameter computations seemed to indicate that the confinement-deconfinement transition disappeared at a large value of the quark mass.⁽¹⁰⁻¹¹⁾ Newer computations using pseudo-fermion techniques or micro-canonical ensembles indicate that the phase transition may persist to zero mass, or at least, if the phase transition is removed, the change in the properties of the quark-gluon plasma is very sharp at a temperature which may be regarded as a remnant temperature of the confinement-deconfinement temperature.⁽¹⁵⁻¹⁷⁾ There is no time to review these methods here, except to note that computations involving fermions are improving very rapidly and an answer to questions about the QCD phase diagram may soon be available.

In spite of all the theoretical understanding of the properties of hadronic matter which has developed in the last few years, almost no experimental data exists which might probe its properties. Such data might provide a striking confirmation of ideas about confinement and chiral symmetry breaking. The production and study of new forms of matter is also of intrinsic scientific interest, and may enlighten conjectures about neutron star structure and the early universe.

There is a good possibility that new forms of matter might

be produced and studied in the collisions of ultra-relativistic nuclei.⁽¹⁶⁻¹⁹⁾ Such a collision is visualized in Fig. 4 in the context of the inside-outside cascade model of hadron interactions, a picture which we shall soon motivate.⁽²⁰⁾ This model describes known features of hadronic collisions, is true in field theory computations of cascade development, and is a consequence of Lorentz invariance and the limited transverse momentum of particles produced in hadronic collisions.

In Fig. 4a the two nuclei approach one another with energy E_{CM} per nucleon. The two nuclei are Lorentz contracted to a thickness $\Delta x \sim 1$ Fermi. This limiting thickness, $\Delta x \gg R/E_{CM}$, where R is the nuclear radius and E_{CM} is measured in GeV, arises because the nucleons couple to low longitudinal momentum degrees of freedom, $\Delta p^z \sim 200$ Mev, and the uncertainty principle guarantees fuzziness on a scale $\Delta x = 1/4p^z$. These low longitudinal momentum degrees of freedom are the mesons which are produced with small momentum in the collisions of hadrons with high center of mass energy. The nucleon degrees of freedom, that is the portion of the nuclear wavefunction which carries baryon number, is Lorentz contracted to a size $\Delta x = R/E_{CM}$.

As the two nuclei pass through one another, Fig. 4b, the low momentum meson degrees of freedom interact and a hot hadronic matter distribution forms. Meson degrees of freedom with higher longitudinal momentum take longer to interact, and Lorentz time dilation slows matter formation. As time proceeds, this higher longitudinal momentum matter forms at

$$ct = p^z/m = x^z,$$

where we assume mesons have large p^z and travel with velocities close to that of light, and m is a typical hadronic momentum scale, $m \sim 200$ Mev.

In the rest frame of the newly formed matter, we are implicitly assuming there is a formation time at -1 fm./c. This is a natural time scale for hadronic interactions. This

formation zone is at $x \sim ct \sim p''/m$ in the center of mass frame and is a distance $\Delta x \sim 1/p''$ from the nuclei. This formation zone gets closer and closer to the nucleons as time evolves until at $t \sim R/ECM$ the nucleons themselves begin to fragment. The matter formed in these nuclear fragmentation regions is baryon rich whereas the matter in the central region was primarily composed of mesons.

A consequence of the inside-outside cascade model is a correlation between space-time and longitudinal momentum. This correlation may provide a powerful analytical framework for ultra-relativistic nuclear collisions.

The consequences of Lorentz time dilation in particle production are most dramatic in the Landau-Pomeranchuk-Migdal effect for electromagnetic cascade development.(21) In electromagnetic cascades, the cascade multiplies by electrons, positrons or photons passing by nuclei and in the strong electric field of the nuclei, the photons pair produce electron-positron pairs and the electrons or positrons bremsstrahlung. The natural time scale for the pair production is roughly of the order of the time it takes light to travel the Compton wavelength of the electron scaled by an inverse power of the fine structure constant. The fine structure constant appears because in the limit of zero electromagnetic coupling, it is not possible for photons to produce electron-positron pairs. This time is about 10^{-9} cm/c.

In the cascade, this natural time is dilated by the Lorentz factor of the particles participating in the cascade development. If this dilated time becomes large compared to the time it takes electromagnetic particles to pass nuclei, and further cascade, the cascade will become inhibited. The particles are still forming while subsequent scatterings are taking place. For emulsions, a typical interaction length might be a tenth of a centimeter, corresponding to 100 Tev before the Landau-Pomeranchuk-Migdal effect becomes appreciable.(21) If this natural time becomes so large that pairs are just beginning to form as an electromagnetic particle passes through an apparatus,

then the apparatus becomes transparent to the high energy electromagnetic radiation. This occurs at an energy of the order of 10^5 Tev. At 10^9 Tev, neutron stars become transparent to electromagnetic radiation.

In nucleus-nucleus collisions, the hadronic counterpart of the Landau-Pomeranchuk-Migdal effect explains limiting transparency. The nuclei pass through one another for the same reasons that at very high energies electrons pass through detectors with little cascading. Correlations between space-time and momentum space develop as a consequence of this mechanism.

The inside-outside cascade model of hadronic interactions describes hadronic interactions such as hadron-hadron, hadron-nucleus, and nucleus-nucleus collisions. Why are nucleus-nucleus collisions better suited to producing a quark-gluon plasma than are ordinary hadron collisions? The most obvious reason is that in nucleus-nucleus collisions, the average multiplicity of produced particles is higher than for hadron-hadron collisions, and higher energy densities result on the average. Another is that nuclei are of large spatial extent, and in order to produce a well thermalized matter distribution, the particles produced in the collisions must rescatter, so that the large spatial size enables the produced particles to rescatter several times before being emitted from the collision region. Yet another reason is that with the large average multiplicities of nucleus-nucleus collisions, the statistical fluctuations are smaller, and collective phenomena may be easier to observe. These collective effects, which may be consequences of processes such as nucleation of hadronic matter in a supercooled quark-gluon plasma, may be crucial for arguing that a quark-gluon plasma has been produced in the collision.

On the other hand, fluctuations in hadron-hadron collisions might also produce a quark-gluon plasma. In very high multiplicity hadron-hadron collisions, very high energy density regions may be produced. The energy density might be so high that even when the system is in a relatively large spatial

volume, there may be sufficiently large energy densities to maintain a plasma.

If the space-time volume is sufficiently large that hydrodynamics may be used to describe a collision, the description greatly simplifies. Hydrodynamic equations require knowledge of the state of the matter at some time, and the equation of state of the matter. Monte-Carlo simulations may soon provide good equations of state for hadronic matter, and the equation of state is already well understood with semi-quantitative models. The initial conditions are semi-quantitatively predicted by the inside-outside cascade model, and the final state of the matter may be experimentally measured. The evolution of the matter at intermediate times appears to be computable, a situation which is much advanced relative to our knowledge of hadron-hadron collisions.

Assuming an initial formation time for the hadronic matter produced in a nucleus-nucleus collision, and knowing the final state distribution of the matter, the hydrodynamic equations may be integrated backwards in time to determine the initial energy density.^(18,22) There are several experimental measurements of the final state hadron distribution in nucleus-nucleus collisions provided by the JACEE cosmic ray experiment.⁽²³⁾ Extrapolating their results to the head on collisions of uranium, the energy density is

$$E/V = \frac{10 \text{ GeV/Fm}^3}{t_0}$$

where t_0 is the initial formation time. This result only depends on the isentropic nature of the hydrodynamic expansion, and not on the details of the equation of state. Theoretical estimates of the formation time to vary, but the range of reasonable values is probably $.2 < t_0 < 1 \text{ Femtosecond}$. The corresponding range of energy densities is $10\text{-}50 \text{ GeV/Fm}^3$. This is 50-250 times the energy density of nuclear matter and is probably sufficient to produce a quark-gluon plasma.

There are of course great uncertainties in this

prognostication. Is the inside-outside cascade picture truly applicable at the energies appropriate to the JACEE experiments? Are non-equilibrium effects not included in the hydrodynamic analysis important? Are the few results of the JACEE analysis typical of nucleus-nucleus collisions? These questions are difficult to assess without accelerator experiments.

There is of course a pressing question about the signals of a quark-gluon plasma if produced in a nucleus-nucleus collision.⁽²⁴⁾ There have been many suggestions. Metastable droplets of quark-gluon matter might produce long lived droplets of dense matter,⁽²⁵⁻²⁶⁾ or might be short lived and detonate explosively.⁽²⁸⁾ Large scale density fluctuations, like steam bubbles in boiling water, might form as the matter non-explosively cools, or as the plasma is formed from hadronic matter. Leptons and photons might probe the plasma in the hot early stages of its existence.⁽²⁹⁻³³⁾ Strange particle production might be copious, and there might be abundant Λ production in the fragmentation region.⁽³⁴⁻³⁵⁾ These signals for plasma production are extremely speculative, and experimental data is needed to channel speculation into quantitative science.

References:

- (1) L. McLerran and B. Svetitsky, Phys. Lett. 98B, 195, (1981); Phys. Rev. D24, 450; (1981)
- (2) J. Kuti, J. Polonyi, and K. Szlachanyi, Phys. Lett. 98B, 199, (1981)
- (3) J. Engels, F. Karsch, I. Montvay, and H. Satz, Phys. Lett. 101B, 39, (1981); J. Engels, F. Karsch, and H. Satz, Phys. Lett. 113B, 398, (1982); Nuc. Phys. 125B, 411 (1983)
- (4) K. Kajantie, C. Montonen, and E. Pietarinen, Zeit. Phys. C9, 253, (1981)
- (5) J. Kogut, M. Stone, H. W. Wyld, W. R. Gibbs, J. Shigemitsu, S. Shenkar, and D. Sinclair, Phys. Rev. Lett. 48, 1140, (1982); 50, 393, (1983); Nuc. Phys. B225, 326, (1983); J. Kogut, H. Matsuoka, M. Stone, H. W. Wyld, S. Shenkar, J.

- Shigemitsu, and D. Sinclair, Phys. Rev. Lett. 51, 869, (1983);
T. Celik, J. Engels, and H. Satz, Phys. Lett. 125B, 411, (1983);
129B, 323, (1983)
- (6) B. Svetitsky and F. Fucito, Phys. Lett. 131B, 165, (1983)
- (7) K. Wilson, Phys. Rev. D10, 2445, (1974)
- (8) M. Creutz, Phys. Rev. Lett. 45, 313, (1980); Phys. Rev. D21, 2308, (1980)
- (9) T. Banks and A. Ukawa, Nuc. Phys. B225, 145, (1983)
- (10) T. De Grand and C. De Tar, Nuc. Phys. B225, 590, (1983)
- (11) P. Hasenfratz, F. Karsch, I. O. Stamatescu, Phys. Lett. 133B, 221, (1983)
- (12) H. Goldberg, Phys. Lett. 131B, 133, (1983)
- (13) R. D. Pisarski and F. Wilczek, Phys. Rev. D29, 338, (1984)
- (14) R. D. Pisarski, ITP at Santa Barbara Preprint, NSF-ITP-83-71 (1983)
- (15) F. Fucito and S. Solomon, Cal. Tech. Preprint Caltech-68-1084, (1984); R. Gava, M. Lev and B. Peterson, Bielefeld Preprint BI-TP-84/01 (1984); J. Polonyi and H. W. Wyld, Proceedings of Quark Matter 84, Brookhaven National Lab. (1984)
- (16) E. V. Shuryak, Phys. Rep. 61, 71 (1980)
- (17) R. Anishetty, P. Koehler, and L. McLerran, Phys. Rev. D22, 2793, (1980); L. McLerran, Proc. 5th High Energy Heavy Ion Study, (1981)
- (18) J. D. Bjorken, Phys. Rev. D27, 140, (1980)
- (19) K. Kajantie and L. McLerran, Phys. Lett. B119, 203, (1982)
- (20) J. Bjorken, Lectures at the DESY Summer Institute, (1975), Proceedings edited by J. G. Korner, G. Kramer, and D. Schildknecht, (Springer, Berlin, 1976)
- (21) K. Kasahara, Proceedings of 18th International Cosmic Ray Conference, Bangalore, India, (1983)
- (22) M. Gyulassy and T. Matsui, LBL Preprint LBL-15947, (1983)
- (23) T. Burnett et al., Phys. Rev. Lett. 50, 2062, (1983)
- (24) M. Gyulassy, Proceedings of Quark Matter 84, Brookhaven National Lab. (1983)
- (25) J. D. Bjorken and L. McLerran, Phys. Rev. D20, 2353, (1979)
- (26) A. Kerman and S. Chin, Phys. Rev. Lett. 43, 1292, (1979)
- (27) M. Gyulassy, K. Kajantie, H. Kurki-Suonio, and L. McLerran, LBL Preprint LBL-16277 (1983)
- (28) L. Van Hove, Zeit. Phys. C21, 93, (1983)
- (29) E. V. Shuryak, Sov. J. Nuc. Phys. 28, 408, (1978); Phys. Lett. 78B, 150, (1978)
- (30) G. Domokos and J. Goldman, Phys. Rev. D23, 203 (1981)
- (31) K. Kajantie and H. Miettinen, Zeit. Phys. C9, 341, (1981)
- (32) G. Domokos, Phys. Rev. D28, 123, (1983)
- (33) J. Badier et al., Proceedings of Quark Matter 82, Bielefeld, W. Germany, (1982)
- (34) J. Rafelski and B. Muller, Phys. Rev. Lett. 48, 1066, (1982)
- (35) T. Biro, B. Lukacs, and J. Zimanyi, Nuc. Phys. A386, 617, (1982)

Figure Captions:

- Figure 1: An ultra-relativistic nucleus-nucleus collision viewed in the center of mass frame. The two Lorentz contracted nuclei have passed through one another leaving not, dense matter in their wake.
- Figure 2: L as a function of T for a first order, —, and a second order, - - -, phase transition.
- Figure 3: Hypothetical phase diagrams in the T , $e^{-1/m}$, plane. In Fig. 3a, the chiral, deconfined world is not isolated from the chiral symmetry broken, deconfined world. In Fig. 3b, these worlds are separated by a phase boundary.
- Fig. 4: Ultra-relativistic nuclear collisions in the center of mass frame. (a) Approach. (b) Passage through one another. (c) Cooling.

Table I
Energy Densities and New Degrees of Freedom

E (Gev/ fm^3)	Degrees of Freedom
10^{-9}	Electron-positron Pairs, photons
1	Leptons, photons, quarks, gluons
10^{10}	The above plus Z^0 , W , and Higgs bosons
10^{62}	The above plus the superheavy particles of Grand Unified theories.
10^{78}	The above plus the completely unknown.

Figure 0-1



Figure 0-2

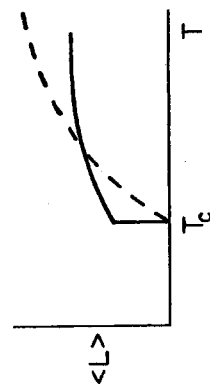


Figure 0-3

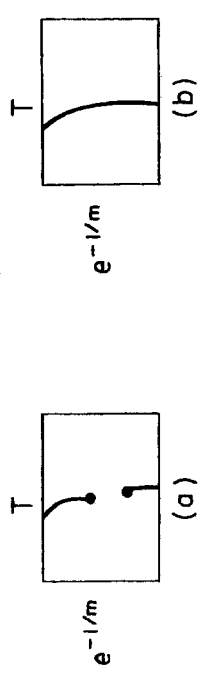


Figure 0-4

LECTURE 1 : Thermodynamics of a Scalar Field Theory

The thermodynamical properties of a system governed by a Hamiltonian H may be abstracted from knowledge of the thermodynamical potential, (1)

$$\Omega(\beta, u) = -1/\beta V \ln \text{Tr } e^{-\beta H} + \beta \vec{J} \cdot \vec{N} . \quad (1)$$

The average number densities associated with conserved charges may be found by differentiating the potential with respect to the chemical potentials, \vec{J} , which are conjugate to the charges \vec{N} ,

$$\rho_i = \langle N_i \rangle / V = -\frac{1}{V} \frac{\partial}{\partial J_i} \Omega(\beta, u) . \quad (2)$$

The average energy density is similarly found by differentiating with respect to u_i and the inverse temperature β ,

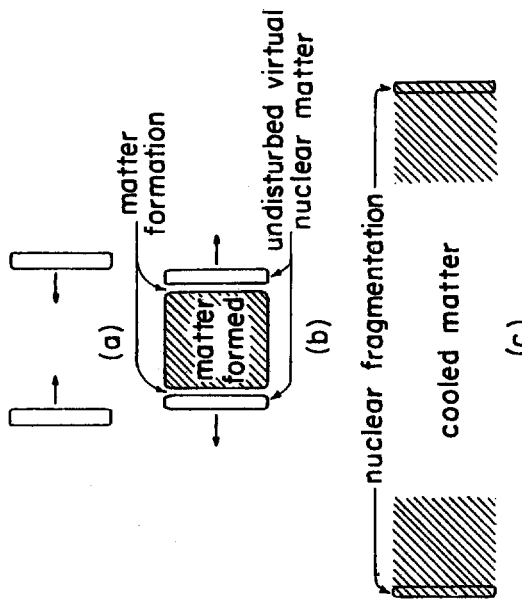
$$\epsilon = \langle H \rangle / V = \frac{1}{V} \left[\frac{\partial}{\partial \beta} - 1/\beta \frac{\partial}{\partial J_i} \right] \Omega(\beta, u) . \quad (3)$$

The simplest example of a thermal system described by a field theory is provided by the thermodynamics of a scalar field. The Hamiltonian for this theory is

$$H = \int d^3x \left\{ \frac{1}{2} \pi^2(x, t) + \frac{1}{2} (\vec{\nabla}\phi(x, t))^2 + \frac{1}{2} m^2 \phi^2(x, t) + V(\phi(x, t)) \right\} \quad (4)$$

where the scalar field ϕ and its conjugate momentum π satisfy the equal time commutation relations

$$[\phi(x, t), \pi(x', t')] = i\delta^3(x - x') . \quad (5)$$



The scalar field ϕ solves the equation of motion

$$\{ -\Box + m^2 \} \phi + \delta V / \delta \phi = 0 . \quad (6)$$

This equation of motion is derived from variation of the action

$$S = \int d^4x \left[\frac{1}{2} (\partial \phi)^2 + \frac{1}{2} m^2 \phi^2 + V(\phi) \right] . \quad (7)$$

The metric in all of these equations is Minkowskian with the convention

$$g^{00} = -1, \quad g_{ii} = 1 . \quad (8)$$

Later we shall deal with Euclidian metric actions, but we shall see that these actions arise from carefully deriving a Feynman path integral representation for the thermodynamical using the fields defined in Minkowski space. (2)

A Feynman path integral representation for the thermodynamical potential arises upon evaluating the trace of Eq. (1) by inserting complete sets of intermediate states. For the scalar field theory we shall take the chemical potential $\mu = 0$. The thermodynamical potential evaluated in basis states which are eigenstates of the field operator ϕ becomes

$$e^{-\beta V_0} = \int d\phi \langle \phi | e^{-\beta H} |\phi \rangle . \quad (9)$$

The integration measure $d\phi$ is a product of integrations over the fields ϕ at all spatial coordinates x defined on some fixed time surface. This product is best defined on a finite spatial grid (lattice), since the product then involves a finite product over a finite number of spatial coordinates and is mathematically well defined.

The representation is not simple to evaluate since the hamiltonian does not have simple properties when it operates on the eigenstates of ϕ . Also the operator $e^{-\beta H}$ is not a simple

operator. To proceed we use the trick of Feynman and write

$$\{ -\beta H = \prod_{i=1}^N e^{-\beta H/N} = \prod_{i=1}^N (1 - \epsilon H) , \quad (10)$$

where

$$\epsilon = \beta/N , \quad (11)$$

and the limit $N \rightarrow \infty$ is to be taken after the product is evaluated.

The product of Eq. 10 may be simply represented by inserting states which alternate between eigenstates of the field operators ϕ and Π ,

$$\begin{aligned} \text{Tr } e^{-\beta H} &= \int (\prod_{i=1}^N d\phi_i d\Pi_i) \langle \phi_{N+1} | e^{-\epsilon H} | \Pi_N \rangle \\ &\quad \langle \Pi_1 | \phi_{N-1} \rangle \langle \phi_{N-1} | e^{-\epsilon H} | \Pi_{N-1} \rangle \cdots \\ &\quad \langle \phi_1 | e^{-\epsilon H} | \Pi_1 \rangle \langle \Pi_1 | \phi_1 \rangle . \end{aligned} \quad (12)$$

The overlap of states $\langle \Pi | \phi \rangle$ is

$$\langle \Pi | \phi \rangle = 1/2\pi e^{i\pi\phi} . \quad (13)$$

The product over the index j in Eq. 12 may be represented as a product of integrals evaluated at different times by making the identification

$$\epsilon = dt \quad (14)$$

$t = j\epsilon = j\beta/N$, so that the path integral becomes

$$\text{Tr } e^{-\beta H} = \int [d\phi d\dot{\phi}] e^{-\int dt d^3x \{ H(\Pi, \phi) - i\dot{\phi} \}} . \quad (15)$$

Notice that the field ϕ is periodic in the interval $0 < t <$

3. This periodicity follows from the trace of Eq. 1. The momenta Π are not required to be periodic. The measure of integration $[d\phi d\phi]$ involves a product over all spatial coordinates and time coordinates. A factor of $1/2\pi$ is included for each Π integration.

The physical interpretation of the Euclidian time variable which is an argument of both Π and ϕ is somewhat obscure. It has been introduced because the operator $e^{-\beta H}$ which appears in the expression may be interpreted as a time translation operator for imaginary time. This is plausible since e^{ith} is the time translation operator for ordinary time. The transformation from Minkowski space, corresponding to real time, to Euclidian space, corresponding to imaginary time, arises since taking $t \rightarrow it$ in scalar products such as $x_\mu x^\nu$ effectively converts the metric tensor from Minkowski to Euclidian. Insofar as $e^{-\beta H}$ translates in imaginary time, the states which contribute to the partition function are propagated through imaginary time by an amount β . These states propagate into themselves by virtue of the trace condition. Since the scalar field ϕ labels these states, ϕ must propagate into itself when propagated an imaginary, Euclidian time of β .

The imaginary Euclidian time must not be confused with real Minkowski time. Real Minkowski time translations are generated by e^{ith} and may operate on the fields which label the states which contribute to the partition function. Such time translations generate the real time response of a thermal system. The theory of this real time response is an immensely interesting and rich study. Of particular interest in this study is the theory of single particle excitations, a theory which closely parallels the theory of single particle excitations in the vacuum. An other interesting application of real time response theory is to the computation of the partition function. The partition function may be computed by real Minkowski time methods rather than by the imaginary time Euclidian methods which are presented here. The Minkowski computation is complicated, and to obtain correct results, the

derivation of the Minkowski space formulation must be carefully deduced from the Euclidian formulation. For lack of time, I shall not attempt to present the theory of real time response, or the Minkowski space method for computing the partition in these lectures.

The final simplification in the path integral representation for the thermodynamic potential comes from performing the integrations over the momentum Π . These integrations are easily done since they all are Gaussian. The effect of these integrations is to replace the momentum dependent terms in the path integral by $-\phi^2$, so that

$$\text{Tr } e^{-\beta H} = \int [d\phi] e^{-S[\phi]} , \quad (17)$$

where S is the Euclidian action,

$$S[\phi] = \int d^4x \left[\frac{1}{2} (a\phi)^2 + \frac{1}{2} m^2 \phi^2 + V(\phi) \right] . \quad (18)$$

the measure of integration in Eq. 16 is a product of $d\phi$'s and factors arising from the integrations over the Π 's,

$$[d\phi] = \prod_{i=1}^N d\phi_i(x) (2\pi)^{-1/2} . \quad (19)$$

In the previous derivation, we have been painstakingly careful to maintain the proper measure factors in the functional integrations. This is necessary since the thermodynamical potential depends in part upon these factors. Thermal expectation values do not since in the quantity

$$\langle O \rangle = \text{Tr } e^{-\beta H} O / \text{Tr } e^{-\beta H} , \quad (20)$$

where O is any operator, the measure factors involving "cancel between numerator and denominator. The contribution to the thermodynamical potential arising from interactions does not depend on these factors since

$$e^{-\beta V_{RI}} = \int [d\phi] e^{-S[\phi]} / \int [d\phi] e^{-S_0[\phi]} , \quad (21)$$

where

$$S_0[\phi] = \int d^4x \left\{ \frac{1}{2} (\partial\phi)^2 + \frac{1}{2} m^2\phi^2 \right\} . \quad (22)$$

The ideal gas contribution does depend on these measure factors, and we shall now derive the ideal gas contribution to the thermodynamical potential.

The ideal gas contribution may be derived using familiar standard arguments⁽¹⁾ This involves inserting inserting multi-particle momentum space eigenstates in the trace of Eq. 1 Since the occupation number of any eigenstate is an arbitrary integer n , and the probability of occupation of any state is $e^{-\beta E}$, the thermodynamical potential is

$$\Omega = -1/\beta V \ln \prod_{\vec{k}} \sum_{n=0}^{\infty} e^{-n\beta E} \\ = 1/\beta \int d^3k/(2\pi)^3 \ln (1 - e^{-\beta E}) . \quad (23)$$

An alternative derivation involves directly evaluating the functional integral representation for the thermodynamical potential⁽⁴⁾ This is easily done after Fourier transforming the fields

$$\Phi(\vec{x}, t) = \int d^3k/(2\pi)^3 e^{i\vec{k}\cdot\vec{x}} \bar{\Phi}(\vec{k}, t) . \quad (24)$$

The functional integral of Eq. 17 becomes

$$\text{Tr } e^{-\beta H} = \int \prod_{j=1}^N (d\bar{\Phi}_j / (2\pi\epsilon)^{-1/2}) \exp -\frac{1}{2} \sum_{j=1}^N \int d^3k/(2\pi)^3 \left\{ [\bar{\Phi}_j - \bar{\Phi}_{j-1}]^2 / \epsilon^2 \right. \\ \left. + \epsilon^2 \bar{\Phi}_j^2 \right\} \quad (25)$$

This product of integrals is simply a product of functional

integrals for elementary harmonic oscillators. If the endpoints in time are constrained by periodic boundary conditions, $\bar{\Phi}_N = \bar{\Phi}_1$, we find the integral for each oscillator corresponding to momentum \vec{k} as

$$I = \{ \epsilon E / \sinh(\beta E) \}^{1/2} \exp -\{ \bar{\Phi}_1^2 E (\cosh(\beta E) - 1) / \sinh(\beta E) \} . \quad (26)$$

The final integration over $\bar{\Phi}_1$ yields

$$\Omega = -1/\beta V \ln \text{Tr } e^{-\beta H} = \frac{1}{\beta} \int d^3k / (2\pi)^3 \ln 2\sinh(\beta E/2) , \quad (27)$$

and the thermodynamical potential becomes

$$\Omega = \frac{1}{\beta} \int d^3k / (2\pi)^3 \ln (1 - e^{-\beta E}) + \frac{1}{2} \int d^3k / (2\pi)^3 E . \quad (28)$$

This result agrees with the result of the direct analysis of Eq. 23 using elementary thermodynamics, except for the temperature independent contribution of

$$\Omega_{VAC} = \frac{1}{2} \int d^3k / (2\pi)^3 E . \quad (29)$$

This is the free energy of the vacuum of the vacuum and is divergent. It must be subtracted from the thermodynamical potential in order to obtain a finite result. This is sensible for physical systems since measurements are only made for the difference of pressures and energies of the system + vacuum and system. (Ignoring the effects of gravity.) Since this divergence is of order Λ^4 in an ultraviolet cutoff Λ , the computation of the thermodynamic potential must be carried out with great care. The finite contribution must be carefully isolated from the divergent contribution, and a sloppy job of carrying out this isolation will give incorrect results. The perturbative methods which we discuss in Lecture 9 are somewhat involved by the necessity of carefully subtracting the divergent thermodynamical potential of the vacuum.

LECTURE 2 : Free fermion field theory.

References:

- (1) Statistical Mechanics, L. D. Landau and E. M. Lifschitz, Addison Wesley Publishing Co. (1958) Reading Mass.
- (2) Quantum Mechanics and Path Integrals, R. P. Feynman and A. R. Hibbs, McGraw-Hill Book Co. (1965) New York.
- (3) C. Bernard, Phys. Rev. D9, 3312 (1974)

$$\{n(x, t), n(y, t)\} = \{n(x, t), n^*(y, t)\} = 0 \quad (1)$$

As shall soon be seen, the periodic boundary conditions in Euclidian time which arose for boson fields reappear here as anti-periodic boundary conditions. To understand these facts we must carefully analyze Eq. 1.1 using fermion "coherent states".

The Hamiltonian is assumed to be a function of fermion fields $\psi(x, t)$ and $\psi^*(x, t)$ which satisfy the equal time anti-commutation relations

$$\begin{aligned} \{\psi_\alpha(x, t), \psi_\beta(y, t)\} &= 0 \\ \{\psi_\alpha(x, t), \psi_\beta^*(y, t)\} &= \delta_{\alpha\beta} \delta(3)(x-y) \end{aligned} \quad (2)$$

The anti-commuting c-numbers anti-commute with these operators. These operators may be interpreted as creation and annihilation operators for fermions at the position x with spinor index α . The occupation numbers for these fermions are 0 and 1. This labeling of states is perhaps best defined if space is discretized on a spatial lattice. The occupation number basis states are labeled by a set of occupation numbers $n_\alpha(x)$ and may be written as

$$| \{n\} \rangle = | x, \alpha (\psi_\alpha^\dagger(x, t))^{n_\alpha(x, t)} | 0 \rangle \quad (3)$$

where $|0\rangle$ is the state of zero occupation number for all x . The

notation $\{n\}$ refers to the set of all occupation numbers $n_a(\vec{x})$.

A particular ordering for the product over coordinates must be chosen for this state since changing the ordering of field operators which appear in the product may change the phase of the state. Notice that the field operator $\psi_a(\vec{x}, t)$ operates on $|[n]\rangle$ and decreases $n_a(\vec{x})$ by one unit if $n_a(\vec{x}) = 1$, or sets the state to zero if $n_a(\vec{x}) = 0$. The phase of the state may change depending upon the occupation of other sites and the ordering chosen in Eq. 3. When $\psi_a^\dagger(\vec{x}, t)$ operates it increases the occupation number $n_a(\vec{x})$ by one unit unless $n_a(\vec{x}) = 1$. The phase may also change.

The thermodynamical potential may be evaluated in these basis states as

$$\text{Tr } e^{-\beta H} = \sum_{\{n\}} \langle \{n\} | e^{-\beta H} | \{n\} \rangle \quad (4)$$

This occupation basis representation for Eq. 1.1 does not give a simple representation. To find a simple representation, fermion "coherent states" may be introduced(1-2) These states are labeled by the anti-commuting c-numbers described above. The states are

$$|x\rangle = e^{-x\psi_a^\dagger} |0\rangle \quad (7)$$

$$\langle x^\dagger | = \langle 0 | e^{-\psi_a} \quad (8)$$

We shall use these states in complete sums over intermediate states. To do this a completeness relation is used

$$I = \int dx dx^\dagger |x\rangle \langle x^\dagger | \quad (9)$$

To verify this completeness relation, we use the rules of Grassmann variable integration. These rules are

$$\int dx = \int dx^\dagger = 0 \quad (10)$$

$$\int dx x = \int dx^\dagger x^\dagger = 1 \quad (11)$$

The integration in the completeness relation of Eq. 9 is computed by expanding the exponential in the integral and the exponentials in the definitions of the "coherent states"

$$\int dx^\dagger dx e^{xx^\dagger} |x\rangle \langle x^\dagger | = \int dx^\dagger dx (1 + xx^\dagger) (|0\rangle - x|1\rangle) \quad (12)$$

$$(\langle 0 | - \langle 1 | x^\dagger) = |0\rangle \langle 0 | + |1\rangle \langle 1 | = I \quad .$$

The thermodynamical potential may be represented in terms of these states as

$$\sum_{\{n\}} \langle \{n\} | e^{-\beta H} | \{n\} \rangle = \sum_{\{n\}} \int [dn] [dn^\dagger] [dn] \quad (13)$$

$$\langle n^\dagger | e^{-\beta H} | n \rangle \in \mathbb{R} \quad e^{\text{Re} \langle n^\dagger | n \rangle} < n^\dagger | n \rangle > .$$

The integration measure is a product over all spatial positions and spinor indices

$$[dn^\dagger] [dn] = \prod_{\vec{x}, \alpha} dn_\alpha^\dagger(\vec{x}) dn_\alpha(\vec{x}) \quad (14)$$

where $|0\rangle$ is the zero occupation number state. We have suppressed the time index on the fields and in this equation since the time may be chosen as $t=0$ in order to construct these states.

We now study the properties of the "coherent states" of Eq. 5. This study is facilitated by studying coherent states at one position and with one spinor index. The generalization of these results to a multi-site, spinor indexed state is straightforward and obvious. A single site, single indexed state and its conjugate are

Now recall that

$$\langle n | \chi \rangle \langle \chi^+ | n \rangle = \langle n | O \rangle \langle O | n \rangle + x \bar{x}^+ \langle n | 1 \rangle \langle 1 | n \rangle,$$

so that

$$\langle n | \chi \rangle \langle \bar{x}^+ | n \rangle = \langle -\bar{x}^+ | n \rangle \langle n | \chi \rangle$$

The thermodynamical potential becomes

$$\begin{aligned} \text{Tr } e^{-\beta H} &= \sum_{\{n\}} f [d\bar{n}^+] [dn] [d\bar{n}^+] \langle n^+ | e^{-\beta H} | \bar{n} \rangle \\ &\quad e^{n^+} \bar{e}^{\bar{n}^+} \langle -\bar{n}^+ | n \rangle \langle n | n \rangle. \end{aligned} \quad (17)$$

Upon using the identity

$$\begin{aligned} f [d\bar{n}^+] [dn] \langle \bar{n}^+ | -n \rangle &= \bar{n}^+ \bar{n}^+ e^{n^+} \bar{e}^{\bar{n}^+} f(n^+, \bar{n}) = \\ f(-n^+, n) &= n n^+ \end{aligned} \quad (18)$$

which may be proved by expanding f in a Taylor's series, using $n^2 = 0$, and the rules of Grassmann integration, we finally obtain

$$\text{Tr } e^{-\beta H} = f [d\bar{n}^+] [dn] \langle -n^+ | e^{-\beta H} | n \rangle \quad (19)$$

Notice that the left ket vector in this expression involves $-n^+$ and not n^+ . We shall soon see that this fact implies anti-periodic boundary conditions on fermion fields in the soon to be derived functional integral representation for the thermodynamical potential.

To derive this representation we must use the following properties of fermion "coherent states"

$$\psi_\alpha | \{n\} \rangle = \eta_\alpha | n \rangle \quad (20)$$

$$\langle \{n^+\} | \psi_d^\dagger = \langle \{n^+\} | n_d^\dagger \quad (21)$$

These states are used to construct a functional integral representation after the operator $e^{-\beta H}$ is written as a product

$$e^{-\beta H} = \prod_{i=1}^N e^{-\beta H/N} = \prod_{i=1}^N (1 - \epsilon H) \quad (22)$$

where

$$\epsilon = \beta/N. \quad (23)$$

and the limit $N \rightarrow \infty$ is to be taken. The product in Eq. 22 may be evaluated using the completeness relation of Eq. 12. We shall now drop the notation $\langle n \rangle$ and leave it as implicit that the state is labeled by values of n at all spatial coordinates.

$$\begin{aligned} \text{Tr } e^{-\beta H} &= f (\prod_{j=1}^N [d\bar{n}_j^\dagger] [dn_j]) \langle -n_j^\dagger | e^{-\beta H} | n_{j-1}^\dagger \rangle \\ &\quad \langle n_{j-1}^\dagger | e^{-\beta H} | n_{j-2} \rangle \langle n_{j-2}^\dagger | e^{-\beta H} | n_{j-3}^\dagger \dots \end{aligned} \quad (24)$$

The overlap of states $\langle n_i^\dagger | n_j \rangle$ is

$$\langle n_i^\dagger | n_j \rangle = e^{-n_j n_i^\dagger}. \quad (25)$$

The product over the index j may be represented as a product over integrals at different times by making the identifications

$$\epsilon = dt \quad (26)$$

$$t = j\epsilon = j\beta/N$$

Assuming that H is linear in ψ and ψ^\dagger , that is

$$H = \int d^3x d^3y \psi^+(x) O(x, y) \psi(y) \quad (27)$$

we may use the identity

$$\langle n_1^\dagger | H(\psi^\dagger, \psi) | n_j \rangle = H(n_1^\dagger, n_j) e^{-n_1^\dagger n_j}$$

For a free Dirac particle this is true since

$$H = \int d^3x \psi^\dagger(\vec{x}) \gamma^0(-i\vec{\gamma}^\dagger + \vec{m}) \psi(\vec{x}).$$

A little algebra yields the functional integral representation for the partition function as

$$\text{Tr } e^{-\beta H} = \int [dn^\dagger] [dn] e^{-\int_0^\beta dt \int d^3x \{ H(n_1^\dagger, n_1) - n_1^\dagger n_1 \}} \quad (30)$$

This representation may be put in a more familiar form upon identifying

$$\text{Tr } e^{-\beta H} = \int [d\psi^\dagger] [d\psi] e^{-\int_0^\beta dt \int d^3x \{ H(\psi^\dagger, \psi) - \psi^\dagger \psi \}} \quad (31)$$

where ψ and ψ^\dagger are "classical" Grassmann fields. We find

$$\text{Tr } e^{-\beta H} = \int [d\psi^\dagger] [d\psi] e^{-\int_0^\beta dt \int d^3x \{ H(\psi^\dagger, \psi) - \psi^\dagger \psi \}} \quad (32)$$

Upon identifying the Euclidian gamma matrix as

$$\gamma_E^0 = i\gamma_M^0$$

and introducing the Euclidian action for the Dirac field as

$$S = \int_0^\beta dt \int d^3x \bar{\psi}(\vec{x}, t) \{ -i\gamma^\dagger \cdot \partial + m \} \psi(\vec{x}, t), \quad (34)$$

we obtain

$$\text{Tr } e^{-\beta H} = \int [d\bar{\psi}] [\psi] e^{-S} \quad (35)$$

The field conjugate to ψ is $\bar{\psi}$ and $\bar{\psi}$ is

$$\bar{\psi} = \psi^\dagger \gamma_M^0 \quad (36)$$

with a Minkowski gamma matrix. The product in the integration measure when written in this manner simply means

$$[\bar{\psi} \bar{\psi}] = \Pi d\psi^\dagger d\psi \quad (37)$$

The fermion fields satisfy antiperiodic boundary conditions

$$\psi(\vec{x}, \beta) = -\psi(\vec{x}, 0) \quad (38)$$

These anti-periodic boundary conditions are different from the periodic boundary conditions derived in the previous lecture for the scalar field. Their origin, like the periodic boundary conditions for the scalar field, are in the trace for the definition of the partition function. The minus sign arises because of the peculiar commutation relations of the scalar products given by Eq. 16. This relation follows from the anti-commuting nature of fermion fields.

This functional is most easily evaluated by Fourier transforming to momentum space. The time Fourier transform involves a sum while the spatial Fourier transform involves a continuous integral. The functional integral for the thermodynamical potential becomes a product over ordinary Grassmann integrals as

$$\begin{aligned} \text{Tr } e^{-\beta H} &= \Pi_{p^0, \vec{p}}^0 \int d\psi^\dagger(p) d\psi(p) e^{-\psi^\dagger(p) \gamma^0(\vec{p}) \psi(p)} \\ &= \Pi_{p^0, \vec{p}}^0 e^{tr \ln \gamma^0(\vec{p}) \psi(p)} = \Pi_{p^0, \vec{p}}^0 e^{2i\ln(p^2+m^2)} \\ &= e^{i p \cdot 2i\ln(p^2+m^2)} = e^{2V \int_{p^0} \int d^3p / (2\pi)^3 \ln(p^2+m^2)} \end{aligned} \quad (40)$$

The momentum p^0 which occurs in this sum is a sum over

$$p^0 = 2\pi(j+1/2)/\beta \quad (41)$$

which arises as a consequence of the anti-periodic boundary conditions on the fermion fields.

The sum which results from this integration is divergent, but the divergence gives a temperature independent contribution to the thermodynamical potential and is therefore a part of the unphysical vacuum energy. The sum is easily evaluated for the temperature dependent pieces, with the result

$$\Omega = -4/\beta \int d^3p/(2\pi)^3 \ln(1+e^{-\beta E}) \quad (42)$$

This result is the same which results from directly inserting momentum space eigenstates into Eq. 1(3),

$$\Omega = -4/\beta \int p \ln(1+e^{-\beta E}) = -4/\beta \int d^3p/(2\pi)^3 \ln(1+e^{-\beta E}) \quad (43)$$

The results of the preceding paragraphs are easily generalized to the case where there is a chemical potential corresponding to a finite fermion number density. The partition function is

$$e^{-\beta V\Omega} = \text{Tr } e^{-\beta H + \mu N} \quad (44)$$

This corresponds to adding

$$-\mu\psi + \bar{\psi}$$

to the Hamiltonian, and results in the modified Euclidian action

$$S = \int_0^\beta dt \int d^3x \bar{\psi}[-i\gamma^a - i\mu\gamma^0 + m]\psi \quad (46)$$

A direct analysis which parallels that described in detail above gives

$$\Omega = -2/\beta \int d^3p/(2\pi)^3 \{ \ln(1+e^{-\beta(E-\mu)}) + \ln(1+e^{-\beta(E+\mu)}) \} \quad (47)$$

The contributions corresponding to positive and negative values of μ arise from particles and anti-particles.

References:

- (1) M. B. Halpern, A. Jevicki, and P. Senjanovic, Phys. Rev. D16, 2474, (1977)
- (2) D. E. Soper, Phys. Rev. D18, 4590, (1978)
- (3) Statistical Physics, L. D. Landau and E. M. Lifschitz, Addison-Wesley Publishing Co. (1958)

Lecture 3: Gauge Theories: QED and QCD

The thermodynamics of gauge theories such as QED and QCD are slightly more complicated than that of theories such as scalar field theory or free fermion field theory. We shall consider QED in some detail in this lecture, and shall generalize the results we find to more complicated gauge theories such as QCD. The results of this analysis are easily generalized to non-abelian gauge theories with scalar fields and spontaneous symmetry breaking such as GUTs.

To understand the problems which arise when gauge theories are studied, we consider the thermodynamics of a photon field. The action for the photon system is

$$S = \int_0^B dt \int d^3x \frac{1}{4} F_{\mu\nu} F^{\mu\nu} \quad (1)$$

where

$$F^{\mu\nu} = \partial^\mu A^\nu - \partial^\nu A^\mu \quad (2)$$

The metric is Euclidian in these equations. This theory is easily quantized in the axial gauge

$$A^3 = 0. \quad (3)$$

The Hamiltonian for this theory is

$$H = \frac{1}{2} \int d^3x (\vec{E}^2 + \vec{B}^2) \quad (4)$$

Since the Gauss's Law constraint

$$\vec{v} \cdot \vec{E} = 0 \quad (5)$$

has the solution

$$E_3 = -1/\partial_3 \vec{v}_\perp \cdot \vec{E}_\perp \quad (6)$$

The Hamiltonian may be expressed entirely in terms of the independent dynamical fields \vec{E}_\perp and \vec{B} as

$$H = \frac{1}{2} \int d^3x (\vec{E}_\perp^2 + \vec{B}^2 + \vec{v}_\perp \cdot \vec{E}_\perp (-\partial_3)^{-2} \vec{v}_\perp \cdot \vec{E}_\perp) . \quad (7)$$

These independent fields satisfy the equal-time commutation relations

$$[E_\perp^i(\vec{x}, t), E_\perp^j(\vec{y}, t)] = [A_\perp^i(\vec{x}, t), A_\perp^j(\vec{y}, t)] = 0 \quad (8)$$

$$[E_\perp^i(\vec{x}, t), A_1^j(\vec{y}, t)] = \delta_{ij} \delta^{(3)}(\vec{x} - \vec{y})$$

The equations of motion for this system follow from Eqs. 7-8 together with the Gauss's Law constraint when Hamilton's equations are computed.

The thermodynamics of this system is that of a free scalar boson with two degrees of freedom. The thermodynamic potential is

$$e^{-\beta V\Omega} = 2/\beta \int d^3p/(2\pi)^3 \ln(1-e^{-\beta E}) \quad (9)$$

This result arises from the functional integral representation

$$e^{-\beta V\Omega} = \int [dE_\perp dA_1] e^{-\int_0^B dt \int d^3x (H(E_\perp, A_1) + iE_1 \cdot \dot{A}_1)} \quad (10)$$

The Gauss's Law constraint may be explicitly used to rewrite Eq. 10 as

$$e^{-\beta V\Omega} = \int [d\vec{E} d\vec{A} dA^0] \delta(A^3) e^{-\int_0^B dt \int d^3x \{ 1/2(\vec{E}^2 + \vec{B}^2) + i\vec{E} \cdot \dot{\vec{A}} + iA^0 \vec{v} \cdot \vec{E} \}} \quad (11)$$

The integrations over \vec{E} may be performed to obtain

$$e^{-\beta V_0} = \int [dA] \delta(A^3) e^{-S[A]} \quad (12)$$

and the functional integral may be performed to find

$$e^{-\beta V_0} = \det^{-1} -\square = e^{-\text{tr} \ln (-\square)} \quad (13)$$

To verify this result, recall that a Gaussian functional integral of the form $\int [d\phi] e^{-\phi O \phi}$ where O is any operator may be evaluated in a basis where the operator O is diagonal. In this basis, the functional integral factorizes into a product of functional integrals, $\prod_i \int [d\phi_i] e^{-\lambda_i \phi_i^2}$ where λ_i are the eigenvalues of O and ϕ_i are the eigenfunctions of O . This functional integral is, up to a normalization constant, the product of the inverse square roots of the eigenvalues of O . The gaussian functional integral is therefore, up to a normalization constant, $\det^{-1/2} O$. The normalization constant for this functional integral may be shown to be independent of the temperature. For the functional integral Eqn. 12, there are integrations over two independent boson fields and each is of the form $\int [d\phi] e^{-\phi(-\square)\phi}$ and the result of Eqn. 13 follows directly.

The thermodynamical potential for this system follows from using Eqn. 13. Inserting a complete set of momentum eigenstates of the operator $-\square$ which satisfy periodic boundary conditions in imaginary time, and performing the summation the discrete frequencies which arise from the Fourier series which arises for the imaginary time variable, we find, up to a temperature independent constant,

$$\Omega = 2/\beta \int d^3 p / (2\pi)^3 \ln (1-e^{-\theta E}) \quad (14)$$

The steps in this computation closely the more detailed derivation presented in Lecture 1, and the details are left to the reader. Notice that this contribution to the thermodynamic

potential is a factor of two larger than that for a system of a single free scalar meson. This is a result which is believable on physical grounds since the thermodynamics of a photon gas involves a degeneracy factor arising from two helicity degrees of freedom.

A problem arises if we consider the photon gas in Feynman gauge (1). The Euclidian action for electrodynamics in this gauge is

$$S = 1/2 \int_0^\beta dt \int d^3x A^\mu \partial_\mu A_\nu \quad (15)$$

Proceeding naively, the path integral representation for the thermodynamical potential is (1)

$$e^{-\beta V_0} = \int [dA] e^{-S[A]} = \det^{-2} -\square \quad (16)$$

and we arrive at the wrong conclusion that the thermodynamics of the photon field involves 4 degrees of freedom.

The problem with this Feynman gauge analysis is that the formula given by Eq. 16 is simply incorrect. The proper result arises from carefully quantizing the theory, writing the Hamiltonian path integral, and then deriving the action path integral by integrating out the electric fields. This was what was done for axial gauge and the path integral of Eq. 11 is a correct result.

The representation of Eq. 11 may be generalized to an arbitrary gauge such as Feynman gauge. To do this, notice that the gauge condition

$$A^3 = 0 \quad (17)$$

may be transformed in Eq. 11 by making the change of variables

$$A^\mu \rightarrow A^\mu + \partial^\mu \Lambda \quad (18)$$

This change of variables corresponds to a change of gauge.

To obtain a proper expression, the Jacobian of the variable transformation

$$\mathcal{J} = \det \delta A^{\mu}/\delta A^{\nu}$$

must be included.

To derive an expression which is valid in an arbitrary gauge, we first express the gauge condition as a constraint of the form (2)

$$F(\Lambda) = 0$$

If we write the functional integral for the partition function as

$$e^{-\beta V\Omega} = \int [dA] \delta(F(A)) e^{-S[A]} \quad (21)$$

we obtain a result which reduces to Eq. 11 in axial gauge. Unfortunately this expression is not gauge invariant. To obtain a gauge invariant expression we must include a factor which cancels the Jacobian of a change of variables corresponding to a gauge transformation. Such a factor modifies Eq. 21 to (2)

$$e^{-\beta V\Omega} = \int [dA] \det \delta F/\delta \Lambda \delta(F) e^{-S[A]} \quad (22)$$

The functional differentiation in this expression is that with respect to a gauge transformation generated by Λ . For axial gauge this factor is

$$\det \delta F/\delta \Lambda = \det \partial_3 \quad (23)$$

and gives a contribution only to the vacuum energy of the theory since

$$\det \partial_3 = e^{8V} d^3 p / (2\pi)^3 \ln P_3 \quad (24)$$

Since the expression of Eq. 22 is gauge invariant, we may

write down an expression which corresponds to Feynman gauge. We let the gauge condition be

$$\partial A = f \quad (19)$$

so that

$$e^{-\beta V\Omega} = \int [dA] \det \delta F/\delta \Lambda \delta(\partial A - f) e^{-S[A]} \quad (26)$$

Since a gauge transformation induces

$$A \rightarrow A + \partial \Lambda \quad (27)$$

the factor $\det \delta F/\delta \Lambda$ is

$$\det \delta F/\delta \Lambda = \det -\square \quad (28)$$

Moreover, the integral given by Eq. 26 is independent of f and integrating over gives only a contribution to the vacuum energy, so that we can compute the finite temperature contribution to Ω as

$$e^{-\beta V\Omega} = \int [dA] [\delta F] \det -\square \delta(\partial A - f) e^{-1/2\alpha^2 e^{-S[A]}} \quad (29)$$

The integral over f yields

$$e^{-\beta V\Omega} = \int [dA] \det -\square e^{-S[A]} - \int (\partial A)^2 / 2\alpha \quad (30)$$

For $\alpha = 1$, the Feynman gauge functional is reproduced except for an extra factor of $\det -\square$. Performing the integrations over the photon field gives

$$\Omega = -1/8V \ln (\det -\square \det -\square) = 1/8V \ln \det -\square \quad (31)$$

a result which corresponds to the correct number of degrees of freedom. The purpose of the "Faddeev-Popov" determinant is

solely to cancel unphysical degrees of freedom and produce a thermodynamical potential with two degrees of freedom.

The results of the preceding paragraphs are easily generalized to the case of a Yang-Mills gas of gluons. The action for this theory is

$$S = 1/4 \int_0^{\beta} dt \int d^3x F_a^{\mu\nu}(x) F_{\mu\nu}^a(x) \quad (32)$$

where

$$F_a^{\mu\nu}(x) = \partial^{\mu}A_a^{\nu} - \partial^{\nu}A_a^{\mu} + g f^{abc} A_b^{\mu} A_c^{\nu} \quad (33)$$

Manipulations which parallel those for a photon gas yield a functional integral for the partition function as

$$e^{-\beta V_R} = \int [dA] \det \delta F/\delta A \delta(F) e^{-S[A]} \quad (34)$$

Since the steps in this derivation closely follow those outlined above, the derivation of this result is left as an exercise. The essential difference between a photon and a gluon gas as far as gauge fixing is concerned is that the determinant in Eq. 23 depends upon the gluon field strength, at least for gauges such as Feynman gauge. In fact, for Feynman gauge this determinant is

$$\det \delta F/\delta A = \det M \quad (35)$$

where

$$M^{ab} = -\square \delta^{ab} + g f^{abc} \partial^{\mu} A_b^{\nu} A_c^{\mu} \quad (36)$$

This fact follows from performing an infinitesimal version of the gauge transformation

$$-i\partial^{\mu} - g A_a^{\mu} \tau^a + U(\Lambda) (-i\partial^{\mu} - g A_a^{\mu} \tau^a) U(\Lambda)^{-1} \quad (37)$$

with

$$U(\Lambda) = e^{i\tau^a \Lambda} \quad (38)$$

This infinitesimal transformation is

$$A_a^{\mu} \rightarrow A_a^{\mu} + \partial^{\mu} \Lambda_a + g f^{abc} A_b^{\mu} \Lambda_c \quad (39)$$

The fact that this determinant depends upon the gluon field means that the presence of this Faddeev-Popov determinant will modify the Feynman rules of the theory. (2)

The Faddeev-Popov determinant may be recast as an integral over anti-commuting c-number pseudo-fermion fields using the identity

$$\det M = \int [d\bar{u}] [du] e^{\bar{u} \cdot M \cdot u} \quad (40)$$

The partition function becomes

$$\begin{aligned} e^{-\beta V_R} &= \int [dA] [d\bar{u}] [du] e^{-S[A, \bar{u}, u]} \\ &= \int [dA] [d\bar{u}] [du] e^{-S[A] - \bar{u} \cdot M \cdot u} \end{aligned} \quad (41)$$

Since the determinant arose from variations of functions which satisfy periodic boundary conditions, the pseudo-fermion fields satisfy periodic conditions

$$\bar{u}(\vec{x}, \beta) = \bar{u}(\vec{x}, 0) \quad (42)$$

$u(\vec{x}, \beta) = u(\vec{x}, 0)$

This is necessary since the determinant which arises from the integration over the fermion fields must generate Bose-Einstein distribution functions, and this is generated from the determinant of an operator satisfying periodic boundary conditions.

In later lectures we shall consider the perturbative expansion of the Yang-Mills thermodynamical potential. In this expansion, the pseudo-fermions ghost fields will play an essential role.

The essential between QCD and QED is that in the properly defined functional integral for the thermodynamical, appropriate to a fixed gauge, ghost fields appear, which form a representation for the determinant which was necessary to make the result for the thermodynamical potential gauge independent. Such a representation for the determinant might also have been introduced for QED, since a determinant appeared there also. In QED, however, this determinant would be trivial and would not depend upon the photon field. In QCD, the determinant depends upon the gluon field and may not be directly evaluated in closed form. It may only be represented by a ghost functional integral which may be systematically evaluated in a weak coupling expansion in powers of g . The non-trivial nature of the determinant in QCD arises from the interweaving of gauge invariance and gluon self interactions. In QED, even when charged fermions are included, no ghost fields appear. This is a consequence of the trivial nature of gauge transformations of fermion fields. The measure of functional integration for fermion fields is gauge invariant, and, most important, the fermion fields are unconstrained by all used gauge fixing conditions. The same applies to Yang-Mills

theories when fermions are included. Fermions do not affect the Faddeev-Popov ghost fields introduced to properly implement a functional integral representation for the thermodynamic potential in a fixed gauge.

References:

- (1) C. W. Bernard, Phys. Rev. D9, 3312, (1974)
- (2) L. Faddev and V. Popov, Phys. Lett. 25B, 29 (1967)

Lecture 4: Confinement and the Center Symmetry

The conjecture that hadronic matter at finite baryon number density and temperature might radically change its properties and perhaps undergo a series of phase transitions at sufficiently high energy densities has its origins in extremely simple pictures of hadrons as composites of quarks and gluons. At some energy density, hadrons will on the average overlap with nearby hadrons. The quarks are no longer confined to individual hadrons and may begin to freely wander unconfined through hadronic matter. This effect might be signalled as a true phase change in the system or, at least, as a dramatic change in the properties of the hadronic matter. As a consequence of these changes in hadronic matter, a variety of other dramatic changes, perhaps phase changes such as chiral symmetry restoration, may take place. The energy density where these changes may take place should be of the order of that inside a proton

$$\rho = \frac{M}{4/3 \pi r^3} \quad (1)$$

where M is the proton mass and r is the proton radius which is taken here as the r.m.s. charge radius. This energy is only a few times that of nuclear matter,

$$\rho_{\text{NM}} = 150 \text{ Mev/Fm}^3 \quad (3)$$

These dramatic changes in the properties of hadronic matter might occur in the cores of neutron stars, $\rho \sim 10-20 \rho_{\text{NM}}$, in ultra-relativistic heavy ion collisions, $\rho \sim 10-200 \rho_{\text{NM}}$, and almost certainly occurred in the early universe.

Examples of dramatic changes which might take place other than that of deconfinement are restoration of chiral symmetry and, at low temperatures and high baryon number density, superconductivity. Chiral symmetry is a symmetry of the QCD equations of motion which if realized would require either that all baryons be massless or occur in parity doublets. This

symmetry is broken at zero temperature and baryon number density. The pion becomes massless as a consequence of this symmetry breaking. Such a symmetry might become restored at an energy roughly that given by Eq. 1. At small temperatures, liberated quarks in high density matter might bind into a variety of Cooper to produce a superconductor or superfluid. At energy densities far above the energy of these rapid changes in the properties of hadronic matter, hadronic matter very probably becomes an almost ideal gas of quarks and gluons. This conjecture follows from the asymptotic freedom of QCD. At short distances, the effective strength of quark-gluon interactions is weak. At high energy densities, quarks and gluons interact most often at short distances, and the effect of these "weak" interactions should be small compared to the effects of free particle propagation. This should be true for the free energy which measures the bulk properties of quark-gluon matter. There may be small non-perturbative contributions arising from long distance interactions, but the dominant effects should be those of an ideal gas. Some quantities may, of course, be sensitive to non-perturbative effects, for example, the long distance behaviour of correlations.

In later lectures, we shall return to the issue of asymptotic freedom and the perturbation theory of the quark-gluon plasma. The remainder of this lecture is a discussion of the confinement-deconfinement "phase transition". (1-9) The words "phase transition" are in quotation marks because there may not be a true phase transition in the system in the statistical mechanical sense that there are discontinuities in the thermodynamical potential or its derivatives. The dramatic change in the properties of hadronic matter which are expected for high energy density hadronic matter will in the remainder of these lectures be sloppily referred to as a phase transition for lack of a better phrase. The chiral phase transition will be described in the next lecture.

The confinement-deconfinement phase transition is clearly illustrated in an $SU(N)$ Yang-Mills theory without dynamical

quarks. For such a theory, this phase transition is a transition in the strict statistical mechanical sense. The word dynamical quark means a quark which interacts with the gluons and contributes to the thermodynamical potential. We shall allow the introduction of non-dynamical static test quarks which probe the dynamics of the gluon matter, but these probes are not allowed to affect the gluon dynamics.

A static test quark placed in the vacuum of such a Yang-Mills system has infinite energy and is confined. In very high energy density hadronic matter, this quark is not confined and has finite free energy. The confinement-deconfinement phase transition occurs when this free energy becomes finite. The free energy difference of a system with a dynamical quark at position r and a system with no dynamical quark will soon be shown to be given as a thermal expectation value of a spatially local operator $L(r)$,

$$e^{-\beta F_q} = \langle L \rangle \quad (3)$$

The operator L is an order parameter for a confinement-deconfinement phase transition since

$$\begin{aligned} \langle L \rangle &= 0 \iff \text{Confinement} \\ \langle L \rangle &\neq 0 \iff \text{Deconfinement} \end{aligned} \quad (4)$$

At low energy densities, $\langle L \rangle$ should be zero for a finite temperature range $0 \leq T \leq T_c$ and is finite for $T \geq T_c$. When dynamical fermions are included in the grand canonical ensemble of a Yang-Mills theory, the free energy of an isolated static test quark is no longer a useful parameter to characterize confinement. Light dynamical fermions may form a bound state with this test quark and the free energy is finite. The order parameter $\langle L \rangle$ is finite for all temperatures, and there is no longer a yes-no signal for a phase transition. Several possibilities arise as a consequence of this fact.

There might be some discontinuity in $\langle L \rangle$ or its derivatives and this might signal a phase transition. There may be another as yet undiscovered order parameter which characterizes a transition. Finally, as suggested by strong coupling lattice gauge theory results, there may be no phase transition. We shall discuss these possibilities in more detail later in this lecture.

To more fully understand the dynamics of confinement, we shall study the operator L in more detail. To compute the free energy of a configuration of static quarks and anti-quarks, we introduce the operators $\psi_a(\vec{r}_i, t)$ and $\psi_a^\dagger(\vec{r}_i, t)$ which create and annihilate static quarks of color a at position \vec{r} and time t , along with their charge conjugate fields ψ^c and $\psi^{c\dagger}$ for anti-quarks. These fields satisfy the equal time anti-commutation relation

$$\{\psi_a(\vec{r}_i, t), \psi_b^\dagger(\vec{r}_j, t)\} = \{\psi_a^c(\vec{r}_i, t), \psi_b^{c\dagger}(\vec{r}_j, t)\} = \delta_{ab} \delta_{ij} \quad (5)$$

with all other equal time anti-commuters set to zero.

The quark fields obey the static time evolution equation

$$(i/\partial_t - \tau A^0(\vec{r}_i, t)) \psi(\vec{r}_i, t) = 0 \quad (6)$$

so that

$$\psi(\vec{r}, t) = T \exp\left[i \int_0^t dt' \tau A^0(\vec{r}, t')\right] \psi(\vec{r}, 0) \quad (7)$$

The symbol T in this expression denotes time ordered exponential.

The operators ψ and ψ^c may be employed to obtain an expression for the free energy of a configuration of N_q quarks and $N_{\bar{q}}$ anti-quarks. This is given by

$$e^{-\beta F(\vec{r}_1, \dots, \vec{r}_{N_q}, \vec{r}_1', \dots, \vec{r}_{N_{\bar{q}}})} = \frac{1}{N_q N_{\bar{q}}} \sum_s \langle s | e^{-\beta H} | s \rangle \quad (8)$$

with the summation indicated over all states $|s\rangle$ with heavy quarks at $\vec{r}_1, \dots, \vec{r}_{N_q}$ and heavy anti-quarks at $\vec{r}_1', \dots, \vec{r}_{N_{\bar{q}}}'$. The

factors of N are to cancel the degeneracy factors on the summation introduced by the color labels of the static quarks. Introducing the quark fields gives this free energy as

$$e^{-\beta F_{N_q N_{\bar{q}}}^0} = 1/(N_q N_{\bar{q}}) \sum_s \langle s' | \psi_a, b \psi_{a1}(\vec{r}_1, 0) \dots$$

$$\begin{aligned} & \psi_{aN_q}(\vec{r}_{N_q}, 0) \psi_{b1}(\vec{r}_1, 0) \dots \psi_{bN_{\bar{q}}}(\vec{r}_{N_{\bar{q}}}, 0) e^{-\beta H} \\ & \psi_{bN_{\bar{q}}}^{c\dagger}(\vec{r}_{N_{\bar{q}}}, 0) \dots \psi_{b1}^{c\dagger}(\vec{r}_1, 0) \psi_{aN_q}^\dagger(\vec{r}_{N_q}, 0) \dots \\ & \psi_{a1}^\dagger(\vec{r}_1, 0) |s'\rangle \end{aligned} \quad (9)$$

where now the sum is over all states $|s'\rangle$ with no heavy quarks. Since $e^{-\beta H}$ generates Euclidian time translations, i.e.,

$$e^{\beta H} O(t) e^{-\beta H} = O(t + \beta) \quad (10)$$

for any operator $O(t)$, Eq. 9 becomes

$$e^{-\beta F_{N_q N_{\bar{q}}}^0} = 1/(N_q N_{\bar{q}}) \sum_s e^{-\beta H} \psi_1(\beta) \psi_1^\dagger(\beta) \psi_{N_q}(\beta) \psi_{N_{\bar{q}}}^\dagger(\beta) \quad (11)$$

Using Eq. 7 and its charge conjugate, together with Eq. 5, and introducing the Wilson line as

$$L(\vec{r}) = 1/N \operatorname{tr} T \exp(i \int_0^\beta dt \tau A^0(\vec{r}, t)) \quad (12)$$

the free energy is

$$e^{-\beta F_{N_q N_{\bar{q}}}^0} = \langle L(\vec{r}_1) \dots L(\vec{r}_{N_q}) L(\vec{r}_1') \dots L(\vec{r}_{N_{\bar{q}}}') \rangle \quad (13)$$

The free energy of an isolated test quark is given by

$$e^{-\beta F_Q} = \langle L(\vec{r}) \rangle \quad (14)$$

As argued above, $\langle L \rangle = 0$ in the deconfined phase of QCD. This fact implies a singular long distance potential for a quark anti-quark pair. The free energy of such a pair is given by

$$e^{-\beta F(\vec{r}_1, \vec{r}_2)} = \langle L(\vec{r}_1) L^\dagger(\vec{r}_2) \rangle \quad (15)$$

If $|\vec{r}_1 - \vec{r}_2|$ is large, this expectation value clusters into

$$\lim |\vec{r}_1 - \vec{r}_2| \rightarrow \infty e^{-\beta F(\vec{r}_1, \vec{r}_2)} = \langle L(0) \rangle^2 \quad (16)$$

In the confined phase, $\langle L \rangle = 0$, and the long distance force is singular. Assuming exponential fall off in correlations of Wilson lines at large separations gives a linear quark anti-quark potential.

The issue of the existence of a confinement-deconfinement phase transition may be reformulated as the issue of whether a global, dynamical Z_N symmetry of gluon interactions is broken or realized. This global symmetry is an invariance of the finite temperature QCD action under gauge transformations which have periodic logarithmic time derivatives at $t=0$ and $t=\beta$, and are periodic up to an element of the center of the gauge group,

$$U(\vec{r}, \beta) = C_N^j U(\vec{r}, 0) \quad (17)$$

$$U^{-1}(\vec{r}, \beta) \frac{d}{dt} U(\vec{r}, t) |_{t=\beta} = U^{-1}(\vec{r}, 0) \frac{d}{dt} U(\vec{r}, t) \quad (18)$$

and the center element is

$$C_N^j = e^{2\pi i j/N} \quad (19)$$

Under such a transformation

$$L(\vec{r}) \rightarrow e^{2\pi i j/N} L(\vec{r}) \quad (20)$$

The periodic boundary conditions on the gluon fields are maintained by this transformation.

The elements of the center of a group are those elements which commute with all the elements of the group. Since all the elements of an $SU(n)$ gauge group have unit determinant, and may be represented by $N \times N$ matrices, the most general center element is $e^{2\pi i j/N}$. The essential ingredient which insures that the transformations of Eqs. 17-19 are symmetries of the Yang-Mills action is the fact that a center element commutes with all the elements of the group. This fact allows the gauge transformations of these equations to maintain the periodic boundary on the gluon fields. These periodic boundary conditions arise as a consequence of the trace in the definition of the thermodynamic potential. The fact that Eqs. 17-19 are gauge transformations is sufficient for the action to be invariant under such a transformation. This discrete symmetry of the Yang-Mills action plus boundary conditions will have dramatic consequences, but a simple physical picture of the dynamical origin of the symmetry is unknown.

If this symmetry is dynamically realized, the free energy of any N -ality non-singlet configuration of quarks and gluons is divergent since

$$e^{-\beta F_{NQ\bar{N}Q}} + e^{-2\pi i j(N_Q - N_{\bar{Q}})} e^{-\beta F_{NQ\bar{N}Q}} \quad (21)$$

implies either

$$e^{-\beta F_{NQ\bar{N}Q}} = 0 \quad (22)$$

or

$$N_Q - N_{\bar{Q}} = IN \quad (23)$$

where I is some integer. If this symmetry is spontaneously broken, N -ality non-singlet configurations of quarks may have finite free energy.

The expectation value of the Wilson line will tend to an element of the center of the gauge group at high enough

temperatures, since the gluon field configurations will tend to gauge transformations of zero field strength. Put another way, the free energy of an isolated quark becomes small, so long as an ultra-violet cut-off is imposed or self-energies are removed, so that $L \rightarrow 1$. The Z_N symmetry allows all possible values so that in the deconfined phase, $\langle L \rangle$ becomes frozen into one of the center elements.

Nathan Weiss proposed that the confinement-deconfinement transition might be understood as a condensation of Z_N domains as measured by L . (10) In different domains, $\langle L \rangle$ is close to different elements of the center. The confined phase of QCD corresponds to a condensate of domains, and $\langle L \rangle = 0$. In the deconfined phase, the system is in one domain and $\langle L \rangle = 0$. This scenario of Weiss has been elaborated and developed by Svetitsky and Yaffe, who provide plausible arguments for the order of the confinement-deconfinement phase transition in $SU(N)$ non-abelian gauge theories. (11) Their argument proceeds by postulating that all the degrees of freedom of an $SU(N)$ gauge theory may be integrated out of the functional integral for the thermodynamical potential except for those degrees of freedom corresponding to a Wilson line. The result of this integration yields a three dimensional gauge theory with enough degrees of freedom to properly describe confinement-deconfinement phase transitions, and with the coupling constant replaced as $g \rightarrow g(T)$. Since the path integral representation for this theory is of the form

$$e^{-\beta V(R)} = \sum_{Z_N \text{ spin values}} e^{-H(Z_N \text{ spins})/g(T)^2} \quad (24)$$

the system of interest is the same universality class as a 3 dimensional classical spin system with a Z_N symmetry and effective temperature

$$T_{\text{eff}} = g^2(T) \quad (25)$$

The origin of this relation arises in the path integral

representation for the thermodynamical potential. This path integral involves a sum over gluon field configurations, weighted by an exponential of the action S . The strength of this action is proportional to $1/g^2$, so that if the fields are all rescaled by $1/g$, the sum is weighted by S/g^2 . The sum over fields weighted by e^{-S/g^2} may be interpreted as a partition function for a classical field theory with temperature $1/g^2$. It is plausible that this effective temperature for the classical field theory becomes temperature dependent when the high frequency contributions to the sum over fields is carried out. The temperature dependence is a consequence of regulating singularities in the sum over fields. The physical origin of this temperature dependence is that the effective interaction strength which controls the sum should depend upon temperature since as the temperature varies, the average separation between the constituents of the thermal system varies. High temperature corresponds to small separation and weak coupling, and low temperature corresponds to large separation and stronger coupling.

Since the Wilson line is a spin variable, the question of confinement or deconfinement is equivalent to whether the system is demagnetized or magnetized. At high effective temperatures we expect confinement and at low effective temperatures we expect deconfinement. Since asymptotic freedom requires that physical temperatures increase as effective temperatures decrease, we have the proper phenomenology of the confinement-deconfinement phase transition.

For $SU(2)$ Yang-Mills theories, the 3 dimensional spin system is the Ising model, which has a second order phase transition. The corresponding system for $SU(3)$ is the 3-state Potts model which has a first order phase transition. The predictions of this crude model are in accord with results of Monte-Carlo simulations of the properties of finite temperature $SU(N)$ gauge theories, results which will be studied in later lectures.

When fermions in the fundamental representation of the gauge

group are introduced into an $SU(N)$ gauge theory, the action becomes

$$S = S_{\text{glue}} + S_{\text{quarks}}$$

where

$$\text{Squarks} = \int_0^\beta dt \int d^3x \bar{\psi}(x) \left\{ \frac{1}{4} \partial_\mu \partial_\nu + m \right\} \psi(x) \quad (27)$$

the center symmetry is explicitly broken. Under a Z_N gauge transformation

$$\psi(\vec{r}, \beta) \rightarrow U(\vec{r}, \beta) \psi(\vec{r}, \beta) = C_N^j U(\vec{r}, \beta) \psi(\vec{r}, \beta) = -C_N^j U(\vec{r}, \beta) \psi(\vec{r}, \beta) \quad (28)$$

and the anti-periodic boundary conditions on the fermion fields are not maintained. This symmetry breaking may be thought of as arising from an effective magnetic field which breaks the symmetry. (12-14) Since large mass fermions should have little effect on the dynamics at temperatures much below the fermion mass scale, we can imagine that the $m \rightarrow \infty$ limit corresponds to $B \rightarrow 0$. We will see how this works more explicitly when finite temperature Yang-Mills theories are formulated on the lattice and effective 3-dimensional systems are considered as models of finite temperature and baryon density theories.

Since an arbitrarily small external magnetic field destroys the magnetization transition in the Ising model, we expect that fermions may destroy the confinement-deconfinement transition in $SU(2)$ Yang-Mills theory. The reason that this occurs is that the magnetization is no longer an order parameter, and there is no longer any characteristic difference between what were once the magnetized and unmagnetized phases. There should still be rapid changes in the properties of the Ising system near the Curie temperature so long as the magnetic field is small. The situation is much more complicated for the $SU(3)$ theory.

Since the phase transition is first order, a small perturbation will not remove the transition. Almost certainly for sufficiently large numbers of zero mass fermions the phase transition disappears. For the masses of fermions in QCD the situation is not clear, and much work on this issue will be done over the next few years which will hopefully clarify the problem. The difficulty is of course that including fermions in Monte-Carlo computations is very difficult, and progress may therefore be slow. It is known that in strong coupling, the phase transition disappears at a finite value of the quark mass and there is indication from a Monte-Carlo computation that this is the case. (14) There is as yet no information on how these results extend to the continuum limit.

References:

- (1) J. C. Collins and M. J. Perry, Phys. Rev. Lett. 34, 1353 (1975)
- (2) M. Kislinger and P. Morley, Phys. Rev. D13, 1130 and 1147 (1976)
- (3) B. Freedman and L. McLerran, Phys. Rev. D16, 1130, 1147, and 1169 (1977)
- (4) J. Kapusta, Nucl. Phys. B148, 461 (1978)
- (5) A. M. Polyakov, Phys. Lett. 72B, 477 (1978)
- (6) L. Susskind, Phys. Rev. D20, 2610 (1979)
- (7) L. McLerran and B. Svetitsky, Phys. Lett. 98B, 195 (1981); Phys. Rev. D24, 450 (1981)
- (8) J. Kuti, J. Polonyi, and K. Szlachanyi, Phys. Lett. 98B, 199 (1981)
- (9) J. Engels, F. Karsch, H. Satz, and I. Montvay, Phys. Lett. 101B, 89 (1981)
- (10) N. Weiss, Phys. Rev. D24, 475 (1981); Phys. Rev. D25, 2667 (1982)
- (11) L. G. Yaffe and B. Svetitsky, Phys. Rev. D26, 963 (1982); Nucl. Phys. B210, 423 (1982)

- (12) T. Banks and S. Ukawa, Nuc. Phys. B225, 590, (1983)
- (13) T. DeGrand and C. Detar Nuc. Phys. B225, 590, (1983)
- (14) P. Hasenfratz, F. Karsch, and I. O. Stamatescu, Phys. Lett. 133B, 221, (1983)

Lecture 5: Chiral Symmetry

The chiral symmetry phase transition involves the restoration of a symmetry of the QCD equations of motion in the limit that the up and down quarks have zero mass. (1-3) Since the up and down quark masses are small but finite, chiral symmetry is only an approximate symmetry of QCD. These quark masses are however very small, so that the massless quark approximation should be very good. In fact if the chiral symmetry phase transition is first order, such a transition should continue to exist if small masses for quarks are added to the QCD action. Another additional chiral symmetry arises if the strange quark is taken as massless. Since the strange quark mass is not so small, such a symmetry may have violations of reasonable magnitude. In most of what follows for the discussion of chiral symmetry breaking, we shall ignore all flavors of quarks except up and down. This simplifies the discussion, and most of our discussion is directly generalized to the cases where additional flavors are included. We shall have some comments about including the effects of strangeness in the last part of this lecture.

Unbroken chiral symmetry would have as its consequence the masslessness of all baryons without parity doubled partners. Since there is not a parity doubled partner of the proton and the proton is not massless, chiral symmetry must be broken. Since we shall soon see that chiral symmetry is a continuous global symmetry, the breaking of chiral symmetry must be accompanied by the appearance of a massless Goldstone boson. We shall soon prove this statement and its corollary at finite temperature. This Goldstone boson is taken to be the pion, and the small value of the pion mass compared to typical meson masses such as that of the rho is explained.

At some temperature or baryon number density, chiral symmetry might be restored. The baryons would presumably become parity doubled or massless, and the pions massive. These comments about mass deserve some comment since the concept of a

mass does not really apply to systems which are not Lorentz invariant. What we mean by massless can be carefully formulated by studying real time response functions. A real time response function for an operator $O(t)$ is given by the correlation function

$$G(t) = \langle O(t)O(0) \rangle = \frac{\text{Tr } e^{-\beta H} e^{itH} O(0) e^{-itH} O(0)}{\text{Tr } e^{-\beta H}} \quad (1)$$

Since the operator O creates states with quantum numbers of O

added on to those of the states on which it operates, we shall say that creates excitations with the quantum numbers of O , and mean by this expression precisely what is stated above. The real time response function describes the propagation in time of disturbances with the quantum number of O when a thermal system is perturbed a small amount from thermal equilibrium. By masslessness, we shall simply mean that there exists a zero frequency disturbance. This might be observed experimentally by Fourier analyzing the response of a thermal system to small perturbations which induce perturbations of appropriate quantum numbers. At zero temperature, only the vacuum state contributes to the partition function, and the intermediate states which contribute to the real time response function truly have the quantum numbers of O . The existence of a zero frequency excitation is equivalent to the existence of a massless particle with the quantum numbers of O .

The experimental study of a chiral symmetry phase transition might be very fruitful since it is straightforward to experimentally measure the masses and widths of resonant states. These masses and widths may be greatly affected by the restoration of chiral symmetry.

Chiral $U(2)$ flavor symmetry is an invariance of the massless QCD action under combined γ^5 and flavor phase rotations. The full $U(2) \times U(2)$ symmetries of $U(2)$ flavor rotations and chiral $U(2)$ flavor rotations correspond to the invariance of the massless QCD action under the rotations

$$\psi \rightarrow e^{i\theta} \psi \quad (2)$$

$$\psi \rightarrow e^{i\alpha \tau_1} \psi \quad (3)$$

$$\psi \rightarrow e^{i\beta \tau_1} \psi \quad (4)$$

$$\psi \rightarrow e^{i\theta \gamma^5} \psi \quad (5)$$

where ψ is a quark field with isospin indices suppressed, and τ_i is the generator of flavor isospin rotations. The electromagnetic, quark flavor, axial $U(1)$, and axial vector quark flavor currents,

$$J^u = \bar{\psi} \gamma^u \psi \quad (6)$$

$$J^u_{\bar{5}} = \bar{\psi} \gamma^u \gamma^5 \psi \quad (7)$$

$$J^u_a = \bar{\psi} \gamma^u \tau_a \psi \quad (8)$$

$$J^u_{5a} = \bar{\psi} \gamma^u \gamma^5 \tau_a \psi \quad (9)$$

are formally conserved as a consequence of Eqs. 2-5,

$$\partial_u J^u = 0 \quad (10)$$

$$\partial_u J^u_{\bar{5}} = 0 \quad (11)$$

$$\partial_u J^u_a = 0 \quad (12)$$

$$\partial_u J^u_{5a} = 0 \quad (13)$$

The axial $U(1)$ current, Eq. 7 is anomalous, however, and quantum corrections to the action give (4-5)

$$\partial_u J^u_{5a} = \frac{1}{3\pi^2} F_{uv} F_d^{uv} \quad (14)$$

where

$$F_d^{\mu\nu} = \frac{1}{2} \epsilon^{\mu\nu\alpha\sigma} F_{\alpha\sigma}$$

The chiral $U(1)$ appears to be broken, but the situation is not quite so simple. The contribution to the right hand side of Eq. 14 is the divergence of a current. This current might be added to the left hand side of Eq. 14 to define a conserved axial $U(1)$ current. The problem with this procedure is that this current is gauge variant. We might think that this would provide no difficulty when we considered the charge corresponding to this current since gauge transformations which approach identity at spatial infinity might not affect the charge. The spectrum of states would possess a chiral $U(1)$ symmetry. This does not however happen since gauge transformations which wind as they approach spatial infinity may change the charge. The symmetry of these big gauge transformations might break dynamically, and the chiral $U(1)$ might again be a symmetry of states. The fact that this symmetry cannot be broken follows from 't Hooft's explicit computation of the effects of instantons. (5-6) Instantons are classical finite action field contributions to the classical field equations and contribute to the thermodynamical potential. Instantons and their ilk provide the only known mechanism for breaking chiral $U(1)$. Since the effect of instantons is exponentially weak in weak coupling, e^{-1/g^2} , we might expect chiral $U(1)$ to be a good approximate symmetry of QCD at high temperatures and density where the coupling g is small.

To illustrate the effects of the symmetries of Eqs. 2-5 imagine an approximation for QCD for which all these symmetries are exact. This approximation might be QCD to all orders in perturbation theory ignoring the effects of instantons, or perhaps requiring that all Feynman graphs which contribute to an anomaly for the $U(1)$ current are ignored. Such an approximation for weak coupling might be very good since, at least for

instantons, we expect effects of strength e^{-1/g^2} .

In this approximation, the mutually commuting charges and Casimirs associated with Q , Q_5 , Q_a , and Q_{5a} label states. To classify these states consider the charge algebra

$$[Q, Q_5] = [Q, \vec{Q}_5] = [Q, \vec{Q}] = [Q_5, \vec{Q}_5] = O \quad (16)$$

$$[Q_i, Q_j] = i \epsilon_{ijk} Q_k \quad (17)$$

$$[Q_5, Q_5] = i \epsilon_{ijk} Q_k \quad (18)$$

$$[Q_i, Q_5] = i \epsilon_{ijk} Q_{5k} \quad (19)$$

This algebra decomposes into $U(1) \times U(1) \times SU(2) \times SU(2)$ under the change of variables

$$\vec{Q}^\pm = 1/2 (\vec{Q} + \vec{Q}_5) \quad (20)$$

and the states are labeled by q , q_5 , $q^{\pm 2}$, and q_z^\pm .

The quantities q , q_5 , $q^{\pm 2}$, and q_z^\pm have simple physical interpretations. Let N_u^+ , N_u^- , N_d^+ , N_d^- , and N_d^\pm be the number of positive (+) chirality (helicity) quarks of flavor up, anti-up, down, and anti-down. These variables solve

$$q^\pm = 1/2 (q \mp q_5) \quad (21)$$

$$q_z^\pm = 1/2 (N_u^\pm - N_d^\pm + N_d^\pm - N_d^\mp) \quad (22)$$

$$q_z^\pm = 1/2 (N_u^\pm - N_d^\pm - N_d^\pm + N_d^\mp) \quad (23)$$

The Casimirs q_z^\pm which label representations of \vec{Q}_+ may be inferred from the maximum and minimum values of q_z^\pm in any multiplet.

The simplest state labeled by these charge operators is the vacuum which has vanishing q , q_5 , $q^{\pm 2}$, and q_z^\pm . The next simplest states are those whose spatial wave function is

independent of the interchange of valence quarks. Our basic assumption in characterizing simple states is that if one quark has a definite helicity, the remaining valence quarks have the same helicity. In order to have particle states of definite parity, we shall have to take simple linear combinations of these states since parity takes $Q_5 \neq -Q_5$ and $\hat{Q}_5 \neq -\hat{Q}_5$. Notice that in the rest frame of a nucleon or a meson that momentum conservation demands that at least one valence quark has momentum opposite to the remaining quarks. The spin of such a state is clearly not just the sum of the helicities of the constituents. (Such an argument as this is useful to illustrate parity doubling and to abstract the SU(2) chiral quantum numbers of the hadrons. The actual structure is somewhat more complicated, and a proper treatment would start with bag model wavefunctions, and the various contributions as chiral eigenstates might be abstracted.)

A nucleon is a state of 2 up and 1 down or 1 up and 2 down quarks. Labeling states by $|q, q_5; q^+, q_z; q^-; q_z\rangle$, the proton and neutron are

$$|\rho\rangle = 1/\sqrt{2} \{ |3, 3; 1/2; 0, 0\rangle + |3, -3; 0, 0; 1/2, 1/2\rangle \} \quad (24)$$

$$|n\rangle = 1/\sqrt{2} \{ |3, 3; 1/2, -1/2; 0, 0\rangle + |3, -3; 0, 0; 1/2, -1/2\rangle \} \quad (25)$$

This state is clearly an isodoublet by the rules for addition angular momentum

$$\hat{Q} = \hat{Q}_+ + \hat{Q}_-$$

As a consequence of Eqs. 24-25, massive nucleons are parity doubled. This follows by multiplying Eqs. 24-25 by either Q_5 or Q_{5z} , and is a consequence of either a chiral $U(1)$ or chiral $SU(2)$ symmetry. This doubling theorem is however evaded for massless nucleons. For massless nucleons, states may never be labeled in a rest frame and nucleons always have non-zero spatial momentum. Parity eigenstates always involve linear

combinations of helicity eigenstates and plane waves of opposite momentum. For an undoubled nucleon, there are two such linear combinations. Multiplication by Q_5 or Q_{5z} interchanges these linear combinations but does not imply an intrinsically doubled spectrum.

The next simplest state is a pion. The π^+ is composed of a u quark and a d anti-quark, so that the π^+ is in the $(1/2, 1/2)$ representation of $SU(2) \times SU(2)$. The odd parity pion wave functions are

$$|\pi^+\rangle = 1/\sqrt{2} \{ |0, 2; 1/2, 1/2; 1/2, 1/2\rangle - |0, -2; 1/2, 1/2; 1/2, 1/2\rangle \} \quad (27)$$

$$|\pi^-\rangle = 1/\sqrt{2} \{ |0, 2; 1/2, -1/2; 1/2, -1/2\rangle - |0, -2; 1/2, -1/2; 1/2, -1/2\rangle \} \quad (28)$$

$$|\pi^0\rangle = 1/\sqrt{2} \{ |0, 2; 1/2, 1/2; 1/2, -1/2\rangle + |0, 2; 1/2, -1/2; 1/2, 1/2\rangle - |0, -2; 1/2, -1/2; 1/2, 1/2\rangle - |0, -2; 1/2, 1/2, -1/2\rangle \} \quad (29)$$

The complicated structure for the π^0 arises since the π^0 is an I=1 linear combination of a u0 and a d0 pair.

If we perform a chiral $SU(2)$ transformation on $|\pi^\pm\rangle$, by multiplying by any component of \hat{Q}_5 , we either produce zero or some multiple of a σ^+ isoscalar state, σ ,

$$|\sigma\rangle = \{ |0, 2; 1/2, 1/2; 1/2, -1/2\rangle - |0, 2; 1/2, -1/2; 1/2, 1/2\rangle - |0, -2; 1/2, 1/2; 1/2, -1/2\rangle + |0, -2; 1/2, 1/2, 1/2\rangle \} \quad (30)$$

A parity doublet, σ' , π' , of this σ, π system is produced by multiplying $|\sigma\rangle$ and $|\pi\rangle$ by Q_5 . The set of parity doubled states and the symmetries which connect them are shown in Table I.

Needless to say, this spectrum bears little resemblance to reality. Some modification of this unrealistic spectrum arises as a consequence of a breakdown of chiral $U(1)$ invariance. This

breakdown is signalled by the anomaly in the axial U(1) current. This breaking will split the σ , π quartet from the σ' , π' quartet.

At finite energy density in hadronic matter, the effects of instantons, which are presumably responsible for driving this symmetry breaking, decrease rapidly as the energy density increases, since the coupling g becomes smaller and therefore $e^{-1/g}$ rapidly decreases. If the σ , π and σ' , π' multiplets existed in matter as boundstates up to relatively weak coupling, their mass splitting would rapidly disappear as the temperature increased. In any case, the spectrum of these states should approach one another as the energy density increases. This might be tested by computing

$$\Delta_{\pm} = 1/2 (1 \pm P) Q_5^2 \quad (31)$$

The parity operator is P and Q_5 is the chiral U(1) charge operator.

Even with a breakdown of chiral U(1), the spectrum of Table I is still unrealistic, since the σ and the π are degenerate in mass. This spectrum becomes more realistic after a dynamical breakdown of chiral SU(2).

If we take

$$\sigma_{op} = \text{flavors } \bar{\psi} \psi \quad (32)$$

as a quantum operator which creates a σ meson, the breakdown of chiral SU(2) is signalled by a condensation of these mesons

$$\sigma = \langle \sigma_{op} \rangle \neq 0 \quad (33)$$

Since the vacuum is taken to be isospin symmetric, the pion is assumed not to condense, so that

$$\hat{\pi} = \bar{\psi} \gamma_5 \gamma_1 \psi \quad (34)$$

satisfies

$$\langle \hat{\pi} \rangle = 0 \quad (35)$$

In high temperature and density hadronic matter, pion condensation might occur and $\langle \hat{\pi} \rangle$ might become non-zero.

The generation of expectation values for σ_{op} and $\hat{\pi}$ is analogous to the spontaneous breakdown of rotational invariance and magnetization in spin systems. If chiral symmetry was unbroken, σ_{op} and $\hat{\pi}$ could not have expectation values since these operators rotate into one another under chiral transformations. In a magnet, rotational invariance is broken by the spontaneous generation of an expectation value for a spin operator

$$\langle S_z \rangle \neq 0 \quad (36)$$

The spectrum of states is no longer rotationally invariant since the Hilbert space of states generated by the magnet when magnetized along any fixed axis of magnetization is orthogonal to the Hilbert space corresponding to any other axis. The analogous situation for chiral SU(2) breaking is that the states which are chiral rotations of the states in a Hilbert of fixed chiral properties

$$|s'\rangle = e^{i\hat{\pi} \cdot \vec{Q}_5^\dagger} |s\rangle \quad (37)$$

are orthogonal. The expectation value

$$\eta(\hat{\pi}) = \langle e^{i\hat{\pi} \cdot \vec{Q}_5^\dagger} \rangle \quad (38)$$

is therefore dual to σ in the sense that $\eta(\hat{\pi}) \neq 0$ in the chirally symmetric phase and is zero in the broken phase for all $\hat{\pi} \neq 0$.

The pions become the Goldstone bosons of chiral SU(2) symmetry breaking. There is no Goldstone boson of chiral U(1)

symmetry breaking since there is an anomaly for the $U(1)$ axial current and $U(1)$ chiral symmetry is explicitly broken. At finite hadronic matter energy density, the concept of a mass loses its meaning, except in the sense of the Fourier decomposition of real time response functions. The concept of a Goldstone boson requires clarification. We shall always mean by a Goldstone boson an excitation corresponding to a real time response which has zero mass as its spatial momentum goes to zero.

To see how these Goldstone bosons arise, consider the partially Fourier transformed real time response function

$$\begin{aligned} J_{ij}^{\mu}(q) = \langle J_{5i}^{\mu}(q) \pi_j^{\dagger}(0) \rangle &= \delta_{ij} \left\{ q_N^O (q^O, |q|) \delta^{ij} \right. \\ &\quad \left. + q^k N(q, |q|) \delta^{ijk} \right\} \end{aligned} \quad (39)$$

The pion field, $\#(0)$, is evaluated at zero spatial coordinate. This expectation value vanishes in the $SU(2)$ chiral symmetric phase, since it is generated as a chiral rotation of $\langle J_i^{\mu}(q) \sigma(0) \rangle$ which vanishes by parity and isospin invariance. Taking the divergence of Eq. 39 gives an equation which relates energy and momentum of pion excitations

$$q^O = |q| \{N/N^O\}^{1/2} \quad (40)$$

and barring any pathological kinematical singularities of $N(O, |q|)$ and $N^O(q^O, |q|)$, we conclude that there is a Goldstone boson. The nature of the singularities of N/N^O should of course be studied to make this conclusion firmer, and if pathological singularities would arise a more complicated new scenario might be concocted for chiral symmetry at finite energy density. Even in such perverse circumstances, the residue of chiral symmetry breaking is embodied in the dispersion relation of Eq. 40.

If light mass strange quarks are included in the description of chiral symmetry breaking, the discussion above goes through essentially unmodified. Instead of chiral pions, the entire octet of pseudoscalar mesons become Goldstone bosons. Since

this picture enjoys some phenomenological success, it may provide a useful description of hadronic matter. In a later lecture where we describe the phenomenology of chiral symmetry breaking, we shall see that strange particles may play an essential role in determining the order of the chiral symmetry phase transition. We shall see that the phase transition is probably first order, and should therefore survive the introduction of small masses for quarks.

References:

- (1) T. D. Lee and G. C. Wick, Phys. Rev. D9, 2291 (1974)
- (2) R. D. Pisarski, Phys. Lett. 110B, 155 (1982)
- (3) E. V. Shuryak, Phys. Lett. 107B, 103 (1981)
- (4) S. L. Adler, Phys. Rev. 177, 2426 (1969); J. S. Bell and R. Jackiw, Nuovo Cimento 60A, 47 (1969)
- (5) G. 't Hooft, Phys. Rev. D14, 3432 (1976)
- (6) C. G. Callan, R. F. Dashen, and D. J. Gross, Phys. Lett. 63B, 334 (1976); R. Jackiw and C. Rebbi, Phys. Rev. Lett. 37, 172 (1976)

Table I
Spectrum of states in a $U(2) \times U(2)$ chirally
symmetric world.

Parity	Particle
-1	π
+1	σ

+1	π'
-1	σ'

+1	N
-1	N'

Q_5 mixes π, σ with π', σ' and N with N' .
 \bar{Q}_5 mixes π with σ , π' with σ' , and N with N' .

Lecture 6: QCD at Finite Temperature and Density on the
Lattice: QED and QCD Without Fermions

The use of lattice gauge theory techniques has revolutionized the study of non-perturbative aspects of field theories. (1) In the last few years, computer Monte-Carlo studies have revealed many interesting aspects of theories such as QCD, and even provide hope for a precise quantitative comparison of computations with experimental data on hadronic spectrum.

Studies of QCD at finite temperature have revealed phase transitions and have made qualitative predictions for the properties of matter at high energy density. (2-4)

In this lecture, we first shall study QED without fermions on the lattice. In the continuum limit, this theory describes free photons. This limit is presumably relevant on the lattice for excitations with wavelengths long compared to the lattice spacing. Photons with short wavelengths however interact in a manner described by a non-polynomial lagrangian which we shall soon derive. This study is of course aimed to the more complicated problem of latticizing QCD, a problem which will be elaborated on later in the lecture.

These lectures always will concern Euclidian field theories. These theories are appropriate for studying thermodynamics. The study of real time Minkowski processes involves analytically continuing computations of Euclidian correlation functions, and is in most cases beyond the realm of current technology. This analytic continuation is nevertheless simple to implement in principle, and perhaps a description of real time processes is possible in the not too distant future.

The derivation of a latticized QED uses Stoke's law. Let S be a two dimensional surface element and $dS_{\mu\nu}$ an infinitesimal surface element imbedded in this surface. Let $\oint dL_\mu$ be a line integral around the edge of this two dimensional surface. Stoke's law is

$$\oint_S d\Gamma_A^{\mu} = \oint_S dS_{\mu\nu} F^{\mu\nu}$$

where

$$F^{\mu\nu} = \partial^{\mu}A^{\nu} - \partial^{\nu}A^{\mu}$$

To derive this result, we consider an infinitesimal surface element in the x-y plane:

$$S^{\mu\nu} + S^{XY} = \frac{dy}{dx} \begin{array}{|c|c|} \hline \hat{x} & \hat{y} \\ \hline \end{array} = dx dy \quad (3)$$

The line integral in Eq. 1 is

$$\oint_{S_{XY}} d\Gamma_A^X = dx A^X(x) + dy A^Y(x+dx\hat{x}) - dy A^Y(x) \quad (4)$$

If the infinitesimal surface element is small on a scale over which the vector potential varies, the vector potential may be expanded in a Taylor's series so that

$$\oint d\Gamma_A^X = dx dy F^{XY} = dS_{\mu\nu} F^{\mu\nu} \quad (5)$$

To proceed to a construction of a gauge invariant Lagrangian, consider the quantity

$$L(x) = \frac{1}{2a^4} \sum_{x \text{ of size } a^2} \text{plaquettes } P \text{ from } \{1-e^{i\Gamma_A^{\mu}(x)}\} \quad (6)$$

The sum over plaquettes is a sum over the twelve distinct orthogonal oriented surfaces of size a^2 whose lower left hand corner originates at the point x . The sum explicitly is

$$A + A/a \quad (12)$$

Now the field variables in Eqn. 11 appear only as $e^{iA^{\mu}(x)}$ where x is a lattice site. These variables link the lattice sites x and $x+a\hat{\mu}$, and are therefore called links. Without

$$\begin{aligned} \text{plaquettes} &= \begin{array}{|c|c|} \hline x & x+a\hat{x} \\ \hline x+a\hat{y} & x+a\hat{y}+a\hat{z} \\ \hline \end{array} + \begin{array}{|c|c|} \hline x & x+a\hat{x} \\ \hline x+a\hat{y} & x+a\hat{y}+a\hat{z} \\ \hline \end{array} \\ &+yz+zx+tx+ty+tz \text{ plaquettes} \end{aligned} \quad (7)$$

Changing the orientation of the arrows changes the sign of $d\Gamma_A^{\mu}$. In the limit that the lattice spacing is small compared to the scale of variation of the vector potential, Stoke's law gives

$$L(x) = \frac{1}{a^4} [6 - \cos(a^2 E_x) - \cos(a^2 E_y) - \cos(a^2 E_z) - \cos(a^2 B_x)] - \cos(a^2 B_y) - \cos(a^2 B_z) \sim \frac{1}{2} [\vec{E}^2 + \vec{B}^2] \quad (8)$$

which is the QED continuum Euclidian action.

To gain contact with the Euclidian QED action of Wilson, we observe that upon rescaling the fields

$$A \rightarrow A/g \quad (9)$$

the QED continuum Lagrangian is

$$L(x) = \frac{1}{2g^2} [\vec{E}^2(x) + \vec{B}^2(x)] \quad (10)$$

Equations 6-8 may be used to motivate a latticeized generalization of Eq. 10 as

$$S = \int d^4x L(x) + \frac{1}{2g^2} \sum_{\text{sites}} \sum_{\text{plaquettes } P} [1 - e^{-i\Gamma_A^{\mu}(x)}] \quad (11)$$

The lattice spacing implicit in Eq. 11 may be removed by rescaling

loss of generality, the field variables $A^{\mu}(x)$ may be chosen to lie in the range

$$-\pi < A < \pi \quad (13)$$

For the continuum fields this range is effectively infinite since for the continuum analog of Eq. 13, we have

$$-\pi/a < A < \pi/a \quad (14)$$

The gauge invariance of this theory is easily demonstrated.

Consider the transformation.

$$e^{i\bar{A}^{\mu}(x)} = e^{i\Lambda(x+\delta x)^{\mu}} e^{iA^{\nu}(x)} e^{-i\Lambda(x)} \quad (15)$$

This transformation is the analog of the continuum transformation

$$\bar{A}^{\mu}(x) = A^{\mu}(x) + \partial^{\mu}\Lambda(x) \quad (16)$$

Using Eq. 15, we have

$$\begin{aligned} e^{i\oint_S v_{\lambda} dx \cdot \bar{A}} &= e^{-i\bar{A}^{\lambda}(x)} e^{-i\bar{A}^{\nu}(x+\delta x)^{\lambda}} e^{i\bar{A}^{\lambda}(x+\delta x)^{\nu}} e^{i\bar{A}^{\nu}(x)} \\ &= e^{i\Lambda(x)} e^{-i\Lambda(x)} e^{-i\Lambda(x+\delta x)^{\lambda}} e^{i\Lambda(x+\delta x)^{\nu}} \dots \\ &= P e^{i\int_S v_{\lambda} dx \cdot A} \quad (17) \end{aligned}$$

and the Lagrangian is gauge invariant.

This theory is quantized by the Euclidian path integral

$$Z = \int [dA] e^{-S[A]} \quad (18)$$

On the lattice, this integral is well defined and finite. The measure factors which we were so careful to compute in the first lectures are not considered here since we may always

compute the thermodynamical potential as expectation values of operators for which these measure factors cancel.

$$\langle F \rangle = \frac{\int [dA] F[A] e^{-S[A]}}{\int [dA] e^{-S[A]}} \quad (19)$$

Correlation functions are of course already in this form. When the continuum limit is abstracted and Feynman graphs are computed, it is convenient to fix a gauge. A path integral of the type described in Lecture 2 will then result. Measure factors may be inserted to obtain conventional forms for the path integral for these integrals.

The lattice theory of QCD in the absence of fermions proceeds in much the same way as QED. We begin by considering the path ordered exponential

$$T(P) = P e^{i \int_S x_F^{\mu} d\Gamma_{\mu} r^{\mu} A^{\mu}} \quad (20)$$

where P denotes an arbitrary path. The matrices r^{μ} are generators of the gauge group in the fundamental representation of the gauge group. This ordering is defined by breaking $T(P)$ into arbitrarily small elements and ordering these elements along the path.

Under the gauge transformation

$$\frac{1}{i} \partial_{\mu} - g r^{\mu} A_{\mu} + U(x) \frac{1}{i} \partial_{\mu} - g r^{\mu} A_{\mu} U^{-1}(x) \quad (21)$$

the path ordered phase transforms as

$$P e^{i \int_S x_F^{\mu} d\Gamma_{\mu} r^{\mu} A^{\mu} + U(x_F) P e^{i \int_S x^{\mu} d\Gamma_{\mu} r^{\mu} A^{\mu}} U^{-1}(x)} \quad (22)$$

To see this, we use the identity that under a gauge transformation of an infinitesimal path ordered phase

$$\begin{aligned} e^{i r^{\mu}(x+\delta x)^{\mu}} e^{i g r^{\mu}(x) dx_{\mu}} e^{-i r^{\mu}(x)} &= e^{i r^{\mu}(x+\delta x)^{\mu}} \\ (1+ig r^{\mu}(x) dx_{\mu}) e^{-i r^{\mu}(x)} &= -U(x) \partial_{\mu} U^{-1}(x) \end{aligned}$$

$$+ U(x) i g r \cdot A^{\mu}(x) dx_{\mu} - e^{i r \cdot \tilde{A}^{\mu}(x)} dx_{\mu} \quad (23)$$

since

$$e^{i r \cdot \tilde{A}^{\mu}(x)} dx_{\mu} = 1 + i g r \cdot \tilde{A}^{\mu} dx_{\mu} = -U(x) \partial_{\mu} U^{-1}(x) \quad (24)$$

Since an arbitrary path ordered phase is a product over these infinitesimal phases, we have the result of Eqn. 22. Notice that the trace of the path ordered phase around a closed path is gauge invariant.

Now consider the trace of the path ordered phase around an infinitesimal closed path. We shall assume that this path is small enough that the fields $A^{\mu}(x)$ may be expanded in a Taylor's series. Since in the end we shall relate the computation of this gauge invariant phase to another gauge invariant quantity, it is convenient to do the evaluation in a gauge where the vector potential vanishes somewhere along the path,

$$A^{\mu}(x(\circ)) = 0 \quad (25)$$

and to a good approximation

$$A^{\mu}(x) = (x - x(\circ))^{\nu} \partial_{\nu} A^{\mu}(x) |_{x=x(\circ)} \quad (26)$$

Expanding the loop integral

$$\begin{aligned} \text{tr } P e^{i g d l_{\mu} r \cdot A^{\mu}} &= \text{tr } P \{1 + i g d l_{\mu} r \cdot A^{\mu} + i^2 g^2 d l_{\mu} r \cdot A^{\mu} d l_{\mu} r \cdot A^{\nu} \\ &\quad + O(S^3)\} \end{aligned} \quad (27)$$

where S is the surface area of the loop. Since

$$\text{tr } r a = 0$$

(28)

$$\text{tr } r a b = \delta^{ab}$$

the path orderings are of no consequence and we obtain

$$\text{tr } P e^{i g d l_{\mu} r \cdot A^{\mu}} = \text{tr } \{1 - \frac{1}{2} r \cdot F^{\mu\nu r} F_{\lambda\sigma} d S_{\mu\nu} d S_{\lambda\sigma}\} \quad (29)$$

where $d S_{\mu\nu}$ is the surface element in the plane of the loop. Summing over all orthogonal surface elements of both orientations which emanate from the point x gives

$$S = \frac{1}{g^2} \int_x \sum_P \text{tr} \{1 - e^{i g d l_{\mu} r \cdot A^{\mu}}\} \quad (31)$$

In particular, on a lattice notice that a typical plaquette which contributes to this sum over plaquettes is

$$\begin{aligned} e^{i g d S_{\mu\nu} d l_{\mu} r \cdot A^{\mu}} &= e^{-i g r \cdot A^{\mu}(x)} e^{-i g r \cdot A^{\mu}(x+d x^{\nu})} e^{i g r \cdot A^{\nu}(x+d x^{\mu})} \\ &e^{i g r \cdot A^{\mu}(x)} \end{aligned} \quad (32)$$

Recall that the action for QCD is

$$S = \frac{1}{4g^2} \int d^4 x F_{\mu\nu} F^{\mu\nu} \quad (33)$$

where

$$F_{\mu\nu}^{\mu\nu} = \partial^{\mu} A_{\mu}^{\nu} + \partial^{\nu} A_{\mu}^{\mu} + \epsilon_{abc} A_{\mu}^{\nu} A_{\nu}^{\mu} \quad (34)$$

This expression is what appears in the action in the gauge specified by Eqn. 25. Since the action is gauge invariant, the result is valid in any gauge. Notice that fields have been rescaled as

$$A \rightarrow A/\beta \quad (35)$$

After this rescaling, link variables are introduced as

phases which connect lattice sites

$$U^\mu(x) = e^{i\tau \cdot A^\mu(x)} = \overbrace{x}^{\longrightarrow} \overbrace{x+dx}^{\longrightarrow}$$

An inverse link is represented as

$$U^{\mu-1}(x) = e^{-i\tau \cdot A^\mu(x)} = \overbrace{x}^{\longleftarrow} \overbrace{x+dx}^{\longleftarrow}$$

The lattice action is represented in terms of these links as

$$S = \frac{1}{g^2} \sum_x \sum_P \text{tr} \{ 1 - U^{\nu-1}(x) U^{\mu-1}(x+d\tau \nu) U^\nu(x+d\tau \nu) U^\mu(x) \} \quad (38)$$

This form of the lattice action is not unique, since the link variables may be constructed from arbitrary dimensional representation generators of the gauge group. In our construction, we have chosen to employ the fundamental representation. This choice presumably makes no difference to the continuum theory, and has been the object of much study.

To study thermodynamics on the lattice, the length of the time direction of the lattice must be chosen to be finite since this length is the inverse temperature. The spatial volume is taken to infinity. At any value of the gauge coupling the lattice spacing may be determined by computing a physical dimensional quantity in terms of the only scale in the theory, the lattice spacing. The continuum limit is obtained by fixing the value of this dimensional physical quantity and adjusting the coupling strength so that the lattice spacing becomes smaller. In the limit of very small lattice spacing, all physical quantities should tend to a fixed limit, and the relationships between these quantities define the content of the theory. Relationships between correlation functions may be derived as the lattice spacing varies, and these relations, along with the dependence of the coupling upon lattice spacing, constitute the renormalization group equations. In QCD, the coupling goes to zero in a computable way as a consequence of asymptotic freedom.

The lattice spacings which have been used in our analysis have been chosen to be symmetric in space and time. We could have chosen asymmetric space-time lattice spacings. This is useful in some applications, and may be carried out by techniques similar to those outlined in the previous lectures.

$$(36)$$

References:

- (1) K. Wilson, Phys. Rev. D10, 2445 (1974)
- (2) L. D. McLerran & B. Svetitsky, Phys. Lett. 98B, 195 (1981); Phys. Rev. D24, 450 (1981)
- (3) J. Kuti, J. Polonyi, & K. Szlachanyi, Phys. Lett. 98B, 199 (1981)
- (4) J. Engels, F. Karsch, I. Montvay, & H. Satz, Phys. Lett. 102B, 332 (1981)

Lecture 7: Considerations on the Order of the Confinement-Deconfinement Phase Transition

The study of the confinement-deconfinement phase transition may either be carried out by Monte-Carlo simulation methods, or by analytic methods which build in much but not all of the structure of a finite temperature gauge theory into simple model analog computations. Monte-Carlo studies are the subject of the next lecture. These studies are severely limited by finite lattice size effects, and the lack of any satisfactory method for including fermions in present day computations. Analytic methods have the ability to sometimes draw firm conclusions about the nature of phase transitions, but are unable to draw quantitative conclusions about the numerical size of various effects. In this lecture we shall use analytic models to study the nature of the confinement-deconfinement phase transition. We shall argue that in SU(3) Yang-Mills theory without fermions, the phase transition is first order. We shall also argue that for sufficiently small quark masses and sufficiently large numbers of quark flavors, the confinement-deconfinement transition disappears, and there is no phase separation between the quark-gluon plasma and ordinary hadronic matter. There may be drastic qualitative changes, similar to the qualitative differences between a gas and a liquid. I shall comment on the physical significance of this result.

I begin by considering SU(N) Yang-Mills theory in the absence of fermions. The theory will be placed on a lattice with N_t sites in the time direction and N_s sites in the space direction. The lattice spacings are taken as assymmetric with a_t in the time direction and a_s in the space direction. The path integral representation for the thermodynamical potential is

$$e^{-\beta V_2} = \int [dU] e^{-S[U]} \quad (1)$$

where the action is

$$S_G[U] = \frac{1}{g^2} \sum_{\text{sites}} \left[\frac{\partial s}{at} L_{\text{space-time}} + \frac{at}{as} L_{\text{space-space}} \right] \text{plaquettes}$$

$$\{1 - e^{-is} d_{\mu} \tau^a A^{\mu}\} \quad (2)$$

To gain some qualitative insight into the phase structure of this theory, we approximate this theory by a theory with one site in the time direction, $N_t = 1$. Since

$$\beta = N_t a_t \quad (3)$$

gives the inverse temperature, the lattice spacing in the time direction is taken to be small and $T \rightarrow \infty$. This limit is strictly valid only for very high temperatures, but the qualitative results which result apply to the SU(N) Yang-Mills theory at all temperatures. This result may be shown in the more general treatment of Svetitsky and Yaffe.⁽¹⁾ In this limit the spatial plaquettes decouple in Eq. 2 and the timelike plaquettes are strongly coupled.

The contributions to the timelike plaquettes are large unless the timelike links are close to elements of the center of $SU(N)$.

$$U^0(x) = e^{2\pi i j/N} = z_j \quad (4)$$

Since the center element commutes with all elements of the group, the action becomes

$$S_G[U] = \frac{N}{g^2} \sum_{\text{sites}} \hat{e}_i \cdot \{1 - z_x z_{x+a_s \hat{e}_i}\} \quad (5)$$

This is the action for a $Z(N)$ spin system in three spatial dimensions. It has been derived assuming high temperature, but even for finite values of T this theory may be shown to faithfully represent the phase structure of the finite temperature $SU(N)$ theory in the sense that if the $Z(N)$ spin system has a first order phase transition, the $SU(N)$ theory also has one. This result was first derived by Svetitsky and Yaffe and is a consequence of universality.

To extract the consequences of the phase structure of the $Z(N)$ spin system for the $SU(N)$ theory, we recall that the physical temperature of the $SU(N)$ gauge theory may be varied by varying the size of the lattice spacing in the time direction. To do this, the coupling g may be varied. If the value of g is decreased, the distance scales at which the theory is being probed decrease as a consequence of asymptotic freedom. Put another way, if a physical length is held constant then as the lattice spacing is decreased so must the lattice spacing be decreased. This fact is a consequence of the lattice renormalization group equations. In this analogy, decreasing g corresponds to increasing temperature, and the effective temperature

$$T_{\text{eff}} = g^2 \quad (6)$$

decreases. The effective $Z(N)$ spin system orders at large physical temperatures and disorders at low physical temperatures.

The $Z(2)$ spin system is the Ising model which has a second order phase transition. The $Z(3)$ system is the three state Pott's model, and has a first order phase transition. We therefore conclude that the confinement-deconfinement for $SU(3)$ Yang-Mills theory in the absence of fermions is first order. A second order transition for the $SU(2)$ theory is suggested. These conclusions are verified by explicit Monte-Carlo computations.

Since these analytic results may also be derived by Monte-Carlo methods, their immediate utility is not so great as when the effect of fermions is considered. Very little is known about the effects of fermions on the confinement-deconfinement phase transition from Monte-Carlo studies. Analytic methods provide useful insight into this murky subject.

The introduction of fermions into a lattice gauge theory is complicated since a naive latticization leads to spurious fermionic states or to explicit chiral symmetry breaking even in

the massless fermion limit. I shall not go into a detailed presentation of the various methods of latticizing fermions and their virtues and evils. A discussion of lattice fermions is included in the lecture notes for the Arctic School of Physics 1982 by C. De Tar, (2) and is referred to in the references. The fermions we shall use in our analysis are those first introduced by Wilson. Their virtue is that they include no spurious unphysical states in the zero mass limit, and in the naive continuum limit the Lagrangian for the fermions reduces to that for continuum fermions. The continuum limit for quantities such as $\bar{\psi}\psi$ or the axial vector current must be taken carefully by point splitting the operators which occur in these expressions. When this is done, the correct anomaly structure of the theory is reproduced. These fermions are perhaps not the best to use for studying the chiral symmetry structure of the theory at finite temperature on the lattice since chiral symmetry is explicitly broken by these fermions for zero mass fermions except in the continuum limit. Only in this limit may chiral symmetry breaking be studied, and the study is no doubt complicated. Since I am interested only in the confinement-deconfinement of the theory, I hope that a mutilation of the chiral properties of the theory will not alter the qualitative nature of the conclusions of my analysis. Studies using other types of fermions would certainly be useful. We shall see in the next lecture that analysis using fermions which maintain chiral symmetry have been used in Monte-Carlo computations in the so called quenched approximation.

The Wilson fermion contribution to the QCD action is

$$\begin{aligned} S_F = \sum_{\text{sites}} & \left\{ \left(M + \frac{6at}{as} + \frac{2as}{at} \right) \bar{\psi}_x \psi_x - \sum_i \left(\frac{3t}{as} \bar{\psi}_x U_x^\dagger \hat{e}_i \right. \right. \\ & \left. \left. (1+\gamma_i) \psi_x \hat{a}_i + \text{c.c.} \right) - \frac{as}{at} \bar{\psi}_x U_O^\dagger (1+\gamma_O) \psi_x + at \hat{e}_O \right. \\ & \left. + \text{c.c.} \right\} \end{aligned} \quad (7)$$

Some of the terms in this expression vanish in the naive

continuum limit. In the naive massless fermion limit, these terms are not chirally invariant. The presence of these terms prevents the appearance of unphysical modes of fermion propagation in the massless limit. Following De Grand and De Tar, this action is rewritten as (3)

$$\begin{aligned} S_F = \Sigma_x \bar{\psi}_x \psi_x - \frac{k\alpha}{a_s} \Sigma_{x,i} & \left\{ \bar{\psi}_{x+\hat{a}_i} (1+\gamma_i) U_{x,i}^\dagger \psi_{x,i} + c.c. \right\} \\ & - \kappa \Sigma_x \left\{ \bar{\psi}_{x+\hat{a}_0} (1+\gamma_0) U_{x,0}^\dagger \psi_x + c.c. \right\} \end{aligned} \quad (8)$$

The overall scale of the action has been redefined in this expression by a rescaling of the fermion fields. The hopping parameter is κ in this expression. The bare fermion mass m_0 is defined as the lowest momentum excitation of the non-interacting theory for large N_t and is

$$\cosh m_0 a_t = \left\{ 4\kappa^2 + \left(1 - \frac{6\kappa a_t}{a_s}\right) \right\} / 4\kappa(1-6\kappa a_t/a_s) \quad (9)$$

This mass is the bare mass of the theory, and when interactions are included, the bare mass will approach infinity so that the physical mass remains finite.

The path integral for the thermodynamical potential is

$$e^{-\beta V_R} = \int [dU d\bar{\psi} d\psi] e^{-S[U, \bar{\psi}, \psi]} \quad (10)$$

The integrations over the fermion fields may be performed to give

$$e^{-\beta V_R} = \int [dU] e^{-S_{\text{eff}}[U]} \quad (11)$$

where

$$S_{\text{eff}}[U] = S_G[U] - \text{Tr} \ln M[U] \quad (12)$$

and where the matrix $M[U]$ is notation for the matrix which appears in the fermion contribution to the action

$$S_F = \Gamma_{n,m} \bar{\psi}_n M_{nm}(U) \psi_m \quad (13)$$

In the limit at $\kappa \rightarrow 0$, appropriate for $N_t = 1$, the fermion action simplifies to

$$S_F = \Sigma_x \left\{ \bar{\psi}_x \psi_x - \kappa \left\{ \bar{\psi}_x (1+\gamma_0) U_{x,0}^\dagger \psi_x + \bar{\psi}_x (1-\gamma_0) U_{x,0} \psi_x \right\} \right\} \quad (14)$$

The fermionic effective action may be easily computed to be

$$\begin{aligned} \text{Tr} \ln M[U] = h_0 + h_1 \Sigma_x \text{Re } U_{x,0} &= 4\ln(1+2\kappa)(1-2\kappa+4\kappa^2) \\ &+ 4\ln \frac{(1+2\kappa)^2}{1-2\kappa+4\kappa^2} \Sigma_x \text{Re } U_{x,0} \end{aligned} \quad (15)$$

For small values of the hopping parameter

$$\text{Tr} \ln M[U] = 24\kappa \Sigma_x \text{Re } U_{x,0} \quad (16)$$

For the case of N_f flavors of quarks, this result is modified to

$$\text{Tr} \ln M[U] = 24N_f \kappa \Sigma_x \text{Re } U_{x,0} \quad (17)$$

The contribution of h_0 does not affect the phase structure of the theory. The contribution h_1 does affect the phase structure since this term generates an effective external magnetic field. For small values of this magnetic field we have

$$\kappa \sim \frac{1}{2} e^{-m_0 a_t} \quad (18)$$

$$(18)$$

and the magnetic field vanishes as the bare quark mass goes to infinity. (-5)

For $SU(2)$ Yang-Mills theory these arguments suggest that the

confinement-deconfinement phase transition disappears for any value of the quark mass since an arbitrarily small external magnetic field destroys a phase transition in the Ising model. This may be seen by considering the effect of an external magnetic field on the effective potential for the Ising model. In Fig. 1, the free energy is plotted as a function of magnetization for temperatures above, Fig 1a, and below the magnetization transition, Fig 1b. The magnetization may be generated by applying an external magnetic field. At the critical temperature the system must decide to settle in to one of the degenerate minimum. This decision depends delicately on the initial conditions, and non-analyticity in the thermodynamical potential results.

In Fig 2, the free energy vs magnetization is plotted for the Ising model in an external magnetic field. Fig 2a is below the transition temperature and Fig. 2b is above the transition temperature. Since the minima are no longer degenerate above the temperature at which these local minima first appear, no non-analyticity is generated, and no phase transition arises. There may be meta-stable states of the spin system which appear as a remnant of the phase transition which appeared in the absence of an external magnetic field.

The situation for SU(3) Yang-Mills theory is slightly more complicated. The confinement-deconfinement transition in the absence of fermions is first order. The introduction of very heavy mass quarks should not remove this transition. A first order transition involves a discontinuous change in the states which give a contribution to the thermodynamical potential, and the introduction of a small perturbation may generate a small change in the magnitude of the discontinuous jump, in for example the energy density of the two different phases, but should not completely remove this discontinuity. Below some critical mass for a sufficiently large number flavors, the confinement-deconfinement transition may disappear. Studies of the three state Pott's model in an external magnetic field indicate that this may very well happen for a finite critical

value of the quark mass.

The confinement-deconfinement phase transition in the presence of fermions may appear as shown in Fig. 3a-b. In Fig 3a, the possibility that the confinement-deconfinement transition disappears at a finite value of the quark mass is shown. This phase diagram is reminiscent of gas-liquid phase diagrams. The quark-gluon plasma and hadronic matter would be qualitatively different aspects of the same phase of matter. In Fig. 3b, the confinement-deconfinement transition is assumed to be reduced to a second order transition at zero renormalized quark mass. In this scenario, the plasma and hadronic matter are different phases. Notice that in these plots, the renormalized masses are plotted. The analysis of the Z(N) spin models and their implications for the continuum theory are complicated since the mass which appears in the spin model is a bare quark mass this mass goes to infinity in the continuum limit, and the external magnetic field goes to zero. The extrapolation to the continuum limit is complicated especially in the Z(3) case. Even in the Z(2) case, the argument that the confinement-deconfinement transition disappears is not rigorous because of this technical complication. Because of this complication, either of the two possibilities shown in Fig 3 are allowed.

These phase diagrams may be more complicated if the possibility of a chiral symmetry phase transition is allowed for.(6) If the chiral symmetry phase transition is second order, the possibilities in Figs 4a-c are allowed. Notice that in Fig. 3c, the second order transition at m=0 may be interpreted as either a chiral symmetry restoration transition or as a deconfinement-confinement transition.

If the chiral symmetry restoration transition is first order, the introduction of small quark masses will not remove the transition. Several interesting phase diagrams are shown in Figs 5 a-d. These possibilities do not exhaust all the possible diagrams, and the reader is invited to draw the complete set. The point I want to make here is that the structure of the

confinement-deconfinement phase transition and its intertwining with chiral symmetry restoration is far from understood, and there is much room for developing qualitative understanding. The reason that there is not necessarily a confinement-deconfinement phase transition in the presence of fermions has its origins in a simple physical argument due to Fradkin and Sherkar. (7) If a static test quark is inserted into a thermal ensemble, it may immediately form a bound state with a dynamical light mass quark. Its free energy is finite for all values of the temperatures regardless of whether quarks are permanently bound as hadrons or are quasi-free in a plasma: A possible definition of an order parameter might be to compute the free energy of a thermal system in the presence of a single extra quark. (8-9) This free energy is always divergent, however. In the confined phase it is obviously divergent, but in the deconfined phase it diverges due to the impossibility of isolating such a quark, that is, no such states contribute to the partition function because of Debye screening. At zero temperature, such an order parameter does characterize confinement, since confinement means the absence of states without triality zero. At finite temperature, thermal fluctuations make such a definition impossible.

References:

- (1) B. Svetitsky & L. Yaffe, Nucl. Phys. B210, 423 (1982); Phys. Rev. D26, 963 (1982)
- (2) C. De Tar Proceedings of the Arctic School of Physics (1983)
- (3) T. Degrand & C. Detar, Nuc. Phys. B225, 590, (1983)
- (4) P. Hasenfratz, F. Karsch, and I. O. Stamatescu, Phys. Lett. 133B, 221, (1983)
- (5) T. Banks & S. Okawa, Nuc. Phys. B225, 145, (1983)
- (6) T. Celik, J. Engels, & H. Satz, Phys. Lett. 125B, 411, (1983); 129B, 323, (1983); J. Kogut, H. Matsuo, M. Stone, H. W. Wyld, S. Shenkar, J. Shigematsu, & D. K. Sinclair, Phys. Rev.

Lett. 51, 869, (1983), B. Svetitsky, Phys. Lett. 131B, 165, (1983)

(7) E. Fradkin & S. Sherkar, Phys. Rev. D19, 3682 (1979)

(8) C. Detar & L. McLerran, Phys. Lett. 119B, 171, (1983)

(9) H. Neuberger, Nucl. Phys. B230, 31, (1984)

Figure Captions:

Figure 1: The free energy as a function of magnetization above, Fig. 1a, and below, Fig. 1b, the magnetization transition.

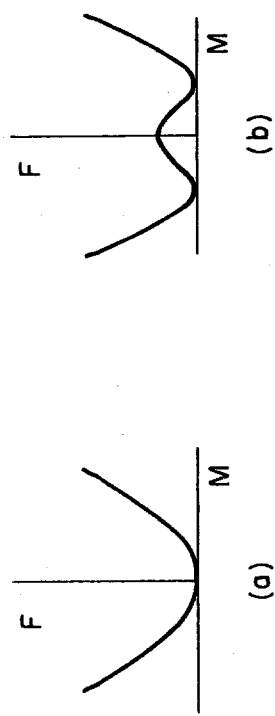
Figure 2: The free energy as a function of magnetization in an external magnetic field above, Fig. 2a, and below, Fig. 2b, the transition temperature of the theory with no external magnetic field.

Figure 3: Possible phase diagrams for QCD in the $T, e^{-1/m}$ plane.

Figure 4: Possible phase diagrams for QCD in the $T, e^{-1/m}$ plane allowing for the possibility of a second order chiral symmetry restoration phase transition.

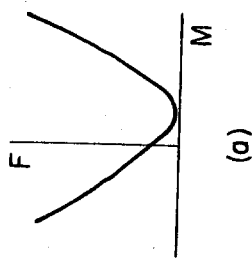
Figure 5: Possible phase diagrams allowing for a first order chiral symmetry restoring transition.

Figure 7-1

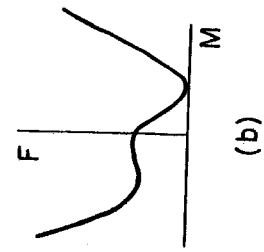


(a)

Figure 7-2

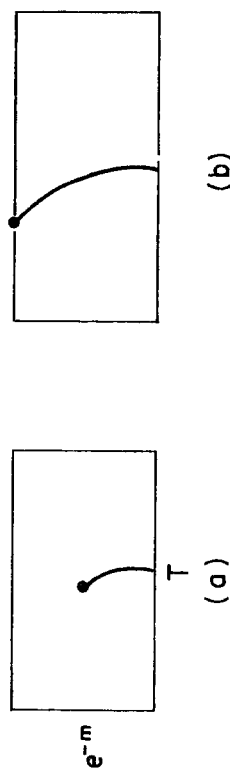


(b)

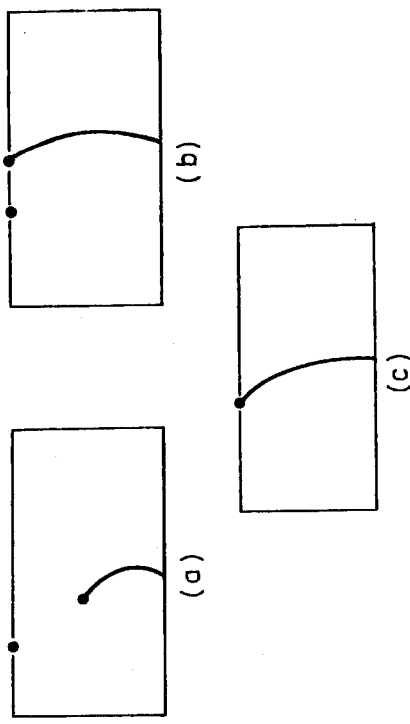


(b)

Figure 7-3



(a)



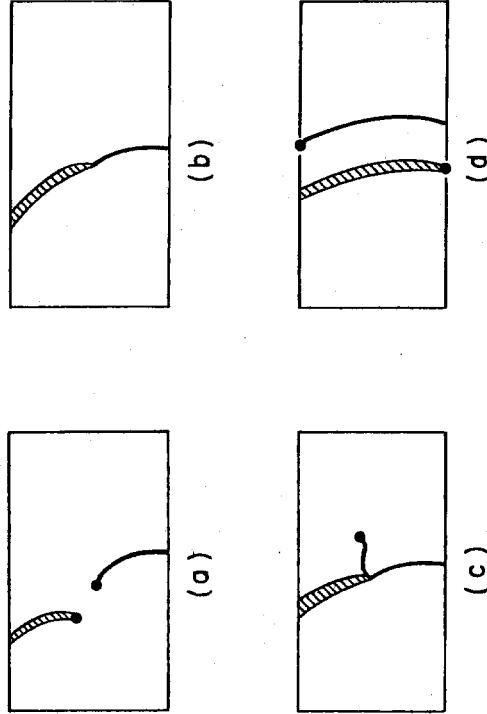
(b)

(c)

Figure 7-4

Lecture 8: Monte-Carlo Simulation Results

Figure 7-5



The study of phase transitions in gauge theories in general have been perturbative aspects of gauge theories revolutionized by lattice gauge theory techniques. In particular, Monte-Carlo evaluations of the path integral representation for correlation functions and the thermodynamical have given a first qualitative and semi-quantitative glimpse at such non-perturbative aspects of gauge theories.

I shall begin by reviewing what is known about finite temperature QCD in the absence of fermions. The methods, and qualitative and semi-quantitative results of studies of such theories will be presented. The next subject I will present is the results of computations with fermions. The results and method of the so-called quenched approximation will be reviewed. Finally, techniques which go beyond the quenched approximation are discussed. In particular, recent results that suggest that the confinement-deconfinement phase transition may disappear when the quenched approximation is removed are discussed.

I shall assume that the theory we shall consider is a Yang-Mills theory in the absence of fermions on a lattice of size $N \times N^3$ and that the lattice spacings are at in the time direction and as in the space direction. I shall assume that $a = s$ unless otherwise stated. The action for such a theory has been discussed several times in the previous lectures. Typically, the quantities which we wish to compute are expectation values of operators such as

$$\langle O \rangle = \frac{\int [dU] e^{-S[U]} O(U)}{\int [dU] e^{-S[U]}} \quad (1)$$

Quantities such as the thermodynamical potential may always be expressed in this form, and it is this form which may be simulated by Monte-Carlo techniques. The basic idea of a Monte-Carlo simulation is to perform the integration in Eq. 1 by choosing field configurations which give a dominant contribution

to Eq. 1. Such a selection involves statistical sampling of those field configurations which dominate the path integral. Since even a modest lattice of 3000 lattice sites involves 3000 integrations, such a statistical evaluation of the path integral provides the only practical method of evaluation.

The evaluation of Eq. 1 proceeds by initially assigning arbitrary values to the links corresponding to an $N \times N^3$ lattice. These links might be chosen randomly or might all be chosen as $U=1$. Starting from this configuration, new configurations are chosen which contribute to Eq. 1 by statistically sampling new values of links at each lattice site with a weight of $e^{-S[U]}$. An iteration of the lattice is completed when each link on the lattice has been sampled and given the opportunity to change. Depending on the quantity computed, a few hundred to sometimes tens of thousand iterations must be performed.

To compute physical dimensionful quantities, a dimensionful quantity must be computed to set the size scale of lattice spacings in the theory. For example, the coefficient of the linear potential in charmonium might be computed. For any fixed value of the coupling g , this would specify the value of the lattice spacing, and the values of all other dimensionful quantities would be determined. Now suppose that another value of g is chosen. If this value of g corresponds to another value of the lattice spacing and if for both these values the physical quantities considered involve computations on a size large compared to a lattice spacing and small compared to the lattice size, the results should agree. This fact is a non-trivial consequence of the renormalizability, or cut-off independence of the theory. Moreover, the lattice spacing and coupling are related by the renormalization group equations, equations which express the invariance of the theory under combined reparameterizations of the coupling and lattice spacing. In theories such as QCD, the limit of small lattice spacing corresponds to small coupling and the relation between lattice spacing and coupling are computable in perturbation theory. For example, the short distance quark-quark potential might be

computed with an ultra-violet cutoff corresponding to the inverse lattice spacing. This computation generates a dimensionful parameter Λ_L which characterizes this interaction, and the renormalization group equations require

$$d\Lambda_L = \left\{ \frac{11Ng^2}{48\pi^2} \right\}^{-51/121} \exp \left\{ \frac{-24\pi^2}{11Ng^2} \right\} \quad (2)$$

(There is some arbitrariness in the scale factor which characterizes this relationship. The scale factor chosen here corresponds to the conventional definition of Λ_L , and must be related by direct computation to the string tension or $\bar{\Lambda}_S$ which characterizes perturbative computations.) With the lattice spacing determined, physical quantities such as the temperature may be computed. Notice that the renormalization may be performed at zero temperature on a symmetric lattice N^4 . Physical quantities at finite temperature will automatically be finite in the continuum limit when such a zero temperature renormalization is performed.

The first quantities which were computed in finite temperature QCD were the free energy of an isolated static test quark, and the energy density of gluonic matter (1-5). The first computations were for $SU(2)$ Yang-Mills theory (1-3). The exponential of the negative of the free energy of an isolated quark is an order parameter, and has zero value in the confined phase and is finite in the deconfined phase. These computations clearly showed a magnetization of the Wilson line which determines this free energy. A curve such as that shown in Fig. 1 results from this computation.

Notice that the quantity $\langle L \rangle$ is plotted vs $1/g^2$ and not vs the temperature. To convert the bottom axis to temperature, the renormalization group equations must be used. This is straightforward, and qualitatively similar curves arise when written in terms of temperature. The overall scale factor is difficult to compute for $SU(2)$ Yang-Mills theory, since there are no naturally occurring scales on which to meter a theory which does not correspond to nature. For $SU(3)$ Yang-Mills

theory, a similar curve results, except that the curve shows a much sharper jump at the critical value of g , and there is evidence of hysteresis in the neighborhood of the transition. This is shown in Fig 2.

The critical temperature for the confinement-deconfinement transition may be expressed in terms of the scale $\Lambda_{\overline{MS}}$ which characterizes deep inelastic scattering. This determination is somewhat ambiguous since quarks contribute to deep inelastic scattering, and the computations are for a quarkless theory. These quarks make only a small contribution to the momentum dependence of the running coupling constant, so such an approximate may be valid. The last lecture should suggest caution when such relations are "derived" since quarks might dramatically alter the structure of the theory. Finally, these results are derived on small lattices, and finite lattice size effects may significantly change the results. The results of such a determination give

$$\Gamma = (1 \pm 1) \Lambda_{\overline{MS}} \quad (3)$$

Since $\Lambda_{\overline{MS}}$ is 50-200 Mev on the basis of deep inelastic muon and neutrino data, the confinement-deconfinement scale is in this range. Values as high as 300-400 Mev cannot be ruled out from the current experiments. Computations using the string tension measured in lattice computations of Creutz gave $\Lambda_{\overline{MS}} = 150-250$ Mev(6). Newer computations of Parisi suggest that these string tension computations were low by as much as a factor of 2 and perhaps $\Lambda_{\overline{MS}} = 300-400$ Mev(7). Such a comparison is probably on even shakier grounds than that using $\Lambda_{\overline{MS}}$ extracted from deep inelastic scattering. The main point of these comments is that due to uncertainties in the value of $\Lambda_{\overline{MS}}$, and uncertainties intrinsic to current lattice computations, only qualitative and semi-quantitative conclusions may be drawn about the nature of the confinement-deconfinement transition in its implications for QCD as it appears in nature where there are dynamical quarks.

The hysteresis of the Wilson line in the neighborhood of the confinement-deconfinement phase transition of $SU(3)$ Yang-Mills theory that the phase transition is first order. This may be tested by trying to find a temperature at which the lattice system is metastable in one of the two phases for arbitrarily long numbers of monte-carlo iterations. The phase which the system is in is determined by the initial conditions. In this situation, the Wilson line will be frozen into different values depending on which phase the system is in. Below and above the critical temperature, the system will stabilize in one phase or the other. The existence of long time scale metastability is convincing of a first order phase transition.

The energy of gluonic matter has been computed using Monte-Carlo methods. This quantity may be abstracted from the path integral for the thermodynamical potential by differentiating with respect to the temperature. This differentiation is best carried out with asymmetric lattice spacings, and in the end taking the symmetric limit. The energy density is

$$\rho = -\frac{1}{V} \frac{\partial \ln Z}{\partial t} |_V = -\frac{1}{Nt^3 a_s^3} \frac{\partial \ln Z}{\partial a t} |_{as} \quad (4)$$

which may be explicitly evaluated, and after considerable straightforward algebra becomes

$$\rho = \frac{2N}{Nt^3 a_s^3 g^2} \left[\frac{\partial t}{a_s} \times \sum_{\text{space-space plaquettes}} (1 - e^{-i/f d_\mu r \cdot A^\mu}) + \frac{a_s}{at} \times \sum_{\text{space-time plaquettes}} (1 - e^{-i/f d_\mu r \cdot A^\mu}) \right] \quad (5)$$

Before presenting the results of the Monte-Carlo simulations, it is useful to review the results expected. At high energy densities, the energy density should approach that of an ideal gas of gluons,

$$\rho/T^4 = \left(\frac{3\pi^2/15}{3\pi^2/15} \frac{SU(2)}{SU(3)} \right) \quad (6)$$

At low temperatures the energy density is that of a dilute glueball gas. In the dilute gas limit, the glueballs should be non-interacting. The energy exponentially approaches zero as T approaches zero, and the slope of this exponential determines the glueball mass. The glueball mass has been estimated by this method.

The energy density of gluonic matter as computed by lattice Monte-Carlo methods are presented for $SU(2)$, Fig 3a, and $SU(3)$, Fig 3b, gauge theories. At high temperatures, the energy density approaches a constant. Due to finite lattice size effects, this constant value is a factor of two different from the predicted value for an ideal gluon gas. The problem is that the lattices considered in the numerical analysis are just too small to extrapolate to infinite volume. It is true however that the result obtained is appropriate for an ideal gluon gas on a finite size lattice of the size considered. This factor of two uncertainty provides some measure of the systematic uncertainties inherent in present day lattice Monte-Carlo simulations. The lattices are too small and the lattice spacings are too big.

At low temperatures, the energy density rapidly approaches zero, corresponding to an ideal glueball gas. At some critical temperature, the energy changes rapidly from a small value to the asymptotic ideal gas limit. For $SU(2)$, the transition appears continuous, but the specific heat

$$C_V = \frac{\partial \rho}{\partial T} |_V \quad (7)$$

seems to be singular, as shown in Fig 4

The jump for $SU(3)$ appears to be discontinuous, corresponding to a first order transition. The magnitude of this jump is the latent heat of the transition. Various estimates of this latent heat give $\delta p \sim 3-1$ Gev/ fm^3 , assuming $\Lambda_{\overline{MS}} = 200$ Mev. Since this result depends upon $\Lambda_{\overline{MS}}$ as $\Lambda_{\overline{MS}}^4$, a factor of two change in this parameterization changes the latent heat by a factor of 16. The major uncertainty in this number

seems to be $\Lambda_{\overline{MS}}$, and not the systematic uncertainties in the lattice computations. As a verification of the first order of the phase transition, the metastability may be observed in the value of the energy density as well as that of the Wilson line at the critical temperature.

The next step in these computations is to include the effects of fermions. Recall that effects of fermions could always be treated in the path integral by directly integrating out the fermion fields. In particular, any path integral of the form

$$\langle Q \rangle = \frac{\int [du d\bar{u} d\psi] O(U, \bar{U}, \psi) e^{-S[U, \bar{U}, \psi]}}{\int [du d\bar{u} d\psi] e^{-S[U, \bar{U}, \psi]}} \quad (8)$$

can be reexpressed as

$$\langle Q \rangle = \frac{\int [du] \det G^{-1}[U] U(U, G[U]) e^{-S[U]}}{\int [du] \det G^{-1}[U] e^{-S[U]}} \quad (9)$$

where $G[U]$ is a fermion Green's function in the external field due to the gluon link U . ($G[U]$ is the inverse of the matrix M corresponding to fermion Propagation as introduced in the preceding lecture.) This fact follows from the bilinear nature of the fermion action, so that all integrals involving fermions are Gaussian and are trivial to compute.

The determinant in Eq. 9 may be expanding in powers of U , and a Feynman graph expansion in fermion-antifermion closed loops results. In the limit of large N for $SU(N)$ gauge theories, these contributions are suppressed, and a good approximation is to ignore the determinant, that is set it to 1. This approximation is gauge invariant for finite N , and is called the quenched approximation. Its utility is not that it is necessarily a good approximation. Recall that the fermion determinant was responsible for removing the confinement-deconfinement transition for sufficiently small quark mass, and the determinant may be essential in some computations. The utility of the quenched approximation is that it is the simplest method of computing effects of fermions at present; other more

systematic methods such as hopping parameter expansions, which systematically expand the determinant about 1, are used but are tedious to compute with(9-10) The hope is that the effects of fermions loops are small, and do not qualitatively alter the structure of the theory, but this statement is one for which there is much dispute.

When fermions are included in the quenched approximation, the temperature of the confinement deconfinement temperature is unaltered and the Wilson line is a good order parameter. Since the fermions do not generate loops, they do not enter the relationship between lattice spacing and $\Lambda_{\overline{\text{MS}}}$. Also since fermions only appear through expectation values, they do not affect the determination of the coupling for which the Wilson magnetizes. The temperature of deconfinement is therefore independent of the presence of fermions in the quenched approximation.

The energy density of hadronic matter may be computed in the quenched approximation. The curves which result are qualitatively similar to those appropriate for gluonic matter, and are not presented here. The numerical value of the latent heat for SU(3) QCD becomes $\delta\rho = 1.-2.$ GeV/fm for $\Lambda_{\overline{\text{MS}}} = 200$ Mev. Perhaps the most interesting application is to the study of chiral symmetry breaking. Kogut et. al. have introduced fermions which maintain an exact continuous chiral invariance on the lattice(8) Such a method may not be applied for a single fermion flavor, since it may be shown that unless there are a sufficiently large number of degenerate zero mass fermions, the fermion action explicitly breaks chiral invariance. The fermions of Kogut et. al. are perhaps not so useful for quantitatively characterizing QCD as they are for probing qualitative aspects of the theory.

An interesting question which may be addressed is whether there is a relationship between the chiral symmetry restoration phase transition and the confinement-deconfinement transition. For quarks, which transform in the adjoint representation of the color gauge group, quenched computations suggest that these

transitions occur at the same value of the temperature. For SU(2) the data is not conclusive and the temperatures might be different, but for SU(3) the data seems conclusive. This observation is somewhat complicated since for fermions in higher dimension representations of the color group, the transition temperatures are different.

Chiral symmetry breaking is presumably generated by a meson condensation. The results in the quenched approximation may be easily understood in this context. At the confinement-deconfinement transition, fermion-antifermion pairs which bind together to form mesons may become ionized. These ionized quark-antiquark pairs for whatever reasons do not condense in the vacuum, and chiral symmetry is restored. For fermions in higher representations of the color group, fermion-antifermion pairs are more tightly bound into mesons, and at the confinement-deconfinement transition are not fully ionized.

Some words of caution are required concerning the quenched approximation and the study of chiral symmetry breaking. The parameter $\bar{\psi}\psi$ is not strictly speaking an order parameter in the quenched approximation. Recall that U(1) chiral symmetry is explicitly broken by the axial-vector anomaly, and dynamically realized by instantons. Since instantons contribute at all temperatures, and since the fermions do not communicate with each other in the quenched approximation and behave as independent flavor chiral fermions, $\bar{\psi}\psi$ is always non-zero. In fact, the one instanton contribution to $\bar{\psi}\psi$ gives a divergent value, and $\bar{\psi}\psi$ only becomes finite due to a zero in the fermion determinant. The claim of Kogut et. al. is that instantons and their ilk only give small contributions to $\bar{\psi}\psi$ and their computations show that other larger dynamical effects generate symmetry breaking.

Several computations have recently tried to go beyond the quenched approximation to study the confinement-deconfinement transition(9-10) As discussed in the last lecture, for some critical value of the bare fermion mass, the transition disappears. This is verified in the computations for Z(3)

theories by DeGrand and Detar, and for $SU(3)$ by Hasenfratz, Karsch, and Stamatescu [9-10]. The $SU(3)$ results suggest that a large value of the mass is sufficient, $m=5-1$. GeV. These computations should be regarded with caution, since no attempt has been made to extrapolate to the continuum limit, and small lattices have been used. Another interesting qualitative result of the $SU(3)$ computation is that as the fermion mass is reduced from infinity, the confinement-deconfinement temperature and latent heat monotonically decrease until the transition disappears. The chiral symmetry restoration temperature, and that of deconfinement if it exists, may be at somewhat lower values than that predicted in the quenched approximation.

References:

- (1) L. D. McLerran & B. Svetitsky, Phys. Lett. 98B, 195 (1981); Phys. Rev. D24, 450 (1981)
- (2) J. Kuti, J. Polonyi & K. Szlachanyi, Phys. Lett. 98B, 199 (1981)
- (3) J. Engels, F. Karsch, I. Montvay, & H. Satz, Phys. Lett. 101B, 89 (1981); Phys. Lett. 102B (1981); Nucl. Phys. B205, 545 (1982)
- (4) K. Kajantie, C. Montonen & E. Pietarinen, Zeit. Phys. C9, 253 (1981)
- (5) I. Montvay & E. Pietarinen, Phys. Lett. 110B, 148 (1982); Phys. Lett. 115B, 151 (1982)
- (6) M. Creutz, Phys. Rev. Lett. 45, 313, (1980); Phys. Rev. D21, 2308, (1980)
- (7) H. Hamber, E. Marinari, G. Parisi, and C. Rebbi, Nucl. Phys. B225, 475, (1983); P. Gutbrod, P. Hasenfratz, Z. Kunszt, and I. Montvay, Phys. Lett. 128B, 415, (1983)
- (8) J. Kogut, M. Stone, H. Wyld, J. Shigematsu, S. Shenkar, & D. Sinclair, Phys. Rev. Lett. 48, 1140 (1982); 50, 393 (1983); Phys. Rev. Lett. 51, 869, (1983)
- (9) T. DeGrand & C. Detar, Nucl. Phys. A225, 590, (1983)
- (9) P. Hasenfratz, F. Karsch & I. O. Stamatescu

Phys. Lett. 133B, 221, (1983)

Figure Captions:

Figure 1: The expectation value of the Wilson line for $SU(2)$ Yang-Mills theory.

Figure 2: The expectation value of the Wilson line for $SU(3)$ Yang-Mills theory.

Figure 3: The energy density as a function of temperature for $SU(2)$, Fig. 3a, and $SU(3)$, Fig. 3b, Yang-Mills theory.

Figure 4: The specific heat for $SU(2)$ Yang-Mills theory.

Figure 8-1

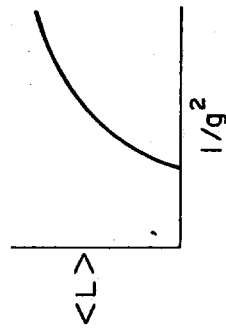


Figure 8-2

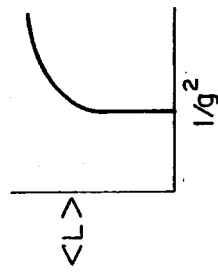
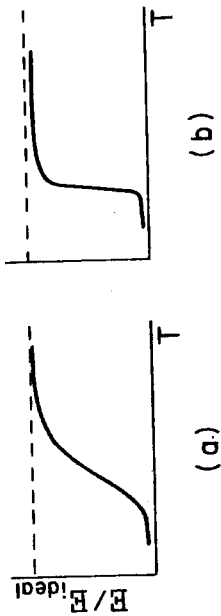
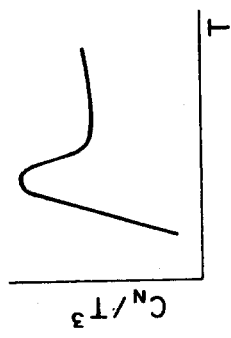


Figure 8-3



(a)

Figure 8-4



(b)

Lecture 9 : Perturbation Theory of the Quark-Gluon Plasma

at Finite Temperature and Baryon Number Density

At very high energy densities, hadronic matter becomes an almost ideal gas of quarks and gluons(1-7) In these circumstances, the effects of particle interactions are small, and to some order in perturbation theory are computable by methods involving weak coupling expansions.

To illustrate the perturbative methods which may be used to compute the thermodynamic potential, I shall review and outline the results and methods which are employed to compute to first order in α_s . The details of this computation are contained in the excellent paper by Kapusta, a paper which should be studied to gain a real flavor for the techniques used in these computations(6) I shall review the problem of the plasmon effect, and the necessity of using non-perturbative methods when going beyond first order in α_s in evaluating the thermodynamic potential. The results at zero temperature and finite baryon number density to second order in α_s are also reviewed. The method of renormalization group improving the weak coupling expansions by replacing the expansion by an expansion in a temperature and baryon number density dependent coupling which approaches zero at high energy densities is discussed. Non-perturbative effects such as instantons are briefly mentioned. The breakdown of perturbation theory for the thermodynamical at order α_s^3 for finite temperature according to the arguments of Linde, and Gross,

Pisarski, and Yaffe is presented(8-9) Since the literature on the subject matter of this lecture is large, this lecture must be viewed as a summary of the existing literature, which must be consulted for details of the results which are discussed.

The perturbation theory of the quark-gluon plasma begins with the path integral representation for the thermodynamic potential

$$e^{-S[\bar{A}, \bar{\psi}, \bar{\phi}, \bar{\omega}]} = \int [d\bar{A} d\bar{\psi} d\bar{\phi} d\bar{\omega}] e^{-S[\bar{A}, \bar{\psi}, \bar{\phi}, \bar{\omega}]} \quad (1)$$

The action in this expression is a sum of terms

$$[\tau^a, \tau^b] = if_{abc}\tau^c \quad (7)$$

$$S = S_G + S_F + S_{Gh} \quad (2)$$

arising from the gluon fields A^μ ,

$$S_G = \int_0^\beta dt \int d^3x \left\{ \frac{1}{4} F_{\mu\nu}^a F_{\mu\nu}^a + \frac{1}{2r_0} (\partial_\mu A^\mu)^2 \right\} \quad (3)$$

where

$$F_{\mu\nu}^a = \partial_\mu A_\nu^a - \partial_\nu A_\mu^a + g_0 f_{abc} A_\mu^b A_\nu^c \quad (4)$$

from the fermion fields $\bar{\psi}$ and ψ ,

$$S_F = \int_0^\beta dt \int d^3x \bar{\psi}_j \gamma^\mu \left\{ \left(\frac{1}{4} \not{D} - i \not{v}_j \not{\gamma}^0 + m_j^0 \right) \delta_{ab} - g_0 \tau^a \not{\tau}^b \right\} \delta_{ab} \quad (5)$$

and from the ghost fields \bar{g} and g ,

$$S_{Gh} = \int_0^\beta dt \int d^3x \bar{g}^\mu \not{\partial}_a \left\{ \not{\partial}_\mu \delta_{ab} - g_0 f_{abc} \not{\tau}^c \right\} g_\mu b \quad (6)$$

The action we have written down is appropriate for generalized Landau gauge with gauge fixing parameter r_0 . This action is written in Euclidian space with metric

$$g^{\mu\nu} = \delta^{\mu\nu} \quad (7)$$

The gamma matrices are Euclidian and satisfy the anti-commutation relations

$$\{\gamma^\mu, \gamma^\nu\} = -2g^{\mu\nu} \quad (6)$$

The quark color indices, a , run over 1-N, while the gluon color indices, a , run over N2-1 + 1. The quark flavor indices, i , run from 1 to N_F , where N_F is the number of quark flavors.

The matrices τ^a are the generators of the color gauge group,

The bare quark mass is m_0 and the bare coupling is g_0 , and both of these quantity will be taken as cutoff dependent singular quantities in order that the resulting thermodynamical potential be finite. The fields A, \bar{A} , and ω satisfy periodic boundary conditions while the fermion fields $\bar{\psi}$ and ψ satisfy anti-periodic boundary conditions.

The derivation of this form for the functional integral and the problem of ghosts has been discussed in previous lectures.

In particular, the delicate mechanics of properly extracting the ideal gas contribution to the thermodynamic potential has been discussed in detail, and we shall concentrate here on the computations of corrections to the thermodynamical potential due to particle interactions. These contributions are given by

$$\Omega_I(\beta, u) = \Omega(\beta, u) - \Omega(\beta, u)|_{g_0=0} = \frac{1}{\beta V} \ln \frac{\int [dA d\bar{A} d\omega d\bar{\omega}] e^{-S}}{\int [dA d\bar{A} d\omega d\bar{\omega}] e^{-S}|_{g_0=0}} \quad (10)$$

Notice that in this ratio delicate factors such as the temperature dependence of the measure cancel.

To properly derive the thermodynamic potential, a trivial renormalization must be performed. The expression given by Eq. 10 yields a non-zero thermodynamic potential for the vacuum, corresponding to the limit $\beta \rightarrow \infty$, $u \rightarrow 0$. This non-zero term is divergent in the limit that an ultraviolet cutoff, Λ , approaches infinity. The order of this divergence is Λ^4 . This divergent term is not of physical consequence, however, since only pressure differences ($P = -\Omega$) between physical systems and the vacuum are physically measurable. Without loss of physical import, we may define the renormalized thermodynamical potential as

$$\Omega^R(\beta, u) = \Omega(\beta, u) - \lim_{\beta \rightarrow \infty, u \rightarrow 0} \Omega(\beta, u) \quad (11)$$

This renormalized thermodynamic potential satisfies a

renormalization group equation. This renormalization group equation follows from the invariance of Eq. 11 under the following rescalings of the numerator of the argument of the logarithm in Eq. 13. These rescalings are

$$\begin{aligned} A &\rightarrow z_3^{1/2} A \\ \bar{\psi}, \psi &\rightarrow z_2^{1/2} \bar{\psi}, \psi \\ \bar{u}, u &\rightarrow \bar{z}_2^{1/2} \bar{u}, u \\ m &\rightarrow m + z_2^{-1} \delta m \end{aligned} \quad (12)$$

The invariance of Eq. 11 is guaranteed if z_1, z_2, z_3, \bar{z}_2 , and δm are temperature and density independent.

The parameters m , r , and g in Eqs. 12 are the renormalized fermion masses, gauge fixing parameter and coupling. A variety of mechanisms are discussed in the literature for invoking renormalization schemes to define z_1, z_2, z_3, \bar{z}_2 , and δm so that m , r , and g and invariant Green's functions of the zero temperature and density theory are ultraviolet finite. I shall not discuss these prescriptions in detail here. I shall merely note that making finite the zero temperature and density Green's functions with a choice of wavefunction renormalization constants and a mass shift also makes finite the finite temperature and density Green's functions for the same parameters. This result is a consequence of the fact that at short distances, the quarks and gluons propagate as if there were no finite density and temperature ensemble of quarks and gluons with which to interact. Over these distances, the quarks and gluons propagate as they would at zero temperature and

density. Since the ultraviolet infinities arise from singular short distance propagation, the finite temperature and density theory should be cutoff independent.

The invariance of Ω under the transformations of Eqs. 12 leads to a renormalization group equation,

$$\Omega(g_0, m_0, \mu_B, Z_A) = \Omega(g_0, m_0, \mu_B, Z_B) \quad (15)$$

The two sets of wavefunction renormalization constants, Z_A and Z_B , correspond to two alternative choices for wavefunction renormalization. The prescriptions A and B both render the theory finite.

The two different prescriptions A and B are in general parameterized by different dimensionful scale parameters μ_A and μ_B . These scale parameters may correspond to a momentum for which the strength of quark-antiquark potential is at some fixed value, or may correspond to some other fixing of a measurable dimensional quantity. In terms of μ_A and μ_B the renormalization group equation, Eq. 15, is

$$\Omega(g_0, m_0, \mu_B, \mu_A) = \Omega(g_0, m_0, \mu_B, \mu_A) \quad (16)$$

The choice of an appropriate value of μ_A or μ_B is essential to facilitate the perturbative expansion for Ω in terms of g . When the thermodynamic potential is expressed as an expansion in β , logarithms of μ/μ_A or μ_B typically occur. These logarithms would invalidate the perturbation expansion for large μ or small β . These singular logarithms may be removed from the perturbation expansion, however, by choosing $\mu_A = (\gamma\mu + \delta T^2)^{1/2}$, where γ and δ are constants of order one. The parameters γ and δ are generally chosen by prescriptions which should render high order perturbative contributions small.

This choice of μ_A converts the perturbative expansion into an expansion in a density and temperature dependent coupling constant,

$$g(\mu_A) = g((\gamma\mu + \delta T^2)^{1/2}) \quad (17)$$

The Gell-Mann-Low equation which determines g 's dependence on follows from Eq. 12

$$\frac{d}{du_A} g_O = \frac{d}{du_A} Z^{-3/2} z_1 g = 0 \quad (18)$$

This equation may be evaluated self-consistently in Perturbation theory when g is small. The integration constant for the equation is the dimensionful Λ parameter of QCD. The result of solving this equation to lowest order in perturbation theory is, with $a_S = g^2/4\pi$,

$$a_S(\mu_A) = \frac{\pi}{(11N-2NF)\ln(\mu_A/\Lambda)} \quad (19)$$

The problem of handling mass renormalization has been briefly discussed in the literature, and I shall not explore it here. In most applications, sufficient accuracy is obtained by using fixed current algebra masses for the quarks

$$m_u = m_d = 0 \quad (20)$$

The perturbative expansion for Ω may be directly obtained from the functional integral representation of Eq. 1 by expansion in powers of g . This expansion generates the sum of all connected vacuum graphs in terms of bare propagators and vertices. The Feynman rules for computing these graphs in covariant gauges are illustrated in Fig. 1.

These rules differ from the ordinary Feynman rules by the Euclidian metric and gamma matrices, the factor of $i\gamma^\mu$ in the fermion propagators, and the frequency sum in k^μ . The Euclidian metric is a consequence of the fact the the thermodynamic Potential is the imaginary time generalization of the ground state expectation value of e^{iH} which governs the Minkowski

space theory. The factor iu^{α} arises from the factor of $\vec{p} \cdot \vec{N}$ in the grand canonical ensemble. The frequency sums arise from the finite Euclidian time periodic or anti-periodic boundary conditions which are imposed on the fields.

The Feynman graphs which appear in lowest order in perturbation theory for are shown in Fig. 2. The fermion mass renormalization is represented by the second diagram. The overall sign and weight of these diagrams are not derived by any simple rule. They may be obtained directly from Eq. 1, or may be extracted by using Legendre transforms and effective potentials.

The individual diagrams which contribute to Fig. 2 are divergent as Λ^4 in the limit that the ultraviolet cutoff approaches infinity. After subtracting the unphysical vacuum pressure and performing a fermion mass renormalization, these graphs are ultraviolet finite.

The situation in three loops and higher and higher order is much more complicated. Coupling constant and wave function renormalizations must be carried out at these orders. The prescriptions for introducing and carrying out these renormalizations follow from the scalings of Eq. 10. A practical method for renormalizing Ω_1 is to express Ω_1 in terms of renormalized propagators and vertices. This method of calculation is the analog of the skeleton graph expansion of the Schwinger-Dyson equations for the propagators and vertices. A closed form expression for Ω_1 has been obtained in QED, but only a computational algorithm has been developed for QCD. In practice, a convenient way of regulating the perturbation for Ω_1 is to continue dimensionally. This continuation not only successfully regulates the ultraviolet divergences, but also regulates complicated overlapping infrared divergences which first appear at three loop order.

The ideal gas contributions to the thermodynamic potential have been discussed in previous lectures. These contributions are represented in Fig. 3. For quarks we have

$$\Omega_0^Q = -2N_C T \sum_{i=1}^N \int \frac{d^3 p}{(2\pi)^3} \left[\ln(1+e^{-\beta(E_i+u_i)}) + \ln(1+e^{-\beta(E_i+u_i)}) \right] \quad (21)$$

which is easily evaluated for massless quarks as

$$\Omega_0^Q = -NN_F/6 \left\{ 7\pi^2 T^4/30 + u^4/2\pi^2 \right\} \quad (22)$$

The gluon and ghost contribution to the thermodynamic potential shown in Fig. 3 is

$$\Omega_0^G = 2(N_C^2-1)T \int \frac{d^3 p}{(2\pi)^3} \ln(1-e^{-\beta|p|}) = -\pi^2/45 (N_C^2-1)T^4 \quad (23)$$

The evaluation of the two loop diagrams shown in Fig. 2 is more involved. A straightforward contour integral evaluation is discussed by Kapusta. The result of this evaluation for the quarks is

$$\begin{aligned} \Omega_2^Q = & \alpha_s \pi (N_C^2-1) \sum_{i=1}^N \int 1/3 \pi^2 \int \frac{d^3 p}{(2\pi)^3} \frac{N_i(p)}{E^i(p)} \\ & + \int \frac{d^3 p}{(2\pi)^3} \frac{d^3 p'}{(2\pi)^3} \frac{1}{E^i(p)E^i(p')} \left[N_i(p)N_i(p') + 2 \right. \\ & \left. \frac{N_i(p)N_i(p')N_i(p')N_i(p)}{(E^i(p)-E^i(p'))^2-(\vec{p}-\vec{p}')^2} \right. \\ & \left. + \frac{N_i(p)N_i(p')N_i(p')N_i(p')}{(E^i(p)+E^i(p'))^2-(\vec{p}+\vec{p}')^2} \right] \end{aligned} \quad (24)$$

The Fermi-Boltzmann distribution functions are

$$N_i^i(p) = \frac{1}{(e^{\beta(E_i(p)+u_i)}+1)} \quad (25)$$

and

$$N = N_+ + N_- \quad (26)$$

This contribution may be thought of as arising from the phase integrals over the Feynman amplitudes shown in Fig. 4. The external lines on these diagrams are on mass shell and

are weighted with the Fermi-Boltzmann distribution functions N_{\pm}^1 for quarks and antiquarks respectively and by

$$M(q) = \frac{1}{1-e^{-B|q|}} \quad (27)$$

the Bose-Einstein distribution function for gluons. All color and spin indices are summed over.

This reduction to phase space integrals over Feynman amplitudes is very general. An advantage of this representation is that ultraviolet divergences manifest in η and proportional to $\Lambda^4, \Lambda^3, \Lambda^2$, and Λ explicitly disappear. The divergences which remain are the standard divergences of the scattering amplitude and are easily renormalized away. A disadvantage is that in three loops and higher orders in perturbation theory, spurious infrared divergences are introduced by this representation.

For massless quarks, the phase space integrals in Eq. 26 are easily carried out with the result

$$x_2^q = (N_c^2 - 1) \alpha_s N_F / 8\pi \left\{ 5\pi^2 T^4 / 18 + T^2 u^2 + u^4 / 2\pi^2 \right\} \quad (28)$$

The two loop gluon contribution to the thermodynamic potential may be evaluated in analogy to that of the quarks with the result

$$x_2^g = \pi / 36 \alpha_s^2 N_c (N_c^2 - 1) \quad (29)$$

To illustrate some of the treacheries of the phase space integral representation, I shall discuss the three loop contribution to the zero temperature potential appropriate for zero mass quarks. These contributions are shown in the vacuum graphs in Fig. 5. As vacuum graphs, only the graph of Fig. 5a represents a contribution which is infrared divergent. This divergence is associated with the well known plasma oscillation, and we shall soon discuss the source and removal of its singular

contribution.

Spurious infrared divergences are however introduced when the remaining vacuum graphs are converted into phase space integrals over Feynman amplitudes. For example when the graph of Fig 5d is converted into the sum of the two phase space integrals over Feynman amplitudes shown in Fig. 6, both resulting integrals are infrared divergent in four dimensions. Space integrals is infrared finite. In $4+\epsilon$ dimensions, $\epsilon > 0$, these integrals are however both finite. The evaluation of these integrals is easily carried out in $4+\epsilon$ dimensions, and the cancellation of the infrared divergences may be explicitly performed. This procedure is also viable for the evaluation of the graph represented by Fig 5c.

The diagram of Fig. 5b presents another hazard. When it is converted to the sum of phase integrals represented by Fig. 7, a mass shell divergence appears.

The intermediate fermion line in the three body scattering shown in Fig 7 is on mass shell. This divergence is an artifact of the phase space integrals over Feynman amplitudes representation. When the phase space integral representation is derived from the vacuum graph representation, a double pole at $p^2 = 0$ must be evaluated. The residue of this pole is finite.

The zero temperature result for the residue of this double pole however yields an incorrect result for this diagram. There are finite corrections associated with taking the zero temperature limit. These corrections terms are discussed by Freedman and McLerran and by Baluni, and only arise when vacuum diagrams have double or higher order poles [3,7]. The lessons which should be learned from this three loop calculation are:

(1) At a minimum, all phase space integrals over Feynman amplitudes which contribute to a single vacuum graph must be summed before an infrared finite result may be expected.

(2) Mass shell singularities should be treated as arising from poles of second order or higher in vacuum graphs. Finite contributions will arise in taking the zero temperature limit

which are not correctly obtained ab initio at zero temperature. The diagram of Fig. 5a possesses a bona-fide infrared divergence. This divergence is generated by an improper treatment of the plasmon effect. The plasmon effect is manifest in the screening of the interaction of two static charge densities when the charge densities are immersed in the plasma. This screening converts the Coulomb potential into a Yukawa potential

$$1/r + e^{-ur}/r \quad (30)$$

where u is the plasmon mass. In perturbation theory, the plasmon mass u is of order g . If we expand the potential of Eq. 30 as a series in g , infrared divergences will be introduced when integrals are performed over this potential. These divergences are spurious and are the result of a naive perturbative analysis.

The way to resolve this difficulty is well known.⁽¹⁰⁻¹²⁾ In momentum space, the longitudinal components of the static gluon propagator are

$$1/q^2 + 1/(q^2+u^2) \quad (31)$$

when proper account is taken of the plasmon effect. In general, the propagator may be treated so as to account for the plasmon effect by summing the diagrams shown in Fig. 8.

In this figure, the difference between the gluon polarization at finite temperature and that at zero temperature and density is $\Delta\Pi$. The plasmon contribution to the thermodynamic potential is properly accounted for by summing the ring diagrams of Fig. 9.

When these contributions are subtracted from Fig. 5a, the remainder is infrared finite.

At finite temperature, the situation is slightly more complicated than that at zero temperature. At finite temperature, propagating gluons make contributions to the

thermodynamic potential. The transverse modes of propagating gluons acquire a mass but the longitudinal modes do not. This situation is the exact opposite to that for the static propagator where the longitudinal propagator acquires a mass but the transverse does not. This difference is reflected in a different dependence of the plasma contribution to the thermodynamic potential at zero temperature, $\alpha_{\text{S}}^2 m^2$, and at finite temperature, $\alpha_{\text{S}}^{3/2}$. The method for handling the effect at finite temperature involves summing the bubble graphs.

A question arises as to whether at any order in perturbation theory, intractable infrared divergences arise which render a further perturbation expansion useless.⁽⁸⁻⁹⁾ This issue may be addressed at finite temperature. To isolate the most singular infrared contribution to the thermodynamic potential, we study vacuum graphs with the Matsubara frequency, q_0 , set to zero for at least one propagator for each loop in the graph. The expansion parameter for these graphs is T^{p+1} where p is the number of loops in the graph, which is effectively an expansion in a dimensional coupling constant T . For $p=4$, the dimension of the resulting three dimensional loop integration must be that of an inverse mass. For the massless gluon propagators which appear in the naive perturbation expansion, this mass can only be generated by an infrared divergence. A mass might be however generated for the gluons and the resulting perturbation expansion would be rendered finite. The expansion is then of the form, $\alpha_{\text{S}}^{p+1} m^{p+3}$, where m is the lightest mass scale in the problem. For $p < 3$, this infrared effect may be ignored since the infrared integrations are finite. At $p=3$, corresponding to order α_{S}^3 , the critical order in perturbation theory where infrared effects are crucial is reached. If the mass is $m < \alpha_{\text{S}} T$, then a weak coupling, although non-perturbative expansion is possible. No mass is however generated for the transverse components of the static transverse gluon propagator and the longitudinal dynamical propagator until at least order α_{S} , corresponding to $m = \alpha_{\text{S}} T$. This has been shown to be a general consequence of gauge invariance by Gross, Pisarski, and Yaffe,⁽⁹⁾

The thermodynamical is therefore not computable at order α_s^3 and higher in perturbation theory. As a consequence of similar arguments involving power counting and the structure of the gluon propagator, it can further be shown that the magnetic screening length is itself not computable in perturbation theory or any weak coupling methods. (These arguments may be shown not to apply to QED since there is always at least one loop in the perturbation expansion for the thermodynamic potential which involves fermions, and the fermion propagator is not singular for the lowest allowed value of the Matsubara frequency (frequency sum.)

I have not discussed the effects of instantons and other topological objects in this lecture[5,9-10] Instantons are finite action classical solutions of the Euclidian Yang-Mills equations. The action associated with these solutions is of order

$$S_{\text{inst}} \sim 1/g^2 \quad (32)$$

and the contribution to the functional integral of Eq. 1 is of order

$$\Omega_1 \sim e^{-1/g^2} \quad (33)$$

The effects of instantons are therefore naively smaller than the effects of any contribution of finite order in perturbation theory. The effects of instantons have been elegantly computed in the article of Gross, Pisarski, and Yaffe, and I shall not consider their computations in detail here except to note that for any value of temperature for which the effects of instantons may be reliably computed, their size is numerically extremely small[9]. This might not be the case for quantities other than the thermodynamical potential. The computation for finite temperature is interesting since temperature provides a natural infrared cutoff, and instantons make infrared finite contributions to the thermodynamical potential.

References:

- (1) C. Bernard, Phys. Rev. D9, 3312 (1974)
- (2) M. Kislinger & P. Morley, Phys. Rev. D13, 2771 (1976)
- (3) B. Freedman & L. McLerran, Phys. Rev. D16, 1130 (1977); 1147 (1977); 1169 (1977); D17 1109 (1977)
- (4) J. Collins & M. Perry, Phys. Rev. Lett. 34, 1353 (1975)
- (5) E. Shuryak, Phys. Lett. 79B, 135 (1978)
- (6) J. Kapusta Nucl. Phys. B148, 461 (1979)
- (7) V. Baluni, Phys. Lett. 72B, 381 (1978); Phys. Rev. D17 2092 (1978)
- (8) A. Linde, Phys. Lett. 96B, 289, (1980)
- (9) D. Gross, R. Pisarski, & L. Yaffe, Rev. Mod. Phys. 53, 43, (1981)
- (10) E. Shuryak, Phys. Rep. C61, 71 (1980)
- (11) M. Gell-Mann & K. Brueckner, Phys. Rev. 106, 364 (1957)
- (12) I. Akhiezer & S. Peletminski, Zh. Eksp. Teor. Fiz. 38, 1829 (1960) (Sov. Phys. 11, 1316 (1960))

Figure Captions:

Figure 1: The Feynman rules in a general covariant gauge.

Figure 2: The Feynman graphs which make a lowest order contribution to the thermodynamic Potential.

Figure 3: A representation for the ideal gas contribution to the thermodynamic potential.

Figure 4: A phase space integral representation over scattering amplitudes representation for the thermodynamical potential.

Figure 5: The three loop contributions to the thermodynamic potential.

Figure 6: The phase space integral over scattering amplitude representation for Fig. 5d.

Figure 9-1

- Figure 7: The phase space integral over scattering amplitude representation for Fig. 5b.
- Figure 8: The contributions to the gluon propagator which give the plasmon effect.
- Figure 9: The contribution of the plasma oscillation to the thermodynamic potential.

$$\text{Diagram: } \overbrace{\text{---}}^{\alpha} \overbrace{k}^k \overbrace{\text{---}}^b = \frac{\delta_{ab}}{k^2} \{ g_{\mu\nu} + (x_0^{-1}) \frac{k_\mu k_\nu}{k^2} \}$$

$$\text{Diagram: } \overbrace{\text{---}}^{\alpha} \overbrace{k}^k \overbrace{\text{---}}^b = \frac{\delta_{ab}}{k^2}$$

$$\text{Diagram: } \overbrace{\text{---}}^{\mu, c} \overbrace{\text{---}}^{\beta} \overbrace{\text{---}}^{\alpha} \overbrace{k}^k = i g_0 f_{abc} k^\mu$$

$$\text{Diagram: } \overbrace{\text{---}}^{\mu, a} \overbrace{\text{---}}^{\beta} \overbrace{\text{---}}^{\alpha} \overbrace{k}^k = i g_0 f_{abc} k^\mu$$

$$\text{Diagram: } \overbrace{\text{---}}^{\mu, c} \overbrace{\text{---}}^{\beta} \overbrace{\text{---}}^{\alpha} \overbrace{k}^k = g_0 \gamma^\mu \delta_{ij} \tau^a_{\alpha\beta}$$

$$\text{Diagram: } \overbrace{\text{---}}^{\mu, a} \overbrace{\text{---}}^{\beta} \overbrace{\text{---}}^{\alpha} \overbrace{k}^k = g_0 \gamma^\mu \delta_{ij} \tau^a_{\alpha\beta}$$

$$\text{Diagram: } \overbrace{\text{---}}^{\alpha, a, k} \overbrace{\text{---}}^{\beta, b, r} \overbrace{\text{---}}^{\gamma, i, q} = i g_0 f_{abc} \{ g_{\beta\gamma} (x-q)_a + g_{\alpha\beta} (k-r)_\gamma + g_{\alpha\gamma} (q-k)_\beta \}$$

$$\text{Diagram: } \overbrace{\text{---}}^{\alpha, a, k} \overbrace{\text{---}}^{\beta, b, r} \overbrace{\text{---}}^{\gamma, c, l} = g_0^2 \left\{ \begin{array}{l} f_{adc} f_{ebc} (g_{\alpha\beta} g_{\delta\gamma} - g_{\alpha\gamma} g_{\delta\beta}) \\ + f_{abc} f_{edc} (g_{\alpha\delta} g_{\beta\gamma} - g_{\alpha\gamma} g_{\beta\delta}) \\ + f_{acc} f_{edb} (g_{\alpha\delta} g_{\beta\gamma} - g_{\alpha\beta} g_{\delta\gamma}) \end{array} \right\}$$

-1 for each closed ghost or fermion loop

$$k^0 = \frac{2\pi n}{\beta} \quad n = \dots -2, -1, 0, 1, 2, \dots \text{ gluons, ghosts}$$

$$= \frac{2\pi(n+\frac{1}{2})}{\beta} \quad " \quad \text{fermions}$$

Integrals are over $\frac{d^3 k}{(2\pi)^3}$, summations all over n.

Figure 9-2

$$\frac{1}{2} - \text{---} + \frac{1}{2} \text{---} - \frac{1}{6} \text{---} - \frac{1}{8} \text{---} - \mu \rightarrow 0, \beta \rightarrow \infty$$

$$\begin{aligned}\Omega_0^q &= \text{Tr ln } \text{---} \\ \Omega_0^{\text{Gh}} &= \text{Tr ln } \text{---} \\ \Omega_0^G &= -\frac{1}{2} \text{Tr ln } \text{---}\end{aligned}$$

Figure 9-3

Figure 9-4

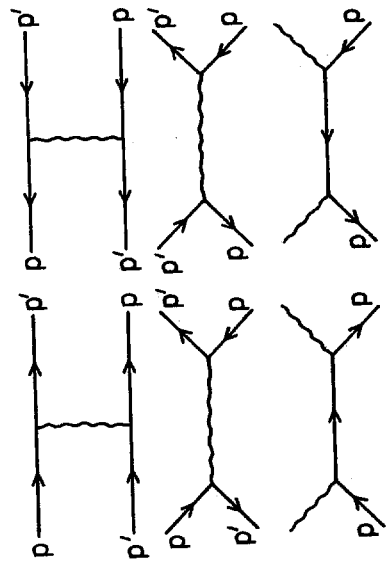


Figure 9-5

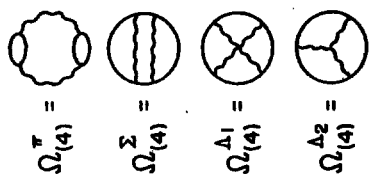


Figure 9-6

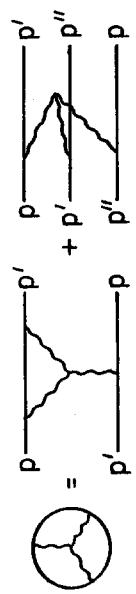


Figure 9-7

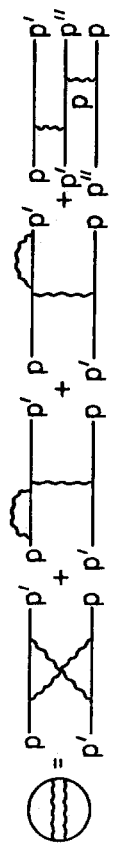
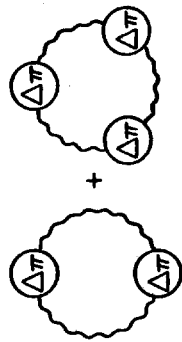


Figure 9-8



Figure 9-9



Lecture 10: Theoretical and Phenomenological Models
The study of phase transitions in QCD is far from a trivial task. We have seen that a great deal of progress has been made in understanding the fundamental dynamics of such phase transitions, and quantitative progress is also being made using lattice Monte-Carlo methods. At present, some insight must also be gleaned from phenomenological models. Historically, such models gave qualitative insight into the nature of confinement-deconfinement transitions. With the recent advances based on lattice computations, such models may be refined to give an even finer insight into the nature of confinement. The problem of chiral symmetry breaking must at present be attacked by such models since there is no completely satisfactory computation of the chiral properties of gauge theories on the lattice.

In the previous lectures, I have presented a $Z(N)$ model of the confinement-deconfinement phase transition. Such a model satisfactorily accounts for the qualitative features of this transition and the effects of fermions when they are included. This model does lack a simple physical intuitive picture of the transition. There has been a recent development of such an intuitive physical picture by Feynman and Patel[1] This picture utilizes a flux-tube model of the confinement-deconfinement transition. Such a picture may not only be regarded as a concrete realization of strong coupling expansions on the lattice, but may also be viewed as a representation of the successful string model phenomenology of high energy physics.

This lecture is taken in large part from the lectures of A. Patel at the Workshop on Phase Transitions in Gauge Theories and Their Physical Applications, July 27 - Aug 22, (1983) held at Seattle, Wash[1]

To derive a flux-tube picture, several assumptions about the nature of the flux-tubes must be made. We shall assume that there is a constant energy per unit length along the string, σ , and that the string has a constant width w . The strings are allowed to terminate only on quarks. Finally, the strings are assumed to be rigid along their length so that the string must

go a distance of a (approximately a fermi) before the string can bend by a right angle. This rigidity assumption is manifest on a strong coupling lattice, since a string cannot bend unless it traverses a lattice spacing a . The parameters of these strings are assumed to be temperature independent. The phase transition is driven by the increasing entropy of strings as the temperature increases.

To understand how such a model works, first consider an SU(2) gauge theory in the absence of quarks. The only structures in this theory are closed rings of strings. The partition function is

$$Z = \sum_l N(l) e^{-E(l)/T} \quad (1)$$

where $N(l)$ is the number of configurations of length l . The lattice spacing or rigidity factor a determines $N(l)$. If backstepping is allowed, the number of distinct random walks of length 1 is $N(1) = 6$. The number of closed loops with backstepping is $N(1) - 1 - 3/2 - 1$. If backstepping is not allowed, as it should not for a physical string, the number of distinct random walks is $N(1) = 5$. The number of closed loops is $N(1) = 5 \times$ (power law corrections in l). The partition function is approximately

$$Z = \sum_l e^{l(\ln 5 - 6a/T)} \quad (2)$$

As T becomes larger the average size of a loop gets larger and larger. At

$$T_c = 6a/\ln 5 \quad (3)$$

the partition becomes singular and the average loop size diverges. The effective string tension,

$$\sigma_{eff} = \sigma - T c^5/a + 0. \quad (4)$$

continuously as

$$T + T_c \quad (5)$$

A second order phase transition is suggested.

Under the circumstances discussed above, the flux tube between two static quarks may wander all over the lattice with no loss in free energy at T_c . The potential is no longer linear. In particular, a single isolated quark has a finite free energy and the expectation of L becomes finite above T_c . To obtain an estimate of T_c in this model, the rigidity parameter a must be determined. Taking the strong coupling result for the 0^+ meson mass as

$$m_{0^+} = 4\sigma a \quad (6)$$

we find

$$m_{0^+}/4T_c = \ln 5 \sim 1.6 \quad (7)$$

Lattice Monte-Carlo computations for T_c give a slightly larger value

$$m_{0^+}/4T_c \sim 1 \quad (8)$$

When this picture is generalized to SU(3) gauge theories, we must account for two new facts. The strings are in general directed, and strings may bifurcate. The diagrammatic rules for drawing closed loops are that each vertex has the structure shown in Fig. 1.

The number of links in each closed loop must also be even. Allowed and disallowed diagrams are shown in Fig. 2.

At zero temperature the vacuum is filled with closed loops formed from networks of these strings. As the temperature increases, the size and density of string bubbles grow. Unlike the case for SU(2), the confinement-deconfinement transition

does not occur when the bubbles acquire infinite size. Before this happens a phase transition to an infinite network takes place. The strings may fuse together in such a way that strings always connect the entire volume of the lattice. This network or percolation phase transition provides a first order deconfining phase transition.

This percolation problem has been studied in the context of polymer chains as a gelation transition by Flory (1941) and Stockmayer (1943). To analyze this problem, the links of networks are divided into two classes. Relevant links are those necessary for the existence of an infinite network. Irrelevant links are those which may be removed without destroying the infinite network. Such links appear in closed loops. To count the possible ratios of relevant to total number of links, we place the vertices of the network on concentric spheres. For the existence of an infinite network, after each bifurcation at least one link must go on to the next concentric sphere, and the other link may either go ahead or turn back and make closed loops. If f is the fraction of relevant links, then $f(T)$ may take on the values $2/3 < f(T) < 1$ with $2/3$ corresponding to a minimally connected network and 1 corresponding to maximally connected. The fraction $f(T)$ may be computed from the dynamics, and at $T=T_c$, the minimally connected network becomes formed. Bubbles exist with non-zero probability.

The energy of an isolated test quark is infinite below T_c because the string attached must terminate at infinity, and is not allowed to terminate on closed flux tube bubbles. Above T_c , the string may terminate on one of the infinite networks. The parameter $\langle L \rangle$ is analogous to the conductivity of the network.

The estimation of T_c requires knowledge of the energy of the three string vertex. Crude estimates give T_c as slightly lower than value estimated for SU(2). For SU(N) gauge theories, there are N string vertices, and each vertex provides N strings which can contribute to the network. The energy of the vertex is of course different. The phase transitions for $N > 2$ are typically first order. At infinite N, the phase transition survives if

the energy of a vertex scaled by $1/N$ approaches a constant as N approaches infinity.

This picture allows an estimation of the effects due to finite mass dynamical quarks. Recall that the pure gauge theory corresponds to the infinite quark mass limit. As m decreases from infinity, the $Z(N)$ symmetry which characterizes the confinement-deconfinement phase transition is explicitly broken. In the flux tube picture, the flux loops are allowed to break up before 1 approaches infinity for any finite value of m . Since $SU(2)$ Yang-Mills theory is characterized by a phase transition corresponding to infinite size flux tubes, this phase transition disappears.

The case for $SU(3)$ is special since first order phase transitions are stable against the introduction of small perturbations. For heavy enough quarks the phase transition will continue to exist. This phase transition corresponds to a boundary between two phases with two different types of screening. In the confined phase, screening is generated by string breakage. In the deconfined phase, screening is generated by strings attaching to large networks. The parameter $\langle L \rangle$ is discontinuous across the phase boundary.

Since there is no symmetry property which characterizes the differences between these phases, the transition may be only defined by the connectedness properties of the networks which characterize the theory. This may itself not be enough either since the networks may break as a consequence of quark-antiquark pair formation. A closely related example of such a transition is that of a gas liquid phase transition. The order parameter for this system is the density or specific volume. As is the case for a liquid gas phase transition, the first order confinement-deconfinement phase transition may be terminated by a second order critical point for some value of the quark mass.

Since the phase transition might be characterized by the connectedness of networks, it is clear that finite quark mass can lead to the disappearance of a connected phase. At infinite m , such a phase exists, and at zero m the string

breaking occurs with no cost in energy so that entropy factors will always force the disappearance of this phase transition. The situation is however complicated by the spontaneous breaking of chiral symmetry since a dynamical mass is always generated when chiral symmetry is broken. Perhaps the confinement-deconfinement transition disappears only at zero mass for sufficiently large numbers of quark flavors or perhaps at a reasonable mass for one flavor. This model does not at present have sufficient resolution to show the difference.

One interesting consequence of this model is that the confinement-deconfinement transition temperature increases as m increases. This is a consequence of the greater difficulty that it takes to make a network if string breaking is permitted. This result appears to be at odds with preliminary Monte-Carlo data, but the discrepancy is not yet serious. The parameters of the string theory could always be allowed some temperature dependence, since after all, thermal loops do renormalize the vertex energy, string tension, and string width.

The phenomenological description of chiral symmetry breaking is not in such good shape as that of confinement-deconfinement. A first step in this direction would be to explore phenomenological lagrangians with approximate $SU(2) \times SU(2)$ and $SU(3) \times SU(3)$ chiral symmetries. Some work in this direction is currently in progress by R. Pisarski and by T. De Grand (2-3). An approximate $U(1)$ chiral symmetry would also be a useful ingredient. Interesting questions are the orders of phase transitions and the effects of finite quark masses. Also, how do the parameters of these phenomenological lagrangians depend on temperature? What consequences for particle spectra are a result of chiral symmetry restoration? How is such a phenomenological lagrangian derived from QCD? What are the best signals of chiral symmetry restoration in ultra-relativistic heavy ion collisions?

References:

- (1) A. Patel, Cal. Tech. Preprints Caltech-68-1073; Calit-68-

1079; Calt-68-1080.

(2) R. D. Pisarski and F. Wiczeck, Phys. Rev. D29, 338,
(1984)

(3) R. D. Pisarski, ITP at Santa Barbara Preprint
NSF-ITP-83-71

Figure 10-1



Figure Captions:

Figure 1: The structure of the string vertex.

Figure 2: Allowed and disallowed diagrams.

Figure 10-2

